

Response to Reviewer 1 are structured as follow: (1) 1.X: comments from Reviewer 1, (2) Response to 1.X: author's response and author's changes in manuscript when any. For sake of clarity, line and page numbering from the revised version are used.

## 5 **Reviewer#1**

Dear Reviewer#1 many thanks for reviewing the manuscript and for highlighting its relevance and interest. Your comments and suggestions led to an improved version of the manuscript. Below is a point by point answer to your specific comments, all your editorial and technical comments were accounted for in the revised version of the manuscript.

1.1 [It would have been interesting to see a comparison of analysis vs. open-loop root-zone soil moisture skill (compared to the International Soil Moisture Network), as this could have a longer memory than the surface zone soil moisture, however, this is not crucial for the conclusions of this study.]

### **Response to 1.1**

Thank your for your highly relevant comment. Following it and similar comments from the other Reviewers, it has been decided to revisit the soil moisture evaluation part of the study:

(1) we have added an evaluation of soil moisture from LDAS-Monde fourth layer of soil (10 to 20 cm) against in situ measurements of soil moisture at 20 cm depth when available (10 networks and 685 stations),

(2) for surface soil moisture (SSM), correlation values (R) were calculated for both absolute and anomaly time-series in order to remove the strong impact from the SSM seasonal cycle on this specific metric,

(3) a 95% Confidence Interval (CI) has been added to R values.

(4) we have added the number of stations for which correlations differences are significant (significant improvement or degradation from the analysis) as well as a map over North America for illustration.

It involves several changes in the revised version of the manuscript, they are listed below.

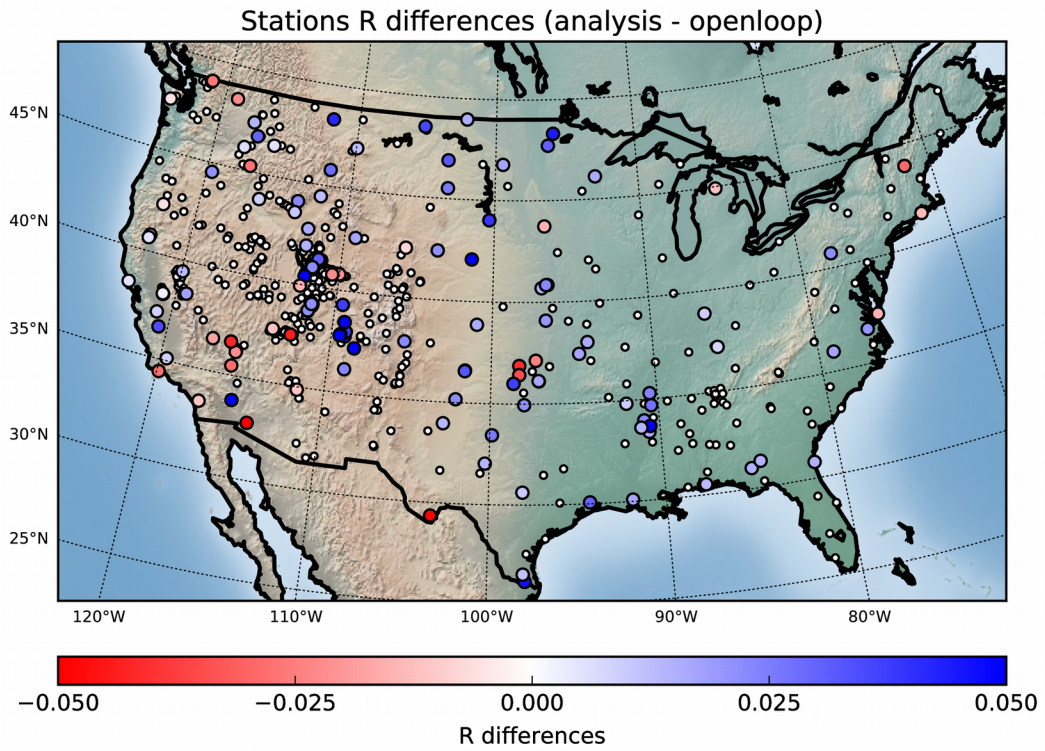
Methodology section, 2.5 Evaluation datasets and metrics

P.11, Lines 358-365: "In situ measurements of surface soil moisture from 19 networks across 14 countries available from the ISMN are also used to evaluate the performance of the soil moisture analysis. They represent 782 stations with at least 2 years of daily data over 2010-2018. Sensors at 5 cm depth (SSM) are compared with soil moisture from LDAS\_ERA5 third layer of soil (4-10 cm), sensors at 20 cm depth with the fourth layer of soil (10-20 cm, 685 stations from 10 networks). Beside 11 stations located in 4 countries of Western Africa (Benin, Mali, Sénégal and Niger) and 21 stations in Australia, most stations are located in North America and Europe, see Table S3."

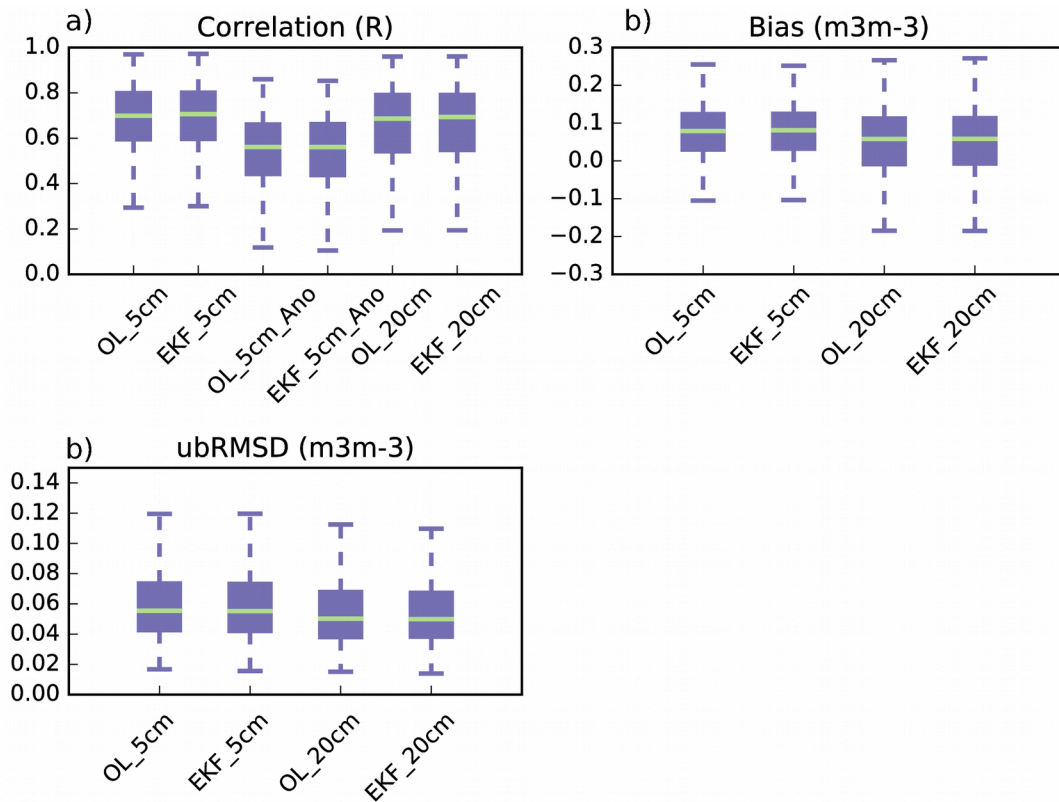
P.12, Lines 374-377: "For global estimates, Normalized RMSD (NRMSD, Eq.(2)) was used, also. Finally, for surface soil moisture, R was calculated for both absolute and anomaly time-series in order to remove the strong impact from the SSM seasonal cycle on this specific metric (see e.g. Albergel et al., 2018a, 2018b)."

Result section, 3..1.2 Ground-based datasets

P.17-18, Lines 548-580: “The statistical scores for soil moisture from LDAS\_ERA5 open-loop and analysis (third and fourth layers of soil, 4-10 cm depth, 10-20 cm depth, respectively) over 2010-2018 when compared with ground measurements from the ISMN (5 cm depth and 20 cm depth) are presented in Table S2 for each individual network. Averaged statistical metrics (ubRMSD, R,  $R_{anomaly}$  and bias) are similar for both LDAS\_ERA5 analysis and open-loop even if local differences exist. For the analysis, averaged R ( $R_{anomaly}$ ) values along with its 95% Confidence Interval (CI) using in situ measurements at 5 cm (782 stations from 19 networks) are  $0.68 \pm 0.03$  ( $0.53 \pm 0.04$ ) ( $0.67 \pm 0.03$  ( $0.53 \pm 0.04$ ) for the open-loop) with averaged-network values going up to  $0.88 \pm 0.01$  ( $0.58 \pm 0.04$ ) for the analysis (SOILSCAPE network, 49 stations in the USA) and always higher than 0.55 except for one network, ARM (10 stations in the USA) presenting an averaged R value of  $0.29 \pm 0.05$ . Averaged ubRMSD and bias (LDAS\_ERA5 minus in situ) are  $0.060 \text{ m}^3\text{m}^{-3}$  and  $0.077 \text{ m}^3\text{m}^{-3}$  for the analysis,  $0.060 \text{ m}^3\text{m}^{-3}$  and  $0.076 \text{ m}^3\text{m}^{-3}$  for the open-loop, respectively. NIC (Eq.1) has also been applied to R values, 65% of the pool of stations present a neutral impact from the analysis (511 stations at NIC ranging between -3 and +3), 12% present a negative impact (91 stations at NIC < -3) and 23% present a positive impact at (180 stations at NIC > +3). The number of stations where R differences between the analysis and the open-loop are significant (i.e. their 95% CI are not overlapping) is 186 out of 782 (about 26%). There is an improvement from the analysis w.r.t. the open-loop for 128 stations (out of 186, i.e. about 69%) and a degradation for 58 stations (about 31%). Figure 7 illustrates R differences between the analysis and the open-loop runs. When differences (analysis minus open-loop) are not significant stations are represented by a small dot. When they are significant, large circles have been used, blue for positive differences (an improvement from the analysis) and red for negative differences (a degradation from the analysis). For most of the stations where a significant difference is obtained, it represent an improvement from the analysis. Averaged analysis R (95%CI), bias and ubRMSD for the fourth layer of soil (685 stations from 10 networks) are  $0.65 \pm 0.03$ ,  $0.049 \text{ m}^3\text{m}^{-3}$  and  $0.055 \text{ m}^3\text{m}^{-3}$ , respectively. For the open-loop, they are  $0.64 \pm 0.03$ ,  $0.048 \text{ m}^3\text{m}^{-3}$  and  $0.056 \text{ m}^3\text{m}^{-3}$ , respectively. For soil moisture at that depth, about 60% of the stations present a neutral impact from the analysis (410 stations at NIC ranging between -3 and +3), 28% a positive impact (189 stations at NIC > +3) and 12% a negative impact (86 stations at NIC < -3). Although differences between the open-loop run and the analysis are rather small, these results underline the added value of the analysis with respect to the model run. Figure S6 represents the distribution of the scores values for LDAS\_ERA5 open-loop and analysis using boxplots centred on the median value. They look very similar and from this figure, it is difficult to see either improvement or degradation from the analysis.”



90 *Figure 7: Map of correlations (R) differences (analysis minus open-loop) for stations available over North America. Small dots represent stations where R differences are not significant (i.e. 95% confidence intervals are overlapping), large circles where differences are significant.*



95 *Figure S6: a) Boxplots representing the distribution of the correlation values on absolute time-series and anomaly time-series (“Ano”) between the stations with in situ measurements of soil moisture either 5cm depth or 20 cm depth and soil moisture from LDAS\_ERA5 open-loop and analysis over 2010-2018 (third and forth layer of soil, respectively). Correlation values are presented for surface soil moisture (5 cm depth measurements against third layer of soil), only. Distribution are centred on the median values. b) Distribution of the Bias values between the stations with in situ measurements of soil moisture either 5cm depth or 20 cm depth and soil moisture from LDAS\_ERA5 open-loop and analysis over 2010-2018 (third and forth layer of soil, respectively).c) Same as b) for ubRMSD.*

## 1.2 [L107-117: Is it necessary to include such details about the datasets in the introduction?]

### 105 **Response to 1.2**

We agree that a lot of information is provided in this bullet. However we believe acronyms should be detailed and appropriate references should be used the first time they appear in the text.

## 110 1.3 [L180: Please specify what you mean by flow dependency between the prognostic variables and the observations.]

### Response to 1.3

115 This sentence has been rephrased: “Flow dependency between the model control variables and the observations are generated using finite differences from perturbed simulations” is now (P.6, Lines 192-195): “The flow-dependency (dynamic link) between prognostic variables and the observations is ensured in the SEKF through the observation operator Jacobians, which propagate information from the observations to the analysis via finite-difference computations (de Rosnay et al., 2013)”

## 120 1.4 [L198-200: Difficult to interpret the difference in LAI error when you use a mix of percent and m2/m2. Please could you clarify this?]

### Response to 1.4

125 We agree that this sentence could be improved. Setting up the observed and modelled LAI standard deviation to 20 % of the LAI value is an empirical option coming from previous studies by Jarlan et al. (2008) and Rudiger et al. (2010), which have underlined the need for a variable LAI error definition. Barbu et al. (2011) further explored the impact of LAI model and background errors on the assimilation results by using diagnostics on model and observation errors (e.g. Desroziers and Ivanov, 2001) on different setups (see figure 2 of Barbu et al., 2011). They found that for small LAI values, it is necessary to use a fixed error standard deviation. This value was set to 0.04 m<sup>2</sup>m<sup>-2</sup> for LAI values lower than 2 m<sup>2</sup>m<sup>-2</sup> and is also used in this study.

135 The following sentence: “The standard deviation of errors for the observed LAI is assumed to be 20% and a similar assumption is made for the standard deviation of errors of the modelled LAI values higher than 2 m<sup>2</sup>m<sup>-2</sup>. For modelled LAI values lower than 2 m<sup>2</sup>m<sup>-2</sup>, a constant error of 0.4 m<sup>2</sup>m<sup>-2</sup> is assumed (Barbu et al., 2011). More details can be found in Albergel et al, 2017 or Tall et al., 2019.” as been reformulated and is now (P.7, Lines 220-224): “Based on previous results from Jarlan et al., 2008, Rüdiger et al., 2010, Barbu et al., 2011, observed and modelled LAI standard deviation errors are set to 20 % of the LAI value itself for values higher than 2m<sup>2</sup>m<sup>-2</sup>. For LAI

values lower than  $2 \text{ m}^2\text{m}^{-2}$ , a fixed value of  $0.04 \text{ m}^2\text{m}^{-2}$  has been used. More detailed can be found in Barbu et al., 2011 (section 2.3 on data assimilation scheme and figure 2).”

Reference (not added to the manuscript):

145 Desroziers, D. and Ivanov, S.: Diagnosis and adaptive tuning of observation-error parameters in a variational assimilation, *Q. J. Roy. Meteorol. Soc.*, 127, 1433–1452, 2001.

Reference (added to the manuscript):

150 Jarlan, L., Balsamo, G., Lafont, S., Beljaars, A., Calvet, J.-C., and Mougin, E.: Analysis of leaf area index in the ECMWF land surface model and impact on latent heat on carbon fluxes: Application to West Africa, *J. Geophys. Res.*, 113, D24117, doi:10.1029/2007JD009370, 2008.

Reference (already in the manuscript):

155 Rüdiger, C.; Albergel, C.; Mahfouf, J.-F.; Calvet, J.-C.; Walker, J.P. Evaluation of Jacobians for leaf area index data assimilation with an extended Kalman filter. *J. Geophys. Res.* 2010.

160 **1.5 [L251: Could you please include why you don’t consider assimilating surface soil moisture observations from the Soil Moisture and Ocean Salinity (SMOS) and/or from the Soil Moisture Active Passive (SMAP) satellite missions? As these satellites are expected to be more sensitive to surface soil moisture than the C-band observations from ASCAT.**

### **Response to 1.5**

165 We find it difficult at this stage to include why a specific dataset has not been used. The development of LDAS-Monde at CNRM has been made possible through different externally funded project including the Copernicus Global Land Service providing, amongst other datasets, the ASCAT Soil Wetness Index used in this study. ASCAT is from 2007 onward an operational product obtained from sensors onboard the METOP satellites and has been used at CNRM for many years. However, it is true than any satellite surface soil moisture products can be assimilate into LDAS-Monde. At CNRM, Albergel et al., 2017 have assimilated the ESA CCI (European Space Agency, Climate Change Initiative) combined surface soil moisture product (e.g. Dorigo et al., 2015), Parrens et al., 2014 have assimilated SMOS surface soil moisture. Future work will assimilate the most recent ESA CCI surface soil moisture dataset (v4.5) up to 2018. It includes the SMOS data.

175 Albergel, C., Munier, S., Leroux, D. J., Dewaele, H., Fairbairn, D., Barbu, A. L., Gelati, E., Dorigo, W., Faroux, S., Meurey, C., Le Moigne, P., Decharme, B., Mahfouf, J.-F., and Calvet, J.-C.: Sequential assimilation of satellite-derived vegetation and soil moisture products using SURFEX\_v8.0: LDAS-Monde assessment over the Euro-Mediterranean area, *Geosci. Model Dev.*, 10, 3889–3912, <https://doi.org/10.5194/gmd-10-3889-2017>, 2017.

180 Dorigo, W.A., A. Gruber, R.A.M. De Jeu, W. Wagner, T. Stacke, A. Loew, C. Albergel, L. Brocca, D. Chung, R.M. Parinussa and R. Kidd: Evaluation of the ESA CCI soil moisture product using ground-based observations, *Remote Sensing of Environment*, <http://dx.doi.org/10.1016/j.rse.2014.07.023>, 2015.

185 Parrens, M., Mahfouf, J.-F., Barbu, A. L., and Calvet, J.-C.: Assimilation of surface soil moisture into a multilayer soil model: design and evaluation at local scale, *Hydrol. Earth Syst. Sci.*, 18, 673–689, <https://doi.org/10.5194/hess-18-673-2014>, 2014.

190 **1.6 [Furthermore, as I understand ASCAT data are already assimilated in the production of the ERA5 dataset. Will the LDAS-Monde assimilation not lead to a “double” counting or usage of the ASCAT data and what are the potential consequences for your analyses results?]**

### **Response to 1.6**

195 Thank you for your comment. ASCAT soil moisture is indeed assimilated in the ERA5 LDAS. However, previous studies showed that its impact is confined to the soil and that it is neutral on the IFS atmospheric analysis and forecasts (de Rosnay et al 2014, Munoz-Sabater et al 2019). In our study we use the ERA5 atmospheric analysis as forcing but we do not use any of the ERA5 soil analysis variables as input of our system. So, we consider the ASCAT SM contribution to the ERA5 atmospheric forcing to be negligible.

200 Reference (already in the manuscript):

de Rosnay, P.; Balsamo, G.; Albergel, C.; Muñoz-Sabater, J.; Isaksen, L. Initialisation of land surface variables for numerical weather prediction. *Surv. Geophys.*, 35, 607–621, doi: 10.1007/s10712-012-9207-x, 2014.

205 Reference (not added to the revised version of the manuscript):

Muñoz-Sabater, J. , Lawrence, H. , Albergel, C. , de Rosnay, P. , Isaksen, L. , Mecklenburg, S. , Kerr, Y. and Drusch, M. (2019), Assimilation of SMOS brightness temperatures in the ECMWF Integrated Forecasting System. *Q J R Meteorol Soc.* Accepted Author Manuscript. doi:10.1002/qj.3577

210 **1.7 [L268: Please could you specify the difference between linear rescaling and CDF-matching (if any)? To my understanding linear rescaling is correction of the mean and standard deviation, while CDF-matching corrects the whole CDF (i.e., all moments of the probability distribution function), hence linear rescaling is not the same as CDF-matching.]**

### **Response to 1.7**

215 We use in this paper a seasonal linear rescaling. Linear rescaling was introduced by Scipal et al. (2008) and has been shown giving results that are very similar to an exact CDF matching. Nevertheless, to avoid any confusion, we have rewritten the sentence as follows (P.9-10, Lines 294-301): “This is done through a linear rescaling as proposed by Scipal et al. (2007), where the observations mean and variance are matched to the modelled soil moisture mean and variance from the second layer of soil (1-4 cm depth). This rescaling gives in practice very similar results to CDF (cumulative distribution function) matching. The linear rescaling is performed on a seasonal basis (with a 3-month moving window) as suggested by Draper et al., (2011), Barbu et al., (2014).”  
225 Further mentions of CDF matching in the manuscript have been replaced by “seasonal linear rescaling”.

230 **1.8 [L292-294: Could you please discuss how this short spinup period could affect your results?]**

### **Response to 1.8**

235 Nine months can be perceived as a short period to spin up the system. Unfortunately, HRES atmospheric forcing is only available from April 2016 and the LDAS-HRES experiment ends in December 2018. We have considered this 9 months period for the spin up in order to have the longest possible time series for land surface variables, thus giving more strength to statistics. We could have considered a longer period for spin up (April 2016 to December 2017) and studied only

240 2018. This gives very similar results on surface soil moisture and LAI (not shown). While not being fully spun-up, results obtained with LDAS-HRES can be considered as representative of the system response to data assimilation. Note that most initial values of the LDAS-HRES run are taken from the ECOCLIMAP-II database. For instance, initial LAI is set from a 1999-2005 climatology derived from MODIS.

245 Another possibility to initialise LDAS-HRES could have been to downscale the state of LDAS-ERA5 run in April 2016 to 0.10°x0.10° spatial resolution. LDAS-ERA5 runs have been set to an equilibrium spinning up 20 times the first year (2010).

250 The following sentence: “The period 2017-2018 is presented, HRES is available at this spatial resolution from April 2016, only, and the time period from April to December 2016 is used as a short spinup.” has been modified and is now (P.10, Lines 327-332): “HRES is available at a 0.1° x 0.1° resolution only from April 2016. April to December 2016 is used as a short period for spinup and results are presented for the period 2017-2018. Although a 9-month spinup period can be seen as rather short, evaluating LDAS-HRES on either 2017-2018 or 2018 (using instead a 21-month spinup) leads to similar results on surface soil moisture and LAI (not shown). While the system is not fully spun-up, it can be considered as representative of the system response to data assimilation.”

260 **1.9 [L383: Could you please provide more details on how this can explain the differences seen between ISBA and GLEAM?]**

**Response to 1.9**

265 GLEAM is an hydrological model and vegetation is mainly driven by observations. On the contrary, ISBA also represents plant growth and leaf-scale physiological processes, models key vegetation variables like LAI and above ground biomass (see section 2.1.1 on ISBA Land Surface Model). Within GLEAM, each grid cell comprises four different land-cover types: (1) bare soil, (2) low vegetation (e.g. grass), (3) tall vegetation (e.g. trees), and (4) openwater (e.g. lakes). Except for the fraction of open water, these fractions are sourced from the Global Vegetation Continuous Fields product (MOD44B), based on observations from the Moderate Resolution Image Spectroradiometer (MODIS). While in ISBA, each grid cell can be composed of up to 12 generic land surface types, bare soil, rocks, and permanent snow and ice surfaces as well as nine plant functional types (needle leaf trees, evergreen broadleaf trees, deciduous broadleaf trees, C3 crops, C4 crops, C4 irrigated crops, herbaceous, tropical herbaceous and wetlands). Those types depart from prevalent land cover products such as CLC2000 (Corine Land Cover) and GLC2000 (Global Land Cover) by splitting existing classes into new classes that possess a better regional character by virtue of the climatic environment (latitude, proximity to the sea, topography).

280 Work is undergoing at CNRM to better understand the differences between terrestrial evaporation from ISBA and GLEAM. In particular, the different components of terrestrial evaporation, i.e. transpiration, bare soil evaporation and, interception loss are investigated.

Paragraph: “However GLEAM only estimates (root-zone) soil moisture and terrestrial evaporation, while ISBA in LDAS\_ERA5 is a physically-based land surface model, accounting for more processes linked to vegetation.”

285 is now (P.14-15, Lines 458-471):

“However GLEAM is an evaporation model designed to be driven by remote sensing observations only. GLEAM only estimates (root-zone) soil moisture and terrestrial evaporation while the CO<sub>2</sub>-

responsive version of ISBA in LDAS\_ERA5 is a physically-based land surface model, accounting for more processes linked to vegetation (see section 2.1.1). It has to be noted that the auxiliary dataset used to e.g. represent the different land cover types are different also. Within GLEAM, the land cover types fractions are sourced from the Global Vegetation Continuous Fields product (MOD44B), based on observations from the Moderate Resolution Image Spectroradiometer (MODIS). Four land cover types are considered, bare soil, low vegetation (e.g. grass), tall vegetation (e.g. trees), and openwater (e.g. lakes). In ISBA the 12 land cover types fraction depart from prevalent land cover products such as CLC2000 (Corine Land Cover) and GLC2000 (Global Land Cover). It can potentially impact the distribution of the terrestrial evaporation between GLEAM and ISBA.”

Further work at CNRM will focus on understanding the differences between ISBA and GLEAM, in particular investigating the sub-components of terrestrial evaporation.”



Response to Reviewer 2 are structured as follow: (1) 2.X: comments from Reviewer 2, (2) Response to 2.X: author's response and author's changes in manuscript when any. For sake of clarity, line and page numbering from the revised version is used.

305

## Reviewer#2

**[...] This paper seems to represent a major milestone in the development of LDAS-Monde (which is in my view a very important undertaking), and hence I recommend publishing the paper after minor revisions.**

310

Dear Reviewer#2 many thanks for reviewing the manuscript and for highlighting its relevance and interest. Your comments and suggestions led to an improved version of the manuscript. Below is a point by point answer to your specific comments, all your editorial and technical comments were accounted for in the revised version of the manuscript.

315

### 2.1 [Line 167: What do you mean by "...is bale to ..."?]

#### Response to 2.1

320

Thanks for pointing out this typo, it should read "[...] *is able to* [...]" it is now corrected in the revised version of the manuscript.

**2.2 [Lines 188ff: The procedure described here results in an observational error field mainly related to soil properties, while the real retrieval errors are mostly dependent on vegetation density. Please discuss implications.]**

325

#### Response to 2.2

You are right that vegetation has a role in ASCAT SSM observational error. The observational SSM error we use is consistent with errors typically expected for remotely sensed SSM (e.g., de Jeu et al., 2008, Gruber et al., 2016). Most of the in-situ measurements sites used in typical evaluation studies are indeed representative of grassland. Going from radar backscatter measurements (ASCAT level1 data,  $\sigma^{\circ}$ ) to SSM (ASCAT level2 data) using the change detection approach developed at TUWIEN implies a lot of assumptions in particular on vegetation variability: only seasonal variability is accounted for (e.g. Wagner et al., 1999, Bartalis et al., 2007). That is why we have an ongoing work at CNRM trying to directly assimilate  $\sigma^{\circ}$  (Shamambo et al., 2019). Assimilating  $\sigma^{\circ}$  also raises the question of how to specify observation, background, and model error covariance matrices. The last decade has seen the development of techniques to estimate those matrices. Approaches based on Desroziers diagnostics (Desroziers et al., 2005) are affordable for land data assimilation systems from a computational point of view and could provide insightful information on the various sources of the data assimilation system.

330

335

340

The following paragraph has been added in the discussion and conclusion section (P.24, Lines 788-796):

345

“CNRM is also investigating the direct assimilation of ASCAT radar backscatter (Shamambo et al., 2019), it is supposed to tackle the way vegetation is accounted for in the change detection approach used to retrieve SSM with an improved representation of its effect. Assimilating ASCAT radar backscatter also raises the question of how to specify observation, background, and model error covariance matrices, so far mainly relying on soil properties (see section 2.1.3 on data assimilation). The last decade has seen the development of techniques to estimate those matrices. Approaches

350

based on Desroziers diagnostics (Desroziers et al., 2005) are affordable for land data assimilation systems from a computational point of view and could provide insightful information on the various sources of the data assimilation system”.

355

References (\* denotes new references added to the manuscript):

Bartalis, Z.; Wagner, W.; Naeimi, V.; Hasenauer, S.; Scipal, K.; Bonekamp, H.; Figa, J.; Anderson, C.: Initial soil moisture retrievals from the METOP-A advanced Scatterometer (ASCAT). *Geophys. Res. Lett.*, 34, L20401, doi: 10.1029/2007GL031088., 2007.

360 Desroziers, G.; Berre, L.; Chapnik, B.; Poli, P. Diagnosis of observation, background and analysis-error statistics in observation space. *Q. J. Roy. Meteor. Soc.* **2005**, 131, 3385–3396.

de Jeu, R.A.; Wagner, W.; Holmes, T.R.H.; Dolman, A.J.; Van De Giesen, N.C.; Friesen, J. Global soil moisture patterns observed by space borne microwave radiometers and scatterometers. *Surv. Geophys.*, 29, 399–420, 2008.

365 Gruber, A.; Su, C.-H.; Zwieback, S.; Crow, W.; Dorigo, W.; Wagner, W. Recent advances in (soil moisture) triple collocation analysis. *Int. J. Appl. Earth Obs. Geoinf.*, 45, 200–211, 2016.

Shamambo, D.C.; Bonan, B.; Calvet, J.-C.; Albergel, C.; Hahn, S. Interpretation of ASCAT Radar Scatterometer Observations Over Land: A Case Study Over Southwestern France. *Remote Sens.* 2019, 11, 2842.

370 Wagner, W.; Lemoine, G.; Rott, H. A method for estimating soil moisture from ERS scatterometer and soil data. *Remote Sens. Environ.*, 70, 191–207, 1999.

### 2.3 [Line 198: Is “20 %” a relative error?]

#### 375 **Response to 2.3**

It is 20% of the LAI itself, this paragraph has been revisited to improve its understanding. Setting up the observed and modelled LAI standard deviation to 20 % of the LAI value is an empirical option coming from previous studies by Jarlan et al. (2008) and Rudiger et al. (2010), which have underlined the need for a variable LAI error definition. Barbu et al. (2011) further explored the impact of LAI model and background errors on the assimilation results by using diagnostics on model and observation errors (e.g. Desroziers and Ivanov, 2001) on different setups (see figure 2 of Barbu et al., 2011). They found that for small LAI values, it is necessary to use a fixed error standard deviation. This value was set to 0.04 m<sup>2</sup>m<sup>-2</sup> for LAI values lower than 2 m<sup>2</sup>m<sup>-2</sup> and is also used in this study.

The following sentence: “The standard deviation of errors for the observed LAI is assumed to be 20% and a similar assumption is made for the standard deviation of errors of the modelled LAI values higher than 2 m<sup>2</sup>m<sup>-2</sup>. For modelled LAI values lower than 2 m<sup>2</sup>m<sup>-2</sup>, a constant error of 0.4 m<sup>2</sup>m<sup>-2</sup> is assumed (Barbu et al., 2011). More details can be found in Albergel et al, 2017 or Tall et al., 2019.” as been reformulated and is now (P.7, Lines 220-224): “Based on previous results from Jarlan et al., 2008, Rüdiger et al., 2010, Barbu et al., 2011, observed and modelled LAI standard deviation errors are set to 20 % of the LAI value itself for values higher than 2m<sup>2</sup>m<sup>-2</sup>. For LAI values lower than 2 m<sup>2</sup>m<sup>-2</sup>, a fixed value of 0.04 m<sup>2</sup>m<sup>-2</sup> has been used. More detailed can be found in Barbu et al., 2011 (section 2.3 on data assimilation scheme and figure 2).”

Reference (not added to the manuscript):

Desroziers, D. and Ivanov, S.: Diagnosis and adaptive tuning of observation-error parameters in a variational assimilation, *Q. J. Roy. Meteorol. Soc.*, 127, 1433–1452, 2001.

400 Reference (added to the manuscript):  
Jarlan, L., Balsamo, G., Lafont, S., Beljaars, A., Calvet, J.-C., and Mougin, E.: Analysis of leaf area index in the ECMWF land surface model and impact on latent heat on carbon fluxes: Application to West Africa, *J. Geophys. Res.*, 113, D24117, doi:10.1029/2007JD009370, 2008.

Reference (already in the manuscript):

405 Rüdiger, C.; Albergel, C.; Mahfouf, J.-F.; Calvet, J.-C.; Walker, J.P. Evaluation of Jacobians for leaf area index data assimilation with an extended Kalman filter. *J. Geophys. Res.* 2010.

410 **2.4 [Section 2.2: Note that ASCAT SSM data are already assimilated in ERA5. Please discuss implications.]**

#### **Response to 2.4**

415 Thank you for your comment. ASCAT soil moisture is indeed assimilated in the ERA5 LDAS. However, previous studies showed that its impact is confined to the soil and that it is neutral on the IFS atmospheric analysis and forecasts (de Rosnay et al 2014, Munoz-Sabater et al 2019). In our study we use the ERA5 atmospheric analysis as forcing but we do not use any of the ERA5 soil analysis variables as input of our system. So, we consider the ASCAT SM contribution to the ERA5 atmospheric forcing to be negligible.

420

Reference (already in the manuscript):

de Rosnay, P.; Balsamo, G.; Albergel, C.; Muñoz-Sabater, J.; Isaksen, L. Initialisation of land surface variables for numerical weather prediction. *Surv. Geophys.*, 35, 607–621, doi: 10.1007/s10712-012-9207-x, 2014.

425 Reference (not added to the revised version of the manuscript):

Muñoz-Sabater, J. , Lawrence, H. , Albergel, C. , de Rosnay, P. , Isaksen, L. , Mecklenburg, S. , Kerr, Y. and Drusch, M. (2019), Assimilation of SMOS brightness temperatures in the ECMWF Integrated Forecasting System. *Q J R Meteorol Soc.* Accepted Author Manuscript. doi:10.1002/qj.3577

430

**2.5 [Line 248: SWI is the Soil Water Index]**

#### **Response to 2.5**

435 Thanks, it has been corrected accordingly

**2.6 [Section 2.3: Describe also the masking of SSM]**

#### **Response to 2.6**

440

Thanks for your comment, the following sentence has been added to section 2.3 (P.9-10, Lines 299-301): “As in Albergel et al. (2018a, 2018b), pixels whose average altitude exceeds 1500 m above sea level as well as pixels with urban land cover fractions larger than 15% were discarded as those conditions may affect the retrieval of soil moisture from space.”

445

**2.7 [Line 493: Only this sub-study focusses on severe conditions, but not “this study” overall.]**

#### **Response to 2.7**

450 We agree with Reviewer#2 and the sentence has been corrected accordingly, it is now: “As this subsection focuses [...]”

Response to Reviewer 3 are structured as follow: (1) 3.X: comments from Reviewer 3, (2) Response to 3.X: author's response and author's changes in manuscript when any. For sake of clarity, line and page numbering from the revised version are used.

455

### **Reviewer#3**

**[...] Overall, the LDAS-Monde system is great, but the paper needs a thorough revision [...]**

460 Dear Reviewer#3 many thanks for reviewing the manuscript and for highlighting its relevance and interest. Your comments and suggestions led to an improved version of the manuscript. Below is a point by point answer to your specific comments, all your editorial and technical comments were accounted for in the revised version of the manuscript.

465 **3.1 [Are the perturbations chosen to get an optimal data assimilation system? Please discuss]**

### **Response to 3.1**

470 Yes, several studies have investigated the size of the perturbations within the ISBA LSM. In particular Draper et al., 2009, for soil moisture, Rüdiger et al., 2010, for LAI. The following sentence has been added to the revised version of the manuscript (as well as the new reference to Draper et al., 2009):

Section 2.1.3 on data assimilation

475 P.7, Lines 202-204: "Several studies (e.g. Draper et al., 2009; Rüdiger et al., 2010) have demonstrated that small perturbations lead to a good approximation of this linear behaviour, provided that computational round-off error is not significant."

References:

480 Draper, C. S., Mahfouf, J.-F., and Walker, J. P.: An EKF assimilation of AMSR-E soil moisture into the ISBA land surface scheme, J. Geophys. Res., 114, D20104, <https://doi.org/10.1029/2008JD011650>, 2009.

485 Rüdiger, C., Albergel, C., Mahfouf, J.-F., Calvet, J.-C., and Walker, J. P.: Evaluation of Jacobians for Leaf Area Index data assimilation with an extended Kalman filter, J. Geophys. Res., 115, D09111, <https://doi.org/10.1029/2009JD012912>, 2010.

**3.2 [How are the cross correlations between the errors in the various soil layers defined, and the error correlations between LAI and soil moisture?]**

### **Response to 3.2**

490

In the SEKF, no covariance is directly prescribed between LAI and soil moisture or soil moisture between the various soil layers. The sensitivity of model variables to observations is entirely driven by the Jacobian of the observation operator, which is defined as the product of the model state evolution from  $t$  to  $t + 24h$  and the conversion of the model state into the observation equivalent (see paragraph 2.3.1 and supplementary material of Bonan et al. (2020)). The value of Jacobian has been heavily studied in previous publications such as Albergel et al. (2017) or Tall et al. (2019).

495 Within LDAS-Monde, cross correlations between the errors in the various variables (soil moisture of the different layers and LAI) will be investigated in a near future based on the Ensemble Square Root Filter (EnSRF) proposed by Bonan et al., 2020.

500

## References:

- 505 Albergel, C., Munier, S., Leroux, D. J., Dewaele, H., Fairbairn, D., Barbu, A. L., Gelati, E., Dorigo, W., Faroux, S., Meurey, C., Le Moigne, P., Decharme, B., Mahfouf, J.-F., and Calvet, J.-C.: Sequential assimilation of satellite-derived vegetation and soil moisture products using SURFEX\_v8.0: LDAS-Monde assessment over the Euro-Mediterranean area, *Geosci. Model Dev.*, 10, 3889–3912, <https://doi.org/10.5194/gmd-10-3889-2017>, 2017.
- 510 Bonan, B., Albergel, C., Zheng, Y., Barbu, A. L., Fairbairn, D., Munier, S., and Calvet, J.-C.: An Ensemble Square Root Filter for the joint assimilation of surface soil moisture and leaf area index within LDAS-Monde: application over the Euro-Mediterranean region, *Hydrol. Earth Syst. Sci. Discuss.*, <https://doi.org/10.5194/hess-2019-391>, accepted, 2020.
- 515 Tall, M.; Albergel, C.; Bonan, B.; Zheng, Y.; Guichard, F.; Dramé, M.S.; Gaye, A.T.; Sintondji, L.O.; Hountondji, F.C.C.; Nikiema, P.M.; Calvet, J.-C. Towards a Long-Term Reanalysis of Land Surface Variables over Western Africa: LDAS-Monde Applied over Burkina Faso from 2001 to 2018. *Remote Sens.*, 11, 735, 2019

### **3.3 [ASCAT has an approximate resolution of 25 km. How are these coarse data assimilated/downscaled into the 0.1° model simulations?]**

#### 520 **Response to 3.3**

The assimilated SWI product is provided by the Copernicus Global Land Service directly on a global 0.1° regular grid. Informations on how the SWI product is derived from ASCAT data at 25-km resolutions can be found in the Product User Manual  
525 ([https://land.copernicus.eu/global/sites/cgls.vito.be/files/products/CGLOPS1\\_PUM\\_SWIV3-SWI10-SWI-TS\\_I2.60.pdf](https://land.copernicus.eu/global/sites/cgls.vito.be/files/products/CGLOPS1_PUM_SWIV3-SWI10-SWI-TS_I2.60.pdf)).

### **3.4 [CDF matching ‘refers to rescaling of the entire CDF, and is not a correct terminology when only rescaling the mean and variance.]**

530

#### **Response to 3.4**

We use in this paper a seasonal linear rescaling. Linear rescaling was introduced by Scipal et al. (2008) and has been shown giving results that are very similar to an exact CDF matching.  
535 Nevertheless, to avoid any confusion, we have rewritten the sentence as follows (P.9-10, Lines 299-301): “This is done through a linear rescaling as proposed by Scipal et al. (2007), where the mean and variance of observations are matched to the mean and variance of the modelled soil moisture from the second layer of soil (1-4 cm depth). This rescaling gives in practice very similar results to CDF (cumulative distribution function) matching. The linear rescaling is performed on a seasonal  
540 basis (with a 3-month moving window) as suggested by Draper et al., (2011), Barbu et al., (2014).” Further mentions of CDF matching in the manuscript have been replaced by “seasonal linear rescaling”.

### **3.5 [How exactly are the LAI data ‘interpolated’ from 1 km to 0.25 degree? Do you mean interpolation to bridge cloudy pixels and then aggregation (upscaling)?]**

545

#### **Response to 3.5**

550 Thanks for this suggestion. As in previous studies (e.g. Barbu et al., 2014, Albergel et al., 2019), observations are aggregated using an arithmetic average to the model grid points (0.25° or 0.10° in this study), if at least 50 % of the model grid points are observed (i.e. half the maximum amount).

555 Future work will focus on looking at the impact of cloud cover on the LAI upscaling process. Instead of 50%, a possibility could be to use an arithmetic average to the model grid point if at least 70% of the model grid point are observed. Then during the assimilation/evaluation ERA5 (or HRES IFS) total cloud cover field (tcc) could be used to mask out grid point if tcc is greater than 30%. This is already used when evaluating e.g. satellite land surface temperature to model data (e.g. Johannsen et al., 2019).

560 Reference:  
Johannsen, F.; Ermida, S.; Martins, J.P.A.; Trigo, I.F.; Nogueira, M.; Dutra, E. Cold Bias of ERA5 Summertime Daily Maximum Land Surface Temperature over Iberian Peninsula. *Remote Sens.*, *11*, 2570, 2019.

565 **3.6 [Is the LAI also ‘converted from the observation space to the model space’ as is done for soil moisture? Please describe how? If there is no such rescaling, then the results may be trivial, i.e. there will be more impact of a non-rescaled LAI assimilation than when doing a gentle nudging with rescaled soil moisture. However, since you use a KF variant, there probably is some rescaling for both (otherwise the KF assumptions would be violated).]**

570 **Response to 3.5**

575 Soil moisture is a very model-specific variable, precipitation, evapotranspiration, soil texture, topography, vegetation, and land use could either enhance or reduce the spatial variability of soil moisture depending on how it is distributed and combined with other factors (Famiglietti et al. 2008). In particular, differences in soil properties between the model grid points and reality could imply important variations in the mean and variance of soil moisture. Furthermore, vegetation effects are not completely corrected when going from the satellite measurement (e.g. radar backscatter in the case of ASCAT) to SSM, leading to potential seasonal biases (e.g. Shamambo et al., 2019). That is why we apply the linear rescaling to the ASCAT SWI. It also acts as an observation operator to go from the observational space (SWI, an index 0 and 1) to the model space (SSM in  $m^3m^{-3}$ ).

585 For LAI, biases between the model and the observations are linked to the way processes are represented in the model as well as uncertainties on the atmospheric forcing (cumulated effect on modelled LAI). The assimilation sequentially removes bias in the modelled LAI (with respect to the observed LAI). This technical difference between SSM and LAI assimilation, combined with the longer memory of LAI compared to SSM contributes to the results presented in this study. See also response to comment 3.14.

590 References:  
Famiglietti, J. S., D. Ryu, A. A. Berg, M. Rodell, and T. J. Jackson, 2008: Field observations of soil moisture variability across scales. *Water Resour. Res.*, *44*, W01423, doi:10.1029/2006WR005804.  
Shamambo, D.C.; Bonan, B.; Calvet, J.-C.; Albergel, C.; Hahn, S. Interpretation of ASCAT Radar Scatterometer Observations Over Land: A Case Study Over Southwestern France. *Remote Sens.* **2019**, *11*, 2842.

600 **3.6 [How exactly is the ‘climatology’ defined? Is it seasonally varying, how much smoothing is applied, etc?]**

### Response to 3.6

605 The following sentence “This 9-yr global reanalysis was then used to provide a climatology for  
estimating anomalies of the land surface conditions.” has been reformulated and is now (P.10, Lines  
317-320) “This 9-yr global reanalysis was then used to provide a monthly climatology for  
estimating anomalies of the land surface conditions. For each month (and variable considered) of  
2018 we have removed the monthly mean and scaled by the monthly standard deviation of the  
2010-2018 period”

610

**3.7 [The spinup period for the 0.1° simulation seems unrealistically short. How was it  
initialized? Could you cycle over the short April-December period multiple times?**

### Response to 3.7

615

Nine months can be perceived as a too short period to spin up the system. Unfortunately, HRES  
atmospheric forcing is only available from April 2016 and the LDAS-HRES experiment ends in  
December 2018. We have considered this 9 months period for the spin up in order to have the  
longest possible time series for land surface variables, thus giving more strength to statistics. We  
620 could have considered a longer period for spin up (April 2016 to December 2017) and studied only  
2018. This gives very similar results on surface soil moisture and LAI (not shown). While not being  
fully spun-up, results obtained with LDAS-HRES can be considered as representative of the system  
response to data assimilation. Note that most initial values of the LDAS-HRES run are taken from  
the ECOCLIMAP-II database. For instance, initial LAI is set from a 1999-2005 climatology derived  
625 from MODIS

Another possibility to initialise LDAS-HRES could have been to downscale the state of LDAS-  
ERA5 run in April 2016 to 0.10°x0.10° spatial resolution. LDAS-ERA5 runs have been set to an  
equilibrium spinning up 20 times the first year (2010).

630

The following sentence: “The period 2017-2018 is presented, HRES is available at this spatial  
resolution from April 2016, only, and the time period from April to December 2016 is used as a  
short spinup.” has been modified and is now (P.10, L.327-332): “HRES is available at a 0.1° x 0.1°  
635 resolution only from April 2016. April to December 2016 is used as a short period for spinup and  
results are presented for the period 2017-2018. Although a 9-month spinup period can be seen as  
rather short, evaluating LDAS-HRES on either 2017-2018 or 2018 (using instead a 21-month  
spinup) leads to similar results on surface soil moisture and LAI (not shown). While the system is  
not fully spun-up, it can be considered as representative of the system response to data  
assimilation.”

640

**3.8 [Table II: An observation operator is a function, not a variable; also explain what you  
mean by control variable (updated variables) for readers who are new to the field. In fact, the  
control vector enters the observation operator, which in turn selects a subset of relevant  
variables to produce the observation prediction.]**

645

### Response to 3.8

Agreed, in Table II “Observations operators” has been replaced by “Model equivalents” and the  
following sentences have been added to the revised version of the manuscript (section 2.1.3 on data  
650 assimilation, P.6, Lines 200-202): “The eight control variables are directly updated using their



sensitivity to observed variables (i.e. defined by the Jacobians). Other variables are indirectly modified through biophysical processes and feedbacks from the model”

### 3.9 [Why is there no skill evaluation in terms of anomalies? Would be interesting.]

655

#### Response to 3.9

Thank you for your highly relevant comment. Following it and similar comments from the other Reviewers, it has been decided to revisit the soil moisture evaluation part of the study:

660

(1) we have added an evaluation of soil moisture from LDAS-Monde fourth layer of soil (10 to 20 cm) against in situ measurements of soil moisture at 20 cm depth when available (10 networks and 685 stations),

665

(2) for surface soil moisture (SSM), correlation values (R) were calculated for both absolute and anomaly time-series in order to remove the strong impact from the SSM seasonal cycle on this specific metric,

(3) a 95% Confidence Interval (CI) has been added to R values.

(4) we have added the number of stations for which correlations differences are significant (significant improvement or degradation from the analysis) as well as a map over North America for illustration.

670

It involves several changes in the revised version of the manuscript, they are listed below.

Methodology section, 2.5 Evaluation datasets and metrics

675

P.11, Lines 358-365: “In situ measurements of surface soil moisture from 19 networks across 14 countries available from the ISMN are also used to evaluate the performance of the soil moisture analysis. They represent 782 stations with at least 2 years of daily data over 2010-2018. Sensors at 5 cm depth (SSM) are compared with soil moisture from LDAS\_ERA5 third layer of soil (4-10 cm), sensors at 20 cm depth with the fourth layer of soil (10-20 cm, 685 stations from 10 networks).  
680 Beside 11 stations located in 4 countries of Western Africa (Benin, Mali, Sénégal and Niger) and 21 stations in Australia, most stations are located in North America and Europe, see Table S3.”

685

P.12, Lines 374-377: “For global estimates, Normalized RMSD (NRMSD, Eq.(2)) was used, also. Finally, for surface soil moisture, R was calculated for both absolute and anomaly time-series in order to remove the strong impact from the SSM seasonal cycle on this specific metric (see e.g. Albergel et al., 2018a, 2018b).”

Result section, 3..1.2 Ground-based datasets

690

P.17-18, Lines 548-582: “The statistical scores for soil moisture from LDAS\_ERA5 open-loop and analysis (third and fourth layers of soil, 4-10 cm depth, 10-20 cm depth, respectively) over 2010-2018 when compared with ground measurements from the ISMN (5 cm depth and 20 cm depth) are presented in Table S2 for each individual network. Averaged statistical metrics (ubRMSD, R,  $R_{anomaly}$  and bias) are similar for both LDAS\_ERA5 analysis and open-loop even if local differences exist.

695

For the analysis, averaged R ( $R_{anomaly}$ ) values along with its 95% Confidence Interval (CI) using in situ measurements at 5 cm (782 stations from 19 networks) are  $0.68 \pm 0.03$  ( $0.53 \pm 0.04$ ) ( $0.67 \pm 0.03$  ( $0.53 \pm 0.04$ ) for the open-loop) with averaged-network values going up to  $0.88 \pm 0.01$  ( $0.58 \pm 0.04$ ) for the analysis (SOILSCAPE network, 49 stations in the USA) and always higher than 0.55 except for one network, ARM (10 stations in the USA) presenting an averaged R value of  $0.29 \pm 0.05$ . Averaged ubRMSD and bias (LDAS\_ERA5 minus in situ) are  $0.060 \text{ m}^3\text{m}^{-3}$  and 0.077

700

$\text{m}^3\text{m}^{-3}$  for the analysis,  $0.060 \text{ m}^3\text{m}^{-3}$  and  $0.076 \text{ m}^3\text{m}^{-3}$  for the open-loop, respectively. NIC (Eq.1) has also been applied to R values, 65% of the pool of stations present a neutral impact from the analysis (511 stations at NIC ranging between -3 and +3), 12% present a negative impact (91 stations at NIC < -3) and 23% present a positive impact at (180 stations at NIC > +3).

705 The number of stations where R differences between the analysis and the open-loop are significant (i.e. their 95% CI are not overlapping) is 186 out of 782 (about 26%). There is an improvement from the analysis w.r.t. the open-loop for 128 stations (out of 186, i.e. about 69%) and a degradation for 58 stations (about 31%). Figure 7 illustrates R differences between the analysis and the open-loop runs. When differences (analysis minus open-loop) are not significant stations are represented by a small dot. When they are significant, large circles have been used, blue for positive differences (an improvement from the analysis) and red for negative differences (a degradation from the analysis). For most of the stations where a significant difference is obtained, it represent an improvement from the analysis.

710  
715 Averaged analysis R (95%CI), bias and ubRMSD for the fourth layer of soil (685 stations from 10 networks) are  $0.65\pm 0.03$ ,  $0.049 \text{ m}^3\text{m}^{-3}$  and  $0.055 \text{ m}^3\text{m}^{-3}$ , respectively. For the open-loop, they are  $0.64\pm 0.03$ ,  $0.048 \text{ m}^3\text{m}^{-3}$  and  $0.056 \text{ m}^3\text{m}^{-3}$ , respectively. For soil moisture at that depth, about 60% of the stations present a neutral impact from the analysis (410 stations at NIC ranging between -3 and +3), 28% a positive impact (189 stations at NIC > +3) and 12% a negative impact (86 stations at NIC < -3). Although differences between the open-loop run and the analysis are rather small, these results underline the added value of the analysis with respect to the model run. Figure S6 represents the distribution of the scores values for LDAS\_ERA5 open-loop and analysis using boxplots centred on the median value. They look very similar and from this figure, it is difficult to see either improvement or degradation from the analysis.”

720

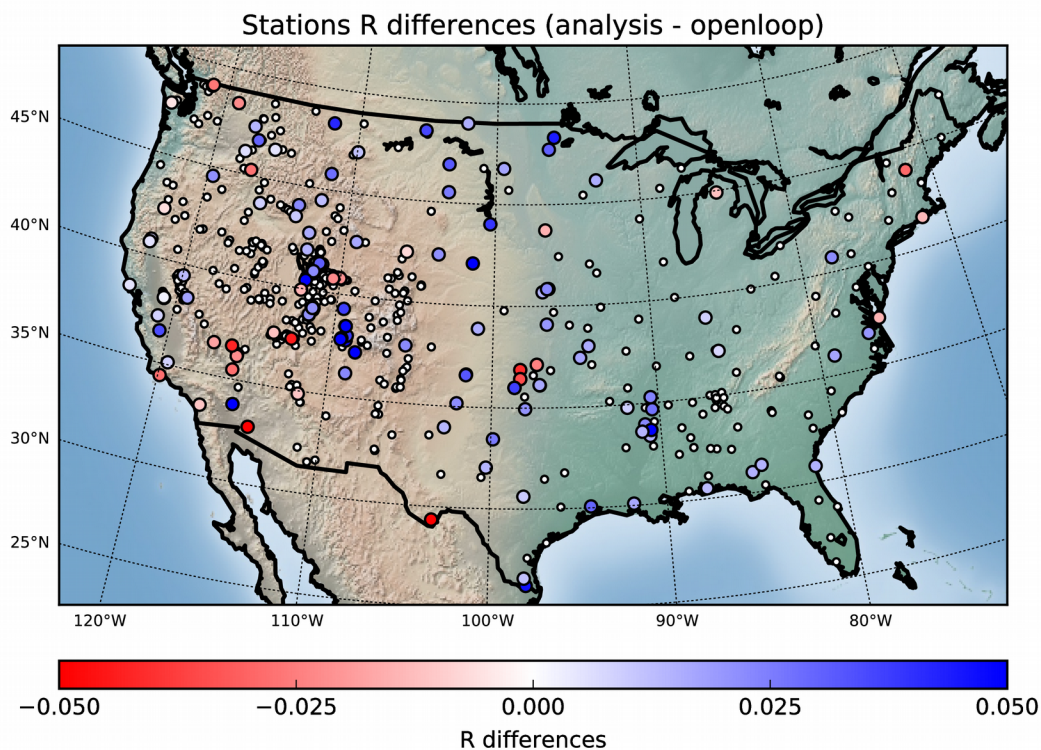
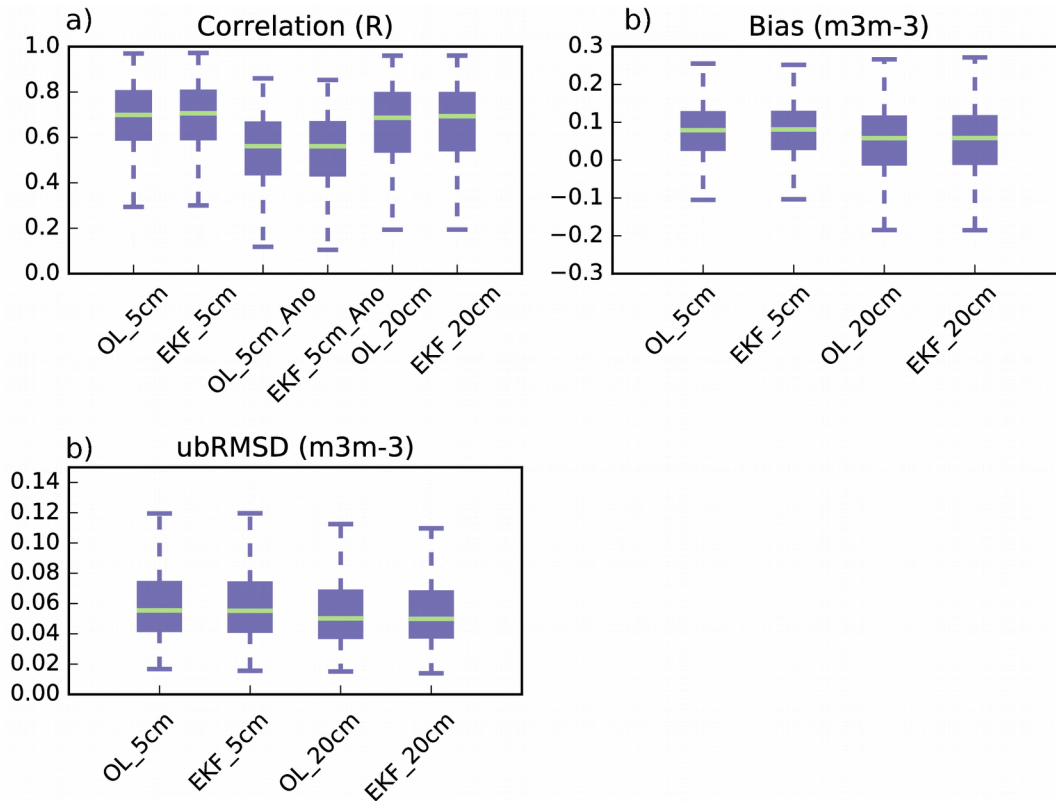


Figure 7: Map of correlations (R) differences (analysis minus open-loop) for stations available over North America. Small dots represent stations where R differences are not significant (i.e. 95% confidence intervals are overlapping), large circles where differences are significant.



735 *Figure S6: a) Boxplots representing the distribution of the correlation values on absolute time-series and anomaly time-series (“Ano”) between the stations with in situ measurements of soil moisture either 5cm depth or 20 cm depth and soil moisture from LDAS\_ERA5 open-loop and analysis over 2010-2018 (third and fourth layer of soil, respectively). Correlation values are presented for surface soil moisture (5 cm depth measurements against third layer of soil), only. Distribution are centred on the median values. b) Distribution of the Bias values between the stations with in situ measurements of soil moisture either 5cm depth or 20 cm depth and soil moisture from LDAS\_ERA5 open-loop and analysis over 2010-2018 (third and fourth layer of soil, respectively). c) Same as b) for ubRMSD.*

740 The following text has been added to the revised version of the manuscript: “Figure S6 represents the distribution of the scores values for LDAS\_ERA5 open-loop and analysis using boxplots centred on the median value. They look very similar and from this figure, it is difficult to see either improvement or degradation from the analysis.”

### 745 **3.10 [Which variable in LDAS-Monde output is related to SIF and how?]**

#### **Response to 3.10**

750 In ISBA, the fluorescence is not simulated directly, but the photosynthesis activity is simulated through the calculation of the GPP, which is driven by plant growth and mortality in the model. Sun et al. (2017) demonstrated that SIF and GPP were driven by the same environmental and biological factors and found that SIF observations from OCO-2 and GPP products from FLUXCOM were highly consistent in time and space. The modelled GPP values are expressed in  $\text{g(C)} \cdot \text{m}^{-2} \cdot \text{day}^{-1}$ , whereas SIF is an energy flux emitted by the vegetation in units of  $\text{mW} \cdot \text{m}^{-2} \cdot \text{sr}^{-1} \cdot \text{nm}^{-1}$ . Thus, GPP and SIF cannot be directly compared as they do not represent the same physical quantities.

755

However, several studies (including Zhang et al., 2016, Sun et al., 2017, Leroux et al., 2018) have found that their time dynamics and their spatial distributions can be investigated.

760 The following paragraph has been added to the revised version of the manuscript (Section 2.5 on evaluation datasets and metrics, P.13, Lines 400-406): “As for SIF, in ISBA the fluorescence is not simulated directly, however photosynthesis activity is simulated through the calculation of the GPP, which is driven by plant growth and mortality in the model. Modelled GPP values are expressed in  $g(C) \cdot m^{-2} \cdot day^{-1}$ , while SIF is an energy flux emitted by the vegetation ( $mW \cdot m^{-2} \cdot sr^{-1} \cdot nm^{-1}$ ). Hence, GPP and SIF cannot be directly compared as they do not represent the same physical quantities.  
765 However, several studies (e.g, Zhang et al., 2016, Sun et al., 2017, Leroux et al., 2018) have found that their time dynamics investigated, highlighting the potential of SIF products to be used as a validation support for GPP models.”

References:

770 Leroux, D.J.; Calvet, J.-C.; Munier, S.; Albergel, C. Using Satellite-Derived Vegetation Products to Evaluate LDAS-Monde over the Euro-Mediterranean Area. *Remote Sens.* **2018**, *10*, 1199.  
Sun, Y.; Frankenberg, C.; Wood, J.D.; Schimel, D.S.; Jung, M.; Guanter, L.; Drewry, D.T.; Verma, M.; Porcar-Castell, A.; Griffis, T.J.; et al. OCO-2 advances photosynthesis observation from space via solar-induced chlorophyll fluorescence. *Science* **2017**, 358, 189.  
775 Zhang, Y.; Xiao, X.; Jin, C.; Dong, J.; Zhou, S.; Wagle, P.; Joiner, J.; Guanter, L.; Zhang, Y.; Zhang, G.; et al. Consistency between sun-induced chlorophyll fluorescence and gross primary production of vegetation in North America. *Remote Sens. Environ.* **2016**, 183, 154–169.

**3.11 [Overall, it is a bit disconcerting that trivial design results are shown repeatedly. Assimilate a variable, and sure, the model will get closer the assimilated observations. The results need to be thoroughly revised (both text and figures) to eliminate the trivial results. They can be mentioned once, but then the focus needs to be on the independent evaluation. It is also not correct to say that results “improve” if they simply get closer to the assimilated observations (e.g. L. 375, L. 516,...). This holds both for the global assessment and for the case studies, e.g. all of L. 505-512 is ‘trivial’ and can be removed.]**  
780  
785

**Response to 3.11**

790 Verifying that the assimilation system works as intended is an important task. This is why several figures have been included for “sanity check”. We have emphasized in the manuscript that several presented evaluations are carried out to check if the assimilation system is working properly.

795 Also, using SSM and LAI as an independent source of information to evaluate the forecast has been further discussed and added in the revised version of the manuscript. While LAI remains an independent source of information for the forecast evaluation (although constrained by the assimilation), ASCAT SWI has been rescaled to match the model climatology. The seasonal rescaling impacts both bias and correlation. In an attempt to have a more independent evaluation, an additional figure has been put in the revised version of the manuscript. It displays maps of correlations between modelled soil moisture (1-4 cm) from the four experiments (LDAS-HRES open-loop, analysis, LDAS\_fc4 and LDAS\_fc8) and ASCAT SWI (i.e. ASCAT data prior rescaling)  
800 for the WEUR domain. Correlations are applied to both absolute values and to anomalies (to assess the short term variability of soil moisture).

***End of section 3.2.2***

805 P.22, Lines 703-724: “Similarly to Figures 13(a, b, c, d), panels of Figure 15 illustrate the impact of the analysis on SSM using correlations., To that end, ASCAT SWI (i.e. no rescaling) has been used. Figure 14 (top panels) shows map of R values based on absolute values while Figure 14 (bottom panels) shows R values on anomalies (short term variability) as defined in Albergel et al., 2018a. Figure 15 (a) and (e) represents R values and anomaly R values for LDAS\_HRES, respectively. As  
 810 expected R values are higher than anomaly R values. Maps of differences (panels b and f) of Figure 15 suggest that after assimilation, both scores are improved rather equally. While the 4 day and 8-day forecast still show an improvement from the initial condition on R values (panels c and d of Figure 15 dominated by positive differences, analysis minus open-loop), maps of anomaly R values forecast don’t show any negative or positive impact (panels g and h of Figure 15).”  
 815

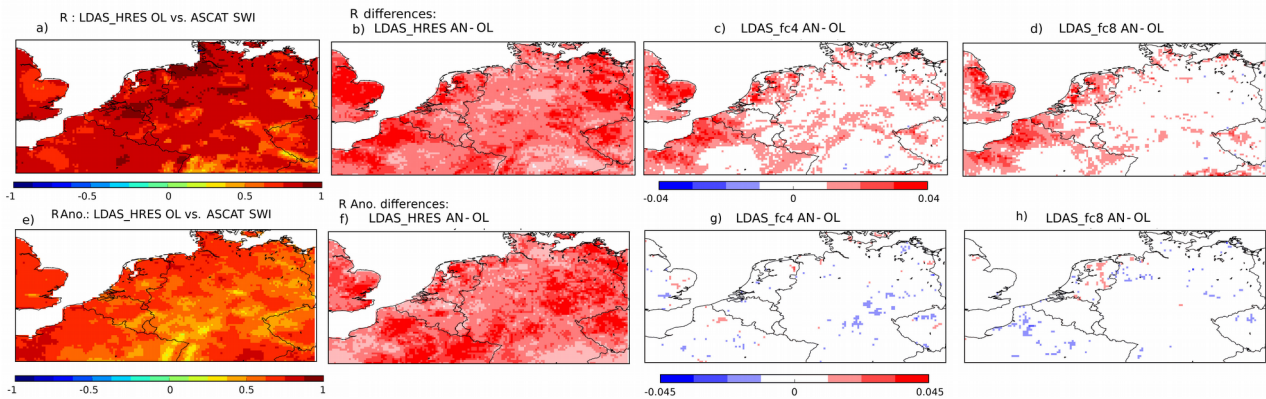


Figure 15: Top row, (a) R values between LDAS\_HRES open-loop and ASCAT SWI estimates from the Copernicus Global Land Service (CGLS) over 2017-2018 for the WEUR domain, (b) R differences between LDAS\_HRES analysis (open-loop) and ASCAT SWI. (c) and (d) same as (b) between LDAS\_fc4 initialised by the analysis (open-loop) and LDAS\_fc8. Bottom row, same as top row for R values based on anomaly time-series.

### Discussion and conclusion sections

820 P.23, Lines 749-754: “For SSM, the assimilation is done after a rescaling to the model climatology (see section 2.3), which removes bias. For LAI, however it is not the case and the assimilation process removes bias in the modelled LAI (w.r.t. to the observation). This technical difference between SSM and LAI assimilation, combined with the longer memory of LAI compared to SSM, contributes to the results presented in this section”

825 **3.12 [The snow cover results (Fig 7-8) can be removed. It is too trivial that there would be no impact on snow cover by assimilating soil moisture or LAI. Or else, explain in detail how either variable would affect the snow cover.]**

### **Response to 3.12**

830 Agreed, both figures have been moved to the supplementary document (Figures S1 and S2) and it has been further emphasized that there is no snow data assimilation yet. Those results are presented to highlight areas of improvements in LDAS-Monde:

835 P.15, Lines 487-492: “As expected, the analysis has an almost neutral impact on snow as both SSM and LAI observations are filtered out from frozen/snow condition and as there is no snow data assimilation in LDAS\_ERA5 (Figure S2 and panels (j), (k) and (l) of Figure S1). This clearly shows however an area of potential improvement of data assimilation within LDAS-Monde using satellite data such as the IMS one (as in e.g. de Rosnay et al., 2014).”

840 **3.13 [The independent validation (e.g against in situ SSM) shows no substantial improvement in any of the metrics due to data assimilation. Have the in situ data been thoroughly filtered to remove bad points? Why exactly do the authors see an advantage of LDAS\_ERA5 for these variables relative to the open loop (L. 458)? There is some added value, but there is also significant degradation, i.e. I would say it is an equal game here.]**

845 **Response to 3.13**

850 Agreed, last paragraph of section 3.1.2 on ground based dataset has been modified and is now (P.18, Lines 582-587): “For evapotranspiration, river discharge and surface soil moisture, there is a slight advantage for LDAS\_ERA5 analysis with respect to its open-loop counterpart. Even if the distribution of the averaged statistical metrics can be rather similar for both (particularly true for surface soil moisture evaluation), there are significant differences for some sites, which shows the added value of the analysis with respect to the open-loop. Note that for fewer sites, a negative impact from the analysis can also be observed.”

855 We have also revisited the soil moisture evaluation part of the manuscript, see response to comment 3.9.

860 **3.14 [L. 535 & L. 545: ‘more sensitive to’ is perhaps not the correct wording? Sensitivity would be quantified by something like the Jacobian. There is simply a larger update in LAI than in SSM by design, and this propagates in time differently due to the difference in memory for both variables (at this point in the paper, I am actually suspecting that LAI is assimilated with a bias, see comment above).]**

865 **Response to 3.14**

865 Agreed, “more sensitive” has been replaced by “relies more”. We also agree on the larger updates allowed when assimilating LAI, and it has been stressed out by adding the following paragraph to the discussions and conclusion section (see also response to 3.5)

870 P.23, Lines 749-754: “For SSM, the assimilation is done after a rescaling to the model climatology (see section 2.3), which removes bias. For LAI, however it is not the case and the assimilation process removes bias in the modelled LAI (w.r.t. the observation). This technical difference between SSM and LAI assimilation, combined with the longer memory of LAI compared to SSM, contributes to the results presented in this section.”

875 **3.15 [Could you evaluate the impact of LAI and SSM assimilation in terms of runoff for the high-resolution simulation?]**

880 **Response to 3.15**

880 Thank you for this suggestion, we have added a figure to show the impact of the assimilation (together with the impact of the initialisation on 4-day and 8-day forecasts) on drainage and runoff over the WEUR domain.

885 The following paragraph and figure have been added to the revised version of the manuscript (section 3.2.2 on Case studies for assessing LDAS-Monde high resolutions (0.1° x 0.1°) experiments, P.22; Lines 713-724): “Top panels of Figure 16 illustrate the impact of the analysis on drainage monitoring and forecast over WEUR. Fig. 16 a) represents drainage from LDAS\_HRES open-loop varying between 0 and 1 kg.m<sup>-2</sup>.day<sup>-1</sup>, as seen in Fig.16 b) (drainage difference between

890 LDAS\_HRES analysis and open-loop) the analysis impact is rather small, about  $\pm 3\%$  and more  
 pronounced in areas where the analysis has affected LAI more (see panels f), g) and h) of Figure  
 16). As seen on panels c) and d), there is also an impact from the initialisation in areas where the  
 analysis was more effectively correcting LAI. Bottom panels of Figure 16 illustrate similar impact  
 on runoff. As for drainage, this variable is affected by the analysis. Initial conditions have an impact  
 895 on its forecast, also. Although we did not present a quality assessment of those two variables, our  
 findings on river discharge analysis impact, but also those from Albergel et al., 2017, 2018a,  
 suggest a neutral to positive impact, propagated from the analysis of SSM and LAI to river  
 discharge through variables such as drainage and runoff.”

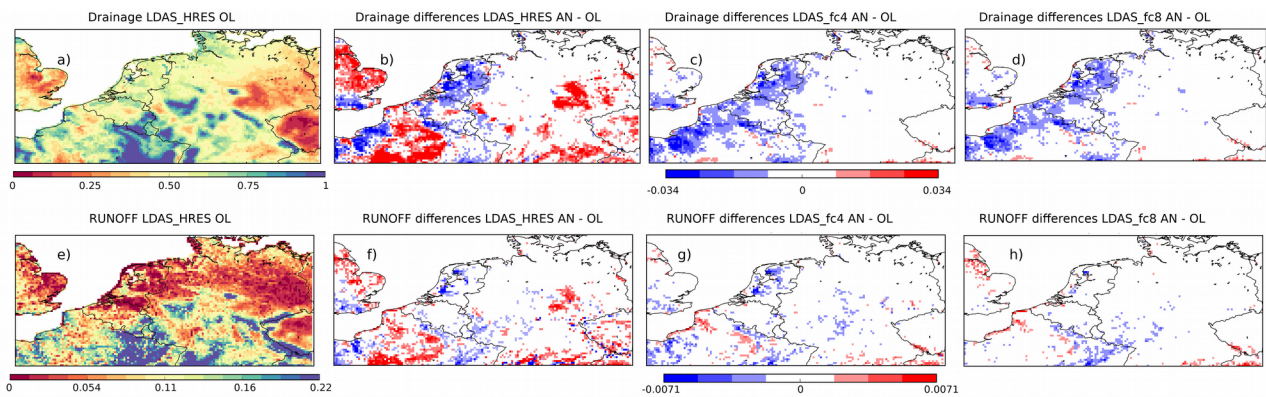


Figure 15: Top row, (a) drainage values for LDAS\_HRES open-loop over 2017-2018 for the WEUR domain, (b) drainage differences between LDAS\_HRES analysis and open-loop. (c), (d), same as (b) between LDAS\_fc4 initialised by the analysis and LDAS\_fc4 initialised by the open-loop, between LDAS\_fc8 initialised by the analysis and LDAS\_fc8 initialised by the open-loop. Bottom row, same as top row for runoff. Units are  $\text{kg.m}^{-2}.\text{day}^{-1}$

900 **References:**

Albergel, C., Munier, S., Leroux, D. J., Dewaele, H., Fairbairn, D., Barbu, A. L., Gelati, E., Dorigo, W., Faroux, S., Meurey, C., Le Moigne, P., Decharme, B., Mahfouf, J.-F., and Calvet, J.-C.: Sequential assimilation of satellite-derived vegetation and soil moisture products using SURFEX\_v8.0: LDAS-Monde assessment over the Euro-Mediterranean area, *Geosci. Model Dev.*, 10, 3889–3912, <https://doi.org/10.5194/gmd-10-3889-2017>, 2017.

905 Albergel, C.; Munier, S.; Bocher, A.; Bonan, B.; Zheng, Y.; Draper, C.; Leroux, D.J.; Calvet, J.-C. LDAS-Monde Sequential Assimilation of Satellite Derived Observations Applied to the Contiguous US: An ERA5 Driven Reanalysis of the Land Surface Variables. *Remote Sens.*, 10, 1627, 2018a

910 Response to Reviewer 4 are structured as follow: (1) 4.X: comments from Reviewer 4, (2)  
Response to 4.X: author's response and author's changes in manuscript when any. For sake of  
clarity, line and page numbering from the first submission is used.

915 **[...]I think the paper can be an important contribution and can eventually be suitable for  
publication in HESS, but at this point I recommend MAJOR revisions with consideration of  
the comments below. [...]**

920 Dear Reviewer#4 many thanks for reviewing the manuscript and for highlighting its relevance and  
interest. Your comments and suggestions led to an improved version of the manuscript. Below is a  
point by point answer to your specific comments, all your editorial and technical comments were  
accounted for in the revised version of the manuscript.

### **Major**

925 **4.1 [1] Six of the thirteen figures that show results (i.e., not counting "data & methods"  
figures 1 and 2) are about evaluating the skill of the assimilation estimates \*exclusively\*  
against the assimilated observations (Figs 3 and 9-13). Comparisons against the assimilated  
observations are also included in Figs 4-6 (along with other variables) and Figs 14-15 (along  
with forecast estimates of SSM and LAI). While I agree that it is important to verify that the  
assimilation system works as intended, the authors overemphasize the comparison against the  
930 assimilated observations.]**

### **Response to 4.1**

935 We agree with Reviewer #4, verifying that the assimilation system works as intended is an  
important task. Part of the figures mentioned are indeed dedicated entirely (Fig. 3) or partially (Figs.  
4-6) to that validation. The other aforementioned figures play a different role. Fig. 9 allows us to  
identify potential hotspots for droughts and heat waves. Figs. 10-11 study the behaviour of LDAS-  
ERA5 in the context of droughts for the WEUR (Western Europe) and the MUDA (Murray-Darling)  
areas. Figs. 12-15 focus on the capacity of our system to forecast the evolution of land surface  
940 variables depending on how it is initialized.

Comment 4.6 on using SSM and LAI as an independent source of information to evaluate the  
forecast has been further discussed and added in the revised version of the manuscript. While LAI  
remains an independent source of information (although constrained by the assimilation as  
explained in Rewiewer#4 4.6), ASCAT SWI has been rescaled to match the model climatology. The  
945 seasonal rescaling impacts both bias and correlation. In an attempt to have a more independent  
evaluation an additional figure has been put in the revised version of the manuscript. It presents  
maps of correlations, between soil moisture (1-4 cm) from the four experiments (LDAS-HRES  
open-loop, analysis, LDAS\_fc4 and LDAS\_fc8) and ASCAT SWI (i.e. ASCAT data prior rescaling)  
950 for the WEUR domain. Correlations are applied to both absolute values and to anomalies (to assess  
the short term variability of soil moisture).

### ***End of section 3.2.2***

955 ***P.22, Lines 703-724: "Similarly to Figures 13(a, b, c, d) panels of Figure 15 illustrates the impact of  
the analysis on SSM using correlations. This time, ASCAT SWI (i.e. no rescaling) has been used.  
Figure 15 (top panels) shows map of R values based on absolute values while Figure 15 (bottom  
panels) shows R values on anomalies (short term variability) as defined in Albergel et al. (2018a).  
Figure 15 (a) and (e) represents R values and anomaly R values for LDAS\_HRES, respectively. As  
expected R values are higher than anomaly R values. Maps of differences (panels b and f) of Figure***



960 15 suggest that after assimilation, both scores are improved rather equally. While the 4 day and 8-day forecast still show an improvement from the initial condition on R values (panels c and d of Figure 15 dominated by positive differences, analysis-open-loop), maps of anomaly R values forecast do not display any negative or positive impact (panels g and h of Figure 15).”

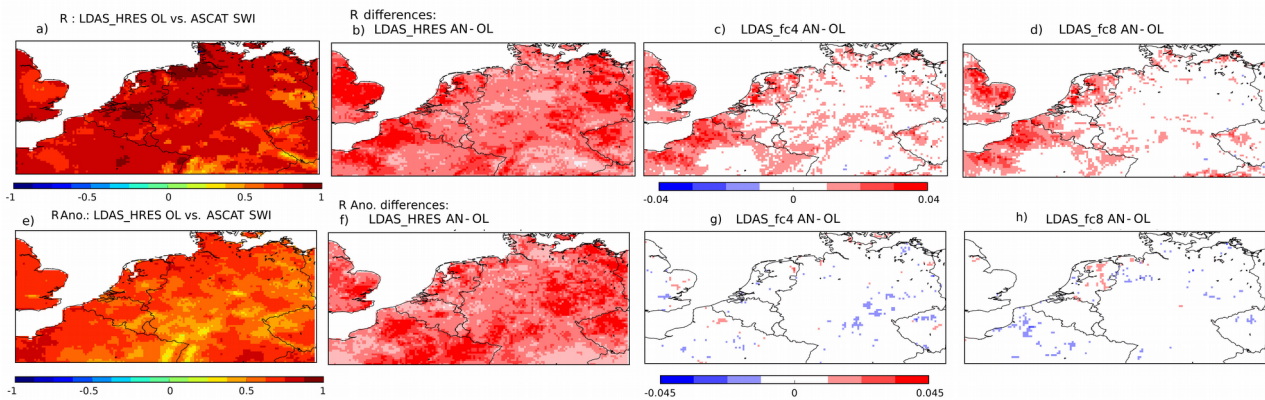


Figure 14: Top row, (a) R values between LDAS\_HRES open-loop and ASCAT SWI estimates from the Copernicus Global Land Service (CGLS) over 2017-2018 for the WEUR domain, (b) R differences between LDAS\_HRES analysis (open-loop) and ASCAT SWI. (c) and (d) same as (b) between LDAS\_fc4 initialised by the analysis (open-loop) and LDAS\_fc8. Bottom row, same as top row for R values based on anomaly time-series.

#### Discussion and conclusion sections

970 P.23, Lines 749-754: “For SSM, the assimilation is done after a rescaling to the model climatology (see section 2.3), which removes bias. For LAI, however, this is not the case and the assimilation process removes bias in the modelled LAI (w.r.t. the observation). This technical difference between SSM and LAI assimilation, combined with the longer memory of LAI compared to SSM, contributes to the results presented in this section”

975 **4.2 [2) The two figures about snow (Figs 7 & 8) could be simplified considerably because there is no meaningful difference between the assimilation estimates and the open-loop estimates, which is a rather trivial result (as the authors discuss).]**

#### Response to 4.2

980 Agreed, both figures have been moved to the supplementary document (Figures S1 and S2) and it has been further emphasized that there is no snow data assimilation yet. Those results are presented to highlight areas of improvements in LDAS-Monde:

985 P.15, Lines 487-492: “As expected, the analysis has an almost neutral impact on snow as both SSM and LAI observations are filtered out from frozen/snow condition and as there is no snow data assimilation in LDAS\_ERA5 (Figure S2 and panels (j), (k) and (l) of Figure S1). This clearly shows, however, an area of potential improvement of data assimilation within LDAS-Monde using satellite data such as the IMS one (as in e.g. de Rosnay et al., 2014).”

990 **4.3 [3) There are no graphics in the main text (only in the supplement) about the validation of the results against \*independent\* in situ measurements (section 3.1.2). This independent validation should be reflected more prominently in the main paper.]**

#### Response to 4.3

995 Most of the in situ evaluation datasets involved in this study are available over North America and  
(western) Europe and two regional-scale studies assessing LDAS-Monde analysis impact have  
already been published (Albergel et al., 2017 over Europe, Albergel et al., 2018a over North  
America). To avoid redundancy with these previous studies, we preferred not to put too much of  
those results in the main part of the study. However to better reflect the findings of this evaluation,  
1000 last paragraph of section 3.1.2 on ground based dataset has been modified and is now (P.18, L.583-  
587): “For evapotranspiration, river discharge and surface soil moisture it can be stated that there is  
a slight advantage from LDAS\_ERA5 analysis with respect to its open-loop counterpart. Even if the  
distribution of the averaged statistical metrics can be rather similar for both (particularly true for  
surface soil moisture evaluation), there are regional significant differences for some sites, which  
1005 shows the added value of the analysis with respect to the open-loop. Note that for fewer sites, a  
negative impact from the analysis can also be observed.”

Also, the whole evaluation against in situ measurements has been revisited and now includes such a  
figure, see response to comment 4.4.

1010 **4.4 [4] The claim about "improvement" of the assimilation estimates vs. the open-loop  
estimates from the independent validation against in situ soil moisture estimates in section  
3.1.2 (~line 460) is on shaky footing. For none of the networks listed in Table S3 is there a  
difference of more than 0.02 in the R values between the assimilation and the open loop. In  
1015 some cases, the 0.02 difference is negative (ie., degradation). For most networks the R  
difference is 0 or 0.01, that is, there really isn't a meaningful change. Here, and also for at  
least the other in-situ based results, it is imperative that the authors provide some estimates of  
whether the differences are meaningful (e.g., by including statistical confidence intervals), and  
then honestly discuss the results. The claim in line 460 about significant improvements at  
1020 some sites may be true, but given the network-average neutral results there must then also be  
sites with a significant degradation, which is not mentioned in the paper.]**

#### **Response to 4.4**

1025 Thank you for your highly relevant comment. Following it and similar comments from the other  
Reviewers, it has been decided to revisit the soil moisture evaluation part of the study:

(1) we have added an evaluation of soil moisture from LDAS-Monde fourth layer of soil (10 to 20  
cm) against in situ measurements of soil moisture at 20 cm depth when available (10 networks and  
685 stations),

1030 (2) for surface soil moisture (SSM), correlation values (R) were calculated for both absolute and  
anomaly time-series in order to remove the strong impact from the SSM seasonal cycle on this  
specific metric,

(3) a 95% Confidence Interval (CI) has been added to R values.

1035 (4) we have added the number of stations for which correlations differences are significant  
(significant improvement or degradation from the analysis) as well as a map over North America for  
illustration.

It involves several changes in the revised version of the manuscript, they are listed below.

1040 Methodology section, 2.5 Evaluation datasets and metrics

P.11, Lines 358-365: “In situ measurements of surface soil moisture from 19 networks across 14  
countries available from the ISMN are also used to evaluate the performance of the soil moisture  
analysis. They represent 782 stations with at least 2 years of daily data over 2010-2018. Sensors at 5

1045 cm depth (SSM) are compared with soil moisture from LDAS\_ERA5 third layer of soil (4-10 cm), sensors at 20 cm depth with the fourth layer of soil (10-20 cm, 685 stations from 10 networks). Beside 11 stations located in 4 countries of Western Africa (Benin, Mali, Sénégal and Niger) and 21 stations in Australia, most stations are located in North America and Europe, see Table S3.”

1050 P.12, Lines 374-377: “For global estimates, Normalized RMSD (NRMSD, Eq.(2)) was used, also. Finally, for surface soil moisture, R was calculated for both absolute and anomaly time-series in order to remove the strong impact from the SSM seasonal cycle on this specific metric (see e.g. Albergel et al., 2018a, 2018b).”

1055 Result section, 3..1.2 Ground-based datasets

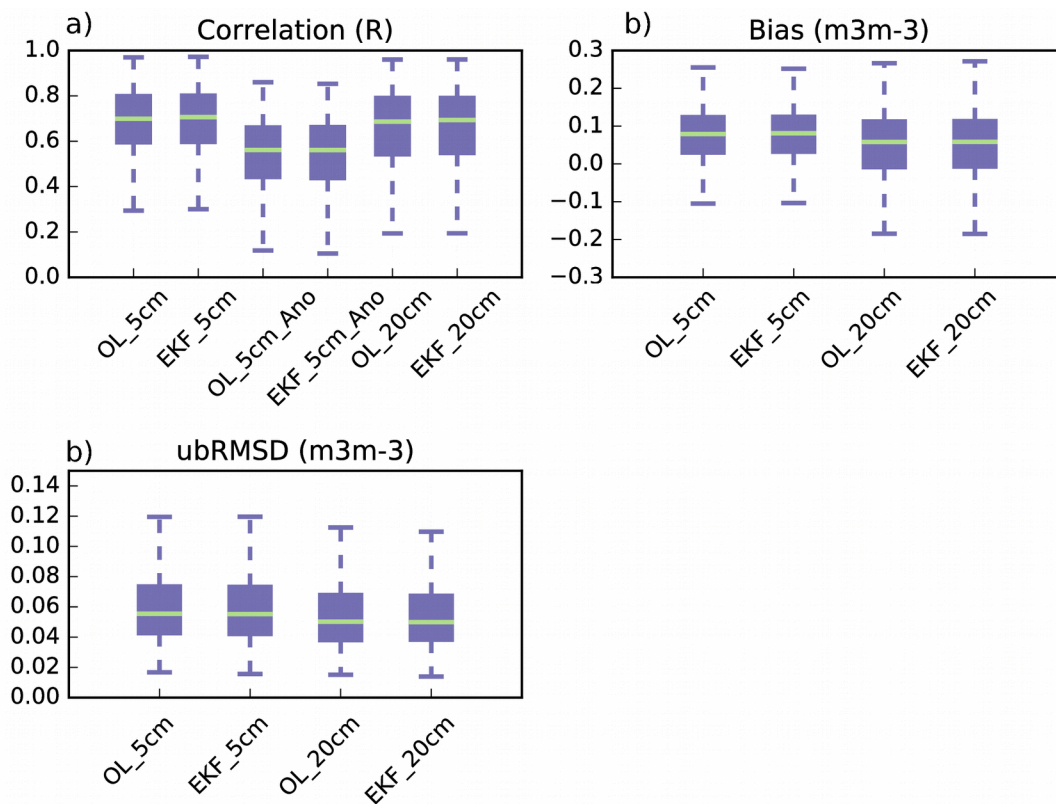
P.17-18, Lines 548-582: “The statistical scores for soil moisture from LDAS\_ERA5 open-loop and analysis (third and fourth layers of soil, 4-10 cm depth, 10-20 cm depth, respectively) over 2010-2018 when compared with ground measurements from the ISMN (5 cm depth and 20 cm depth) are presented in Table S2 for each individual network. Averaged statistical metrics (ubRMSD, R,  $R_{anomaly}$  and bias) are similar for both LDAS\_ERA5 analysis and open-loop even if local differences exist. For the analysis, averaged R ( $R_{anomaly}$ ) values along with its 95% Confidence Interval (CI) using in situ measurements at 5 cm (782 stations from 19 networks) are  $0.68 \pm 0.03$  ( $0.53 \pm 0.04$ ) ( $0.67 \pm 0.03$  ( $0.53 \pm 0.04$ ) for the open-loop) with averaged-network values going up to  $0.88 \pm 0.01$  ( $0.58 \pm 0.04$ ) for the analysis (SOILSCAPE network, 49 stations in the USA) and always higher than 0.55 except for one network, ARM (10 stations in the USA) presenting an averaged R value of  $0.29 \pm 0.05$ . Averaged ubRMSD and bias (LDAS\_ERA5 minus in situ) are  $0.060 \text{ m}^3\text{m}^{-3}$  and  $0.077 \text{ m}^3\text{m}^{-3}$  for the analysis,  $0.060 \text{ m}^3\text{m}^{-3}$  and  $0.076 \text{ m}^3\text{m}^{-3}$  for the open-loop, respectively. NIC (Eq.1) has also been applied to R values, 65% of the pool of stations present a neutral impact from the analysis (511 stations at NIC ranging between -3 and +3), 12% present a negative impact (91 stations at NIC < -3) and 23% present a positive impact at (180 stations at NIC > +3).

The number of stations where R differences between the analysis and the open-loop are significant (i.e. their 95% CI are not overlapping) is 186 out of 782 (about 26%). There is an improvement from the analysis w.r.t. the open-loop for 128 stations (out of 186, i.e. about 69%) and a degradation for 58 stations (about 31%). Figure 7 illustrates R differences between the analysis and the open-loop runs. When differences (analysis minus open-loop) are not significant stations are represented by a small dot. When they are significant, large circles have been used, blue for positive differences (an improvement from the analysis) and red for negative differences (a degradation from the analysis). For most of the stations where a significant difference is obtained, it represent an improvement from the analysis.

Averaged analysis R (95%CI), bias and ubRMSD for the fourth layer of soil (685 stations from 10 networks) are  $0.65 \pm 0.03$ ,  $0.049 \text{ m}^3\text{m}^{-3}$  and  $0.055 \text{ m}^3\text{m}^{-3}$ , respectively. For the open-loop, they are  $0.64 \pm 0.03$ ,  $0.048 \text{ m}^3\text{m}^{-3}$  and  $0.056 \text{ m}^3\text{m}^{-3}$ , respectively. For soil moisture at that depth, about 60% of the stations present a neutral impact from the analysis (410 stations at NIC ranging between -3 and +3), 28% a positive impact (189 stations at NIC > +3) and 12% a negative impact (86 stations at NIC < -3). Although differences between the open-loop run and the analysis are rather small, these results underline the added value of the analysis with respect to the model run. Figure S6 represents the distribution of the scores values for LDAS\_ERA5 open-loop and analysis using boxplots centred on the median value. They look very similar and from this figure, it is difficult to see either improvement or degradation from the analysis.”

1095

Figure 7: Map of correlations ( $R$ ) differences (analysis minus open-loop) for stations available over North America. Small dots represent stations where  $R$  differences are not significant (i.e. 95% confidence intervals are overlapping), large circles where differences are significant.



1100

Figure S6: a) Boxplots representing the distribution of the correlation values on absolute time-series and anomaly time-series (“Ano”) between the stations with in situ measurements of soil moisture either 5cm depth or 20 cm depth and soil moisture from LDAS\_ERA5 open-loop and analysis over 2010-2018 (third and fourth layer of soil, respectively). Correlation values are presented for surface soil moisture (5 cm depth measurements against third layer of soil), only. Distribution are centred on the median values. b) Distribution of the Bias values between the stations with in situ measurements of soil moisture either 5cm depth or 20 cm depth and soil moisture from LDAS\_ERA5 open-loop and analysis over 2010-2018 (third and fourth layer of soil, respectively). c) Same as b) for ubRMSD.

1105

1110

The following text has been added to the revised version of the manuscript: “Figure S6 represents the distribution of the scores values for LDAS\_ERA5 open-loop and analysis using boxplots centred on the median value. They look very similar and from this figure, it is difficult to see either improvement or degradation from the analysis.”

**4.5 [5] The editing of the paper is rather careless. There are many small mistakes, and the organization of the text is lacking.]**

1115

The 4 Reviewers have provided many editorial comments, corrected several mistakes. Thanks to their work we have an improved version of the manuscript.

1120 **4.5a [a] The Introduction lacks a clear statement of the paper’s objectives. The text in Lines 107-121 simply states what will be presented (with lots of references and details). It’s hard to tell what the objectives might be.]**

**Response to 4.5a**

1125 *Agreed. In order to make the paper’s objectives clearer, the following paragraph in the introduction has been revisited:*

1130 *“In this study, stemming from previous works referenced above, this global, offline, joint integration of Surface Soil Moisture (SSM) and Leaf Area Index (LAI) EOs into the ISBA (Interaction between Soil Biosphere and Atmosphere) LSM (Noilhan and Planton, 1989, Noilhan and Mahfouf, 1996) are presented: [...]”*

*is now (P.4, Lines 108-114):*

1135 *“In this study, stemming from previous works referenced above, it is shown that LDAS-Monde global, offline, joint integration of Surface Soil Moisture (SSM) and Leaf Area Index (LAI) EOs into the ISBA (Interaction between Soil Biosphere and Atmosphere) LSM (Noilhan and Planton, 1989, Noilhan and Mahfouf, 1996) can be used to detect, monitor and forecast the impact on extreme events on LSVs. Are presented in this study: [...]”*

1140 **4.5b [b] There are several instances in the Results section of text that belongs in the Methods section, incl: Lines 384-387 - IMS snow cover product description Lines 405-409 -Fluxnet description Lines 440-447 - ISMN description]**

**Response to 4.5b**

1145 *Agreed. When appropriate, those instances were moved to the section dedicated to methodology (description of IMS data; ISMN and FLUXNET-2015 networks, river discharge).*

**Response to 4.5c [c] Section 3.2.2 is a \*single\* paragraph that stretches over nearly two pages. Really? There are several other paragraphs of excessive length.]**

1150 **Response to 4.5c**

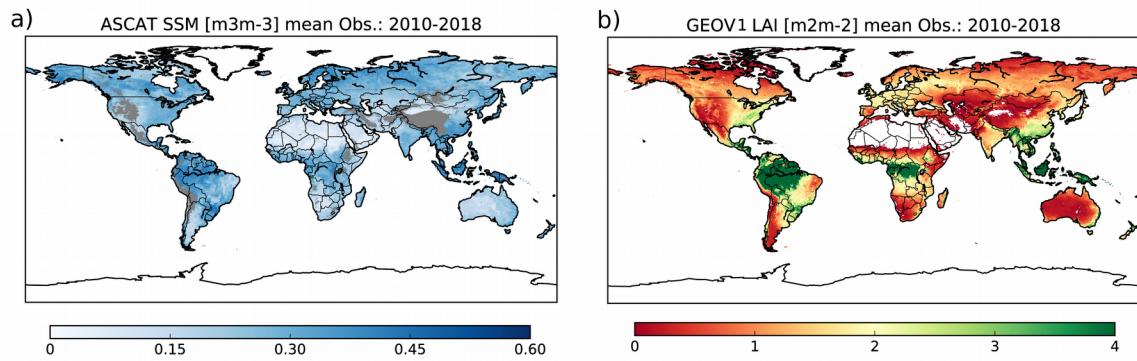
*Section 3.2.2 has now been reshuffled with one paragraph per group of 2 figures.*

1155 **d) Graphics:**

**4.5d\_f1 [Figure 1a: Use different color for zero values and no-data value. (currently, both are white, making it unclear whether there are data in, e.g., the western US, or whether those are screened, perhaps because of topography.)]**

1160 **Response to 4.5d\_f1**

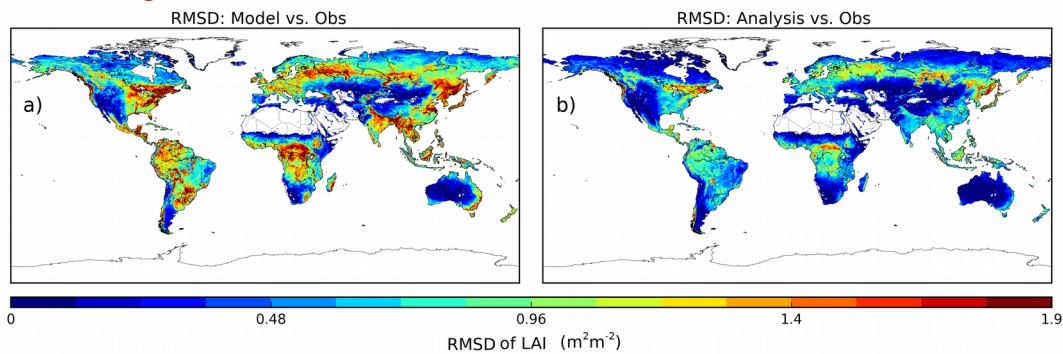
*Agreed, see new figure below.*



1165 4.5d\_f2 [Figure 3: The label of the colorbar should read "RMSD of LAI [m2 m-2]", not just "LAI [m2 m-2]"]

**Response to 4.5f\_f2**

Agreed, see new figure below



1170 4.5d\_f5 [Figure 5: Units are missing for RMSD panels. (This is particularly important because this information is needed to judge whether the differences are in fact meaningful.)]

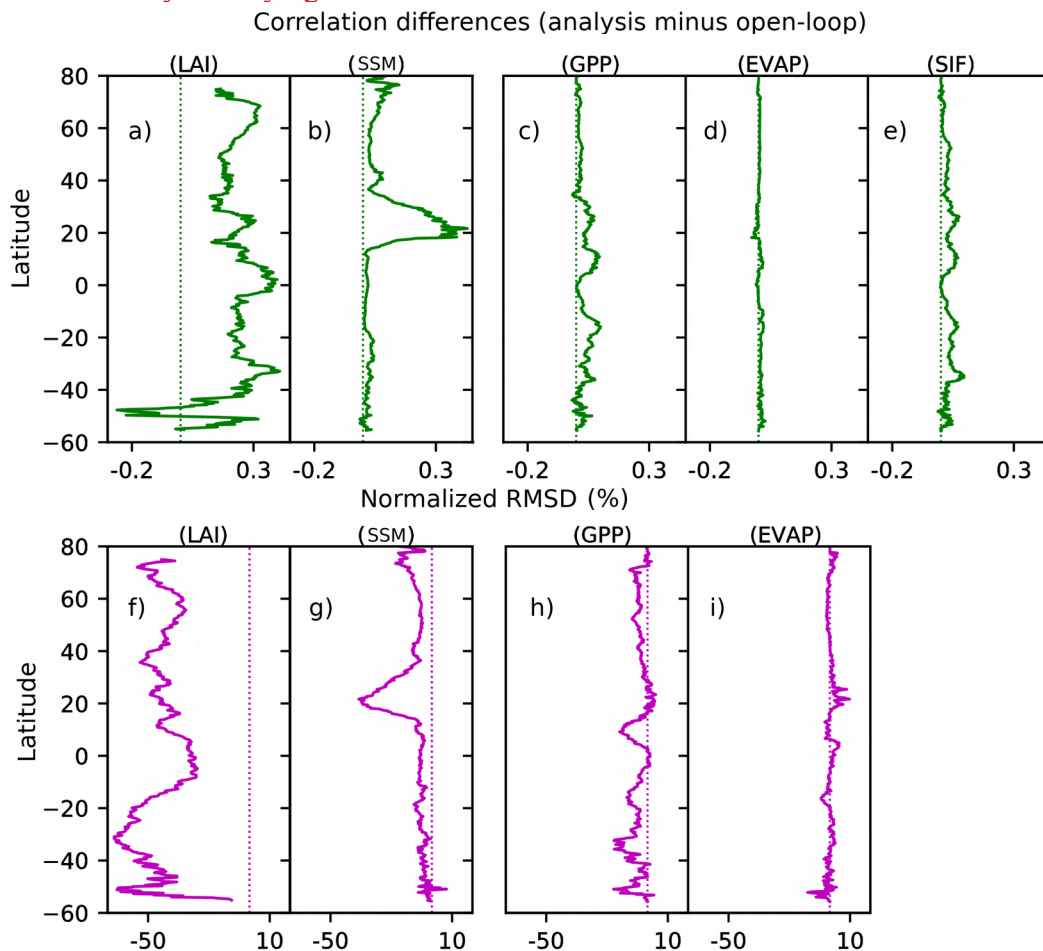
**Response to 4.5d\_f5**

1175 Thank you for this suggestion, for RMSD panels it has been decided to use normalized RMSD (% of improvement and/or degradation) so one can really see the impact on each evaluated variable, it also echoes Reviewer 4's comment 4.7 on analysis impact on GPP. Using similar x-axis limits provides a better information at a glance. For instance it minimizes the previous visual impact of the analysis on GPP, and as such addressing your comment 4.7. Also panels of new Figure 5 separate the assimilated and independent variables, see new figure below.  
1180

1185 Also, in section 3.1.1 on gridded dataset:the following sentence "For SSM a noticeable improvement in both correlation and RMSD is found around 20°N corresponding mainly to an improvement in the Sahara desert (not shown). GPP is also improved across almost all latitude with a particularly positive impact below 20°N which is also true for EVAP. This variable is less impacted by the analysis and some parts of the world show a decrease in e.g. RMSD values." is now (P.14, Lines 436-441):

1190

“For SSM a noticeable improvement in both correlation and RMSD is found around 20°N corresponding mainly to an improvement in the Sahara desert (not shown). Being linked to LAI, GPP is also improved across almost all latitudes (to a lesser extent than LAI) with a particularly positive impact below 20°N. As seen on Figure 5 d) and i), there is little impact on variable EVAP which can be considered negligible. It highlights the difficulty of land surface data assimilation to impact model fluxes by modifying model states.”



1195

**4.5d\_f6 [Figure 6: Three panels only have a single tick & tick label on the y-axis. At least two are required to interpret the axis scale.]**

**Response to 4.5d\_f6**

1200

Agreed, it has been added in the revised version of the manuscript.

**4.5d\_f7 [Figure 7: The color choices should be made consistent with Fig 4.]**

1205

**Response to 4.5d\_f7**

Agreed, Figure 7 is now in the supplementary.

**4.5d\_f9 [Figure 9: I could not find out what the thin cyan lines depict.]**

1210

**Response to 4.5d\_f9**

1215 The following sentence has been added to the caption of the considered figure's caption: "Solid red line, dashed red line and solid green line represent regions MUDA, WEUR and EAFR. Solid cyan lines represent all other boxes (see Table 1 and Figure 2)."

**4.5d\_f10+11 [Figures 10+11: add "LAI" to plot title of c) and d); add "SSM" to plot title of g) and h)]**

1220 **Response to 4.5d\_f10+11**

Agreed, it has been added in the revised version of the manuscript.

1225 **4.5d\_fs2 [Figure S2: NSE should vary from -infinity to 1. The colorbar is from -20 to 20, and darker blue values would clearly be greater than 1. Either the colorbar is wrong or the values show something other than NSE.]**

**Response to 4.5d\_fs2**

1230 Thanks for spotting this issue resulting from a wrong call in a python script, it has been corrected in the revised version of the manuscript.

**4.5d\_ts3 [Table S3: The column headings on the 2nd page of the table still include French words.]**

1235

**Response to 4.5d\_ts3**

Corrected, thanks for spotting this issue.

1240 **4.6 [6] In section 3.2.2, the authors no longer make it clear that the verification is against the assimilated datasets. While verification of forecast data against the assimilated dataset can be viewed as independent validation because the verification data have not (yet) been assimilated, there is an important distinction here between SSM and LAI. For SSM, the assimilation is done after rescaling (cdf-matching), which removes bias. For LAI, however, the assimilation uses the raw LAI observations (I think). That is, the assimilation removes bias in the modeled LAI (w.r.t. the observed LAI). This technical difference between SSM and LAI assimilation, combined with the longer memory of LAI compared to SSM, should contribute to the results in section 3.1.2. Put differently, the LAI results of section 3.1.2 are not likely to hold if an independent LAI dataset had been used for validation that is itself biased against the assimilated LAI observations. (Different LAI datasets may not be as biased against each other as typical satellite SSM datasets, but there are considerable biases between LAI products.)]**

1245

1250

**Response to 4.6**

1255

Verifying that the assimilation system works as intended is an important task. This is why several figures have been included for "sanity check". We have emphasized in the manuscript that several presented evaluations are carried out to check if the assimilation system is working properly.

1260 Also, using SSM and LAI as an independent source of information to evaluate the forecast has been further discussed and added in the revised version of the manuscript. While LAI remains an



independent source of information for the forecast evaluation (although constrained by the assimilation), ASCAT SWI has been rescaled to match the model climatology. The seasonal rescaling impacts both bias and correlation. In an attempt to have a more independent evaluation, an additional figure has been put in the revised version of the manuscript. It displays maps of correlations between modelled soil moisture (1-4 cm) from the four experiments (LDAS-HRES open-loop, analysis, LDAS\_fc4 and LDAS\_fc8) and ASCAT SWI (i.e. ASCAT data prior rescaling) for the WEUR domain. Correlations are applied to both absolute values and to anomalies (to assess the short term variability of soil moisture).

1270

**End of section 3.2.2**

P.22, Lines 703-724: “Similarly to Figures 13(a, b, c, d), panels of Figure 15 illustrate the impact of the analysis on SSM using correlations., To that end, ASCAT SWI (i.e. no rescaling) has been used. Figure 14 (top panels) shows map of R values based on absolute values while Figure 14 (bottom panels) shows R values on anomalies (short term variability) as defined in Albergel et al., 2018a. Figure 15 (a) and (e) represents R values and anomaly R values for LDAS\_HRES, respectively. As expected R values are higher than anomaly R values. Maps of differences (panels b and f) of Figure 15 suggest that after assimilation, both scores are improved rather equally. While the 4 day and 8-day forecast still show an improvement from the initial condition on R values (panels c and d of Figure 15 dominated by positive differences, analysis minus open-loop), maps of anomaly R values forecast don’t show any negative or positive impact (panels g and h of Figure 15).”

1280

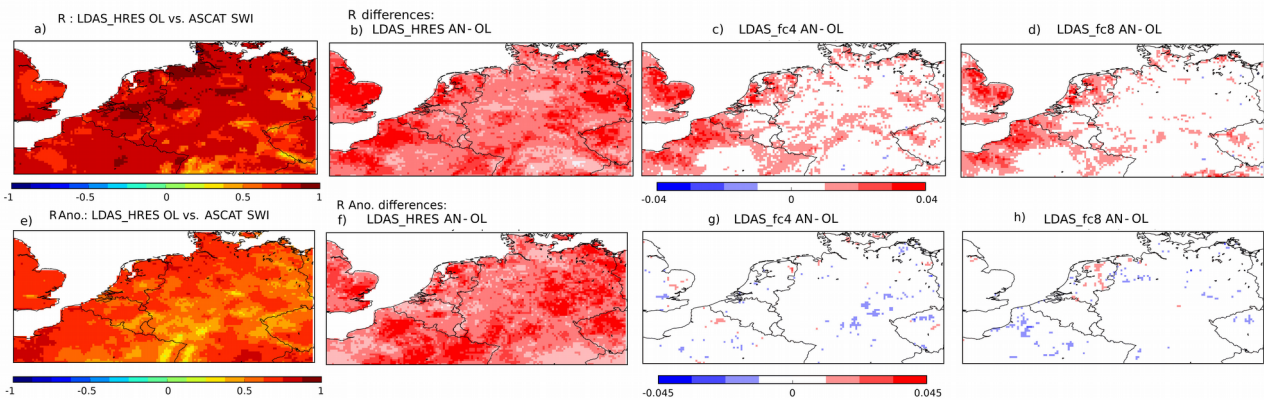


Figure 15: Top row, (a) R values between LDAS\_HRES open-loop and ASCAT SWI estimates from the Copernicus Global Land Service (CGLS) over 2017-2018 for the WEUR domain, (b) R differences between LDAS\_HRES analysis (open-loop) and ASCAT SWI. (c) and (d) same as (b) between LDAS\_fc4 initialised by the analysis (open-loop) and LDAS\_fc8. Bottom row, same as top row for R values based on anomaly time-series.

1285 Discussion and conclusion sections

P.23, Lines 749-754: “For SSM, the assimilation is done after a rescaling to the model climatology (see section 2.3), which removes bias. For LAI, however it is not the case and the assimilation process removes bias in the modelled LAI (w.r.t. to the observation). This technical difference between SSM and LAI assimilation, combined with the longer memory of LAI compared to SSM, contributes to the results presented in this section”

1290

**4.7 [7] Figure 3c suggests that the change in GPP is negligible, at least in the zonal mean sense although Figure 4f suggests that GPP does change in terms of RMSD. Given the considerable change in the (zonal mean) LAI (Fig 3a), I would have expected a lot more change in the mean GPP. I suspect that the disconnect between the LAI and GPP changes is rooted in how these**

1295

**variables are connected in ISBA and how exactly the assimilation system goes about updating LAI. This rather counter-intuitive result requires clarification in the paper.]**

**Response to 4.7**

1300

We believe that Figure 5 was rather confusing and that the new Figure proposed (see Response 4.5d\_f5, also) permits to clarify this point. In section 2.1.1 on ISBA land surface model, the following sentence is now “In the CO<sub>2</sub>-responsive versions of ISBA, photosynthesis is in control of the evolution of vegetation variables.” is now (P.5, Lines 157-160) “In the CO<sub>2</sub>-responsive versions of ISBA, ISBA-A-gs, the model can simulate the CO<sub>2</sub> net assimilation and GPP by considering the functional relationship between the photosynthesis rate (A) and the stomatal aperture (gs) based on the biochemical A-gs model proposed by Jacob et al. (1996). Photosynthesis is in control of the evolution of vegetation variables.”

1305

References:

1310

Jacobs, C.M.J.; van den Hurk, B.J.J.M.; de Bruin, H.A.R. Stomatal behaviour and photosynthetic rate of unstressed grapevines in semi-arid conditions. *Agric. For. Meteorol.* 80, 111–134, 1996.

**4.8 [8] Fig 5h: The changes in EVAP are with +/- 0.02 (mm/d???) . If my guess about the units is correct, this would amount to only a few mm per year, which is well within the uncertainty of in situ measurements. That is, the EVAP changes are not likely to be meaningful in a practical sense. This should be discussed more explicitly.]**

1315

**Response to 4.8**

1320

Agreed, the new figure 5 also helps to clarify that the impact on variable EVAP is rather negligible. See also Responses to 4.5d\_f5, 4.13

**Minor**

1325

**4.9 [9] Line 167: typo "bale" -> "able"]**

**Response to 4.9**

Typo corrected in the revised version of the manuscript, thanks.

**4.10 [10] Line 209: "fifth generation of European reanalyses produced by ECMWF" I recommend phrasing this differently to avoid the misunderstanding that the reanalyses are just for the European domain. E.g.,: "fifth generation of global reanalyses produced by ECWMF"]**

1330

**Response to 4.10**

1335

Rephrased in the revised version of the manuscript, thanks.

**4.11 [11] Lines 293-295: How did you address the heterogeneity within the 0.25-deg grid cells during spin-up? It is not obvious that the short spin-up period from April 2016 suffices for properly spinning up grid cells with strong heterogeneity at the sub-0.25-degree scale.]**

1340

**Response to 4.11**

The global LDAS-ERA5 runs were spun-up by running 20 times the first year (2010). For LDAS\_HRES, nine months can be perceived as a too short period to spin up the system. Unfortunately, HRES atmospheric forcing is only available from April 2016 and the LDAS-HRES

1345

1350 experiment ends in December 2018. We have considered this 9 months period for the spin up in order to have the longest possible time series for land surface variables, thus giving more strength to statistics. We could have considered a longer period for spin up (April 2016 to December 2017) and studied only 2018. This gives very similar results on surface soil moisture and LAI (not shown). While not being fully spun-up, results obtained with LDAS-HRES can be considered as representative of the system response to data assimilation. Note that most initial values of the LDAS-HRES run are taken from the ECOCLIMAP-II database. For instance, initial LAI is set from a 1999-2005 MODIS climatology.

1355 Another possibility to initialise LDAS-HRES could have been to downscale the state of LDAS-ERA5 run in April 2016 to 0.10°x0.10° spatial resolution. LDAS-ERA5 runs have been set to an equilibrium spinning up 20 times the first year (2010).

1360 The following sentence: “The period 2017-2018 is presented, HRES is available at this spatial resolution from April 2016, only, and the time period from April to December 2016 is used as a short spinup.” has been modified and is now (P.10, Lines 327-332): “HRES is available at a 0.1° x 0.1° resolution only from April 2016. April to December 2016 is used as a short period for spinup and results are presented for the period 2017-2018. Although a 9-month spinup period can be seen as rather short, evaluating LDAS-HRES on either 2017-2018 or 2018 (using instead a 21-month spinup) leads to similar results on surface soil moisture and LAI (not shown). While the system is not fully spun-up, it can be considered as representative of the system response to data assimilation.”

1370 **4.12 [12] Line 379: Do you mean a decrease in RMSD or a decrease in skill?]**

**Response to 4.12**

This sentence has been revised and “[...] shows a degradation” is now “[...] shows a decrease in skill”

1375 **13) Line 412: If I’m reading this correctly RMSD decreases while both bias and ubRMSD increase. This is quite counter-intuitive and requires a rather odd distribution of the metrics across the sites or networks included in the average. In any case, since bias and ubRMSD get worse, I do not think that the statement about "a small advantage of the analysis over the open-loop" is justified.**

1380

**Response to 4.13**

Agreed, the considered sentence has been reformulated and is now: “If these numbers depict a small advantage of the analysis over the open-loop configuration, it is worth mentioning that differences are rather small and likely to fall within the uncertainty of the in situ measurements.”

1385

**14) Line 429: "NSE values below -2 were discarded" requires a justification, otherwise it reads like cherry-picking.**

**Response to 4.14**

1390 Agreed, this threshold has also been used for previous studies at CNRM as we did not want to look at river discharges we do not represent well. The pool of stations we have used are monitoring all types of rivers and streams including those where human impacts (dams and reservoirs, irrigation, water uptake, not represented in ISBA yet) is affecting the natural flow of rivers. As we expect the impact of the analysis on river discharge to be small (based on previous work), we did not find  
1395 necessary to include stations we badly represent in ISBA, possibly for known reasons. Futur work

will focus on preparing a more robust in situ pool of station, separating e.g. managed and unmanaged rivers and stream.

1400 The following paragraph has been added to the methodology section (P.12-13, Lines 394-399):  
1405 “Stations with NSE values lesser than -2 were discarded. A similar threshold has already been used in previous studies evaluating LDAS-Monde (e.g. Albergel et al., 2017, 2018a). Many processes, most of them linked to water management such as the presence of dams and reservoirs, irrigation, water uptake in urban areas, are not yet represented in ISBA leading to a poor representation of river discharges. As previous evaluations studies have suggested a neutral to positive impact from the assimilation, only, it has been decided to focus on stations with reasonable NSE values.”

**4.15 [15] Line 535: "the analysis is of better quality" Given the numbers, I see at best "slightly better quality"]**

1410 **Response to 4.15**

Emphasized in the revised version of the manuscript, “Note however that for the MUDA area, a 4-d forecast of surface soil moisture initialised by the analysis is of better quality than a 4-d forecast initialised by the open-loop” is now (P.21, Lines 664-666): “Note, however, that, for the MUDA area, there is a small positive impact of the initialisation on the 4-d and 8-d forecast of surface soil moisture (blue areas on Figure 13 c) and d)).”

1415

**4.16 [4.16 [16] Line 592: "surface (0-1 cm)" In section 3.2.2 the discussion was about the "(1-4cm)" layer. Which is it?]**

1420 **Response to 4.16**

Thanks, it should read 1-4cm, it is now corrected in the revised version of the manuscript

## Data assimilation for continuous global assessment of severe conditions over

### 1425 terrestrial surfaces

Clément Albergel<sup>1</sup>, Yongjun Zheng<sup>1</sup>, Bertrand Bonan<sup>1</sup>, Emanuel Dutra<sup>2</sup>, Nemesio Rodríguez-Fernández<sup>3</sup>, Simon Munier<sup>1</sup>, Clara Draper<sup>4</sup>, Patricia de Rosnay<sup>5</sup>, Joaquin Muñoz-Sabater<sup>5</sup>, Gianpaolo Balsamo<sup>5</sup>, David Fairbairn<sup>5</sup>, Catherine Meurey<sup>1</sup>, Jean-Christophe Calvet<sup>1</sup>

<sup>1</sup> CNRM, Université de Toulouse, Météo-France, CNRS, Toulouse, France

1430 <sup>2</sup> Instituto Dom Luiz, IDL, Faculty of Sciences, University of Lisbon, Portugal

<sup>3</sup> CESBIO, Université de Toulouse, CNRS, CNES, IRD, Toulouse, France

<sup>4</sup> CIRES/NOAA Earth System Research Laboratory, Boulder, CO, USA

<sup>5</sup> European Centre for Medium-Range Weather Forecasts, Shinfield Road, Reading RG2 9AX, UK

\* Correspondence: [clement.albergel@meteo.fr](mailto:clement.albergel@meteo.fr)

1435

**Abstract-**This study demonstrates that LDAS-Monde, a global and offline Land Data Assimilation System (LDAS), that integrates satellite Earth ~~Q~~observations into the ISBA (Interaction between Soil Biosphere and Atmosphere) Land Surface Model (LSM), is able to detect, monitor and forecast the impact of extreme weather on land surface states. LDAS-Monde jointly assimilates satellite derived Earth observations of surface soil moisture (SSM) and Leaf Area Index (LAI). It is run at global scale forced by ~~ERA5 (LDAS\_ERA5)~~, the latest atmospheric reanalysis from the European Centre for Medium Range Weather Forecast (ECMWF), [ERA5 \(ECMWF fifth global Re Analysis, LDAS\\_ERA5 hereafter\)](#) over 2010-2018 leading to a 9-yr,  $\sim 0.25^\circ \times 0.25^\circ$  spatial resolution reanalysis of Land Surface Variables (LSVs). This reanalysis is then used to compute anomalies of land surface states, in order to (i) detect regions exposed to extreme weather such as droughts and heatwave events and (ii) address specific monitoring and forecasting requirements of LSVs for those regions. In this study, LDAS\_ERA5 analysis is first ~~successfully~~ evaluated worldwide using several satellite-based datasets (SSM, LAI, ~~e~~Evapotranspiration, Gross Primary Production and Sun Induced Fluorescence), as well as in situ measurements (SSM, evapotranspiration and river discharge). The added value of assimilating the soil moisture and LAI is demonstrated with respect to a model simulation (open-loop, with no assimilation). Since the global LDAS\_ERA5 has relatively coarse resolution, two higher spatial resolution experiments over two areas particularly affected by heatwaves and/or droughts in 2018 were run: North Western Europe and the Murray-Darling basin in South Eastern Australia. These experiments were forced with ECMWF Integrated Forecasting System (IFS) high resolution operational analysis (LDAS\_HRES,  $\sim 0.10^\circ \times 0.10^\circ$  spatial resolution) over 2017-2018, and both open-loop and analysis experiments compared once again. Since the IFS is a forecast system, it also allows LDAS-Monde to be used in forecast mode,

1455

and we demonstrate the added value of initializing 4- and 8-day LDAS-HRES forecasts of the LSVs, from the LDAS-HRES assimilation run, compared to the open-loop experiments. This is particularly true for LAI that evolves on longer time space than SSM and is more sensitive to initial conditions than to atmospheric forcing, even at an 8-day lead time. This confirms that slowly evolving land initial conditions are paramount for forecasting LSVs and that LDAS-systems should jointly analyse both soil moisture and vegetation states. Finally evaluation of the modelled snowpack is presented and the perspectives for snow data assimilation in LDAS-Monde are discussed.

## 1 Introduction

Extreme weather and climate events like heatwaves and droughts are likely to increase in frequency and/or magnitude (IPCC, 2012, Ionita et al., 2017). Amongst all the natural disasters, droughts are the most detrimental (Bruce, 1994; Obasi, 1994; Cook et al., 2007; Mishra and Singh, 2010; WMO 2017) and about one-fifth of damages caused by natural hazards can be attributed to droughts (Wilhite 2000). They also cost society billions of dollars every year (WMO 2017). It is therefore of paramount importance to implement tools that can monitor and warn about drought conditions (Svoboda, 2002; Luo and Wood, 2007; Blyverket et al., 2019) as well as their impact on land surface variables (LSVs) and society (Di Napoli et al., 2019). A major scientific challenge in relation to the adaptation to climate change is to observe and simulate how land biophysical variables respond to those extreme events (IPCC, 2012).

Droughts can be described as a deficit of water caused by a lack of precipitation. ~~The concept of drought is broad and they are generally~~ However its concept is broader and they are generally classified according to which part of the hydrological cycle suffers from a water deficit (IPCC, 2014; Barella-Ortiz and Quintana-Seguí, 2018). Drought types are all related to precipitation deficit and ~~they have severe impacts in regions with rain-fed crops and no irrigation~~ most severe in areas of ~~rain-fed crops agriculture with no irrigation~~. They include meteorological droughts (lack of precipitation), agricultural droughts (deficit of water in the soil), hydrological droughts (deficit of streamflow, water level in rivers) and environmental droughts (a combination of the previous droughts types). Because of the effect of precipitation deficit propagating through the whole hydrological system, it can be stated that all drought types are related (Wilhite, 2000). Complex interactions between continental surface and atmospheric processes have to be combined with human action in order to representfully understand the wide ranging impacts of droughts on land surface conditions (Van Loon, 2015). As a consequence, Land Surface Models (LSMs) driven by high-quality gridded atmospheric variables and coupled to river-routing system are key tools to

address these challenges (Dirmeyer et al., 2006; Schellekens et al., 2017). Initially developed to provide boundary conditions to atmospheric models, the role of LSMs has evolved and they can now be used to monitor and forecast land surface conditions (Balsamo et al., 2015; Balsamo et al., 2018; Schellekens et al., 2017). Additionally, the representation of LSVs by LSMs can be improved through the integration of Earth Observations (EOs) (e.g. Reichle et al., 2007; Lahoz and de Lannoy, 2014; Kumar et al., 2018; Albergel et al., 2017, 2018a, 2019; Balsamo et al., 2018) as well as by coupling them with other models of the Earth system like atmosphere, oceans, river routing systems (e.g., de Rosnay et al., 2013, 2014; Kumar et al., 2018, Balsamo et al., 2018; Rodríguez-Fernández et al., 2019; Muñoz-Sabater et al., 2019). Satellite products are particularly relevant for such application. Satellite EOs related to the terrestrial hydrological, vegetation and energy cycles are now unrestrictedly available at a global scale with high spatial resolution (at kilometric scale and below) and with long-term records (e.g., Lettenmaier et al., 2015, Balsamo et al., 2018). Combining EOs and LSMs through Land Data Assimilation Systems (LDASs) could leads to enhanced initial land surface conditions which, in turn, lead to improved forecasts of weather patterns, sub-seasonal temperature and precipitation, agricultural and vegetation productivity, seasonal streamflow, floods and droughts, as well as the carbon cycle (Banzai and Shukla, 1999; Schlosser and Dirmeyer, 2001; Bierkens, M. and van Beek, 2009; Koster et al., 2010; Bauer et al., 2015; Massari et al., 2018; Albergel et al., 2018a, 2019, Rodríguez-Fernández et al., 2019; Muñoz-Sabater et al., 2019). Amongst the current land-only LDAS activities ~~are~~ several are NASA-led (National Aeronautics and Space Administration) projects. Examples of such activities are the Global Land Data Assimilation System (GLDAS, Rodell et al., 2004) which is run at a global scale. While the~~Amongst them are the Global Land Data Assimilation System (GLDAS, Rodell et al., 2004) run at global scale.~~ The North American Land Data Assimilation System (NLDAS, Xia et al., 2012a, b) and the National Climate Assessment-Land Data Assimilation System (NCA-LDAS, Kumar et al., 2016, 2018, 2019) are run over the continental United States of America and the Famine Early Warning Systems Network (FEWS NET) Land Data Assimilation System (FLDAS, McNally et al., 2017) is run e.g. over Western, Eastern and Southern Africa. Finally, the Carbon Cycle Data Assimilation System (CCDAS, Kaminski et al., 2002), the Coupled Land Vegetation LDAS (CLVLDAS, Sawada and Koike, 2014, Sawada et al., 2015), the Data Assimilation System for Land Surface Models using CLM4.5 proposed by Fox et al., 2018, the SMAP (Soil Moisture Active Passive) level 4 system (Reichle et al., 2019) as well as LDAS-Monde (Albergel et al., 2017, 2018, 2019) developed by the research department of Météo-France are additional initiatives of combining EOs and LSMs through data assimilation. Few studies have, however, ~~have~~ included the assimilation of multiple EOs and considered global applications (Kumar et al., 2018, Albergel et al.,

1525 2019). A more detailed description of the various existing LDASs is available in Kumar et al., 2018, Albergel et al., 2019 and references therein.

After several applications at regional and continental scales (Albergel et al., 2017, 2018, 2019, Leroux et al., 2018, Tall et al., 2019, Blyverket et al., 2019, Bonan et al., 2019), LDAS-Monde was run at global scale forced by the latest atmospheric reanalysis from the European Centre for  
1530 Medium Range Weather Forecast (ECMWF), ERA5, over 2010-2018 leading to a 9-yr, 0.25° x 0.25° spatial resolution reanalysis of the LSVs (LDAS\_ERA5). In this study, stemming from previous works referenced above, it is shown that this LDAS-Monde global, offline, joint integration of Surface Soil Moisture (SSM) and Leaf Area Index (LAI) EOs into the ISBA (Interaction between Soil Biosphere and Atmosphere) LSM (Noilhan and Planton, 1989, Noilhan and Mahfouf, 1996)  
1535 can be used to detect, monitor and forecast the impact of extreme events on LSVs. are presented in this study:

- An evaluation at global scale using diverse and complementary datasets such as evapotranspiration from the GLEAM project (Miralles et al., 2011, Martens et al., 2017), Gross Primary Production (GPP) from the FLUXCOM project (Tramontana et al., 2016, Jung et al.,  
1540 2017), Solar Induced Fluorescence (SIF) from the GOME-2 (Global Ozone Monitoring Experiment-2) scanning spectrometer (Munro et al., 2006, Joiner et al., 2016) and snow cover data from the Interactive Multi-sensor Snow and Ice Mapping System (or IMS, <https://www.natice.noaa.gov/ims/>, last accessed June 2019). It is also validated using reference observations including in situ evapotranspiration from the FLUXNET 2015 synthesis data set  
1545 (<http://fluxnet.fluxdata.org/>, last accessed June 2019), soil moisture from the International Soil Moisture Network (ISMN, <https://ismn.geo.tuwien.ac.at/en/>, last accessed June 2019) as well as river discharge from several networks across the world.

- An estimation of the mean LSVs climate over 2010-2018, used as reference for computing anomalies of the land surface conditions to (i) detect regions severely-exposed to extreme weather  
1550 such as drought and heatwave events in 2018 and (ii) trigger more detailed monitoring and forecasting activities of the LSVs for those regions at higher spatial resolution.

The paper is organised in four sections as it follows: section 2 details the various components constituting LDAS-Monde: the ISBA LSM, the data assimilation scheme and the EOs assimilated as well as the different atmospheric forcing datasets used, followed by the experimental and  
1555 evaluation setup. Section 3 describes and discusses the impact of the analysis on the representation of the LSVs. The selection of 2 case studies over regions particularly affected by extreme events during 2018 and their detailed monitoring at higher spatial resolution combined with land surface



forecasting activities is also presented. Finally section 4 provides conclusions and prospects [for future work](#).

## 1560 2 Material and methods

The following subsections briefly describe the main components of LDAS-Monde: the ISBA LSM, its data assimilation scheme and two other key elements of the setup: atmospheric forcing and assimilated satellite derived observations. The experimental setup and the evaluation datasets used in this study are also presented.

### 1565 2.1 LDAS-Monde

#### 2.1.1 ISBA Land Surface Model

Embedded within the SURFEX (SURFace EXternalisée, Masson et al., 2013, version 8.1) modelling platform developed by the research department of Météo-France (CNRM, Centre National de Recherches Météorologiques), LDAS-Monde (Albergel et al., 2017) allows the joint  
1570 integration of satellite derived SSM and LAI into the CO<sub>2</sub>-responsive (Calvet, et al., 1998, 2004, Gibelin et al., 2006), multilayer diffusion scheme (Boone et al., 2000, Decharme et al., 2011) version of the ISBA LSM (Noilhan and Planton, 1989, Noilhan and Mahfouf, 1996) using a simplified version of an Extended Kalman Filter (SEKF, e.g. Mahfouf et al., 2009, Barbu et al., 2011, Fairbairn et al., 2017). It can be coupled to the ISBA-CTRIP hydrological model (ISBA-  
1575 CTRIP for ISBA-CNRM, Total Runoff Integrating Pathways) as detailed in Decharme et al., (2019). In such a configuration, ISBA is able to represent the transfer of water and heat through the soil based on a multilayer diffusion scheme, as well as plant growth and leaf-scale physiological processes. ISBA models key vegetation variables like LAI and above ground biomass, the diurnal cycle of water, carbon and energy fluxes. It computes a soil-vegetation composite using a single-  
1580 source energy budget. [In the CO<sub>2</sub>-responsive versions of ISBA, ISBA-A-gs, the model can simulate the CO<sub>2</sub> net assimilation and GPP by considering the functional relationship between the photosynthesis rate \(A\) and the stomatal aperture \(gs\) based on the biochemical A-gs model proposed by Jacob et al., 1996.](#) ~~In the CO<sub>2</sub>-responsive versions of ISBA,~~ photosynthesis is in control of the evolution of vegetation variables. It makes vegetation growth possible as a result of  
1585 an uptake of CO<sub>2</sub>. Oppositely, a deficit of photosynthesis triggers higher mortality rates. Ecosystem respiration (RECO) is represented by the CO<sub>2</sub> being released by the soil-plant system and GPP by the carbon uptake related to photosynthesis. Finally, the net ecosystem exchange (NEE) consists of the difference between GPP and RECO. Each ISBA grid cell can be composed of up to 12 generic land surface types, bare soil, rocks, and permanent snow and ice surfaces as well as nine plant

1590 functional types (needle leaf trees, evergreen broadleaf trees, deciduous broadleaf trees, C3 crops, C4 crops, C4 irrigated crops, herbaceous, tropical herbaceous and wetlands). The ECOCLIMAP-II land cover database (Faroux et al., 2013) provides ISBA parameters for all of them.

ISBA multilayer diffusion scheme's default discretization is 14 layers over 12 m depth. The following configuration is used in this study: thickness (depth) of each layers are (from top to  
1595 ~~downbottom~~), 1 cm (0-1 cm), 3 cm (1-4 cm), 6 cm (4-10 cm), 10 cm (10-20 cm), 20 cm (20-40 cm), 20 cm (40-60 cm), 20 cm (60-80 cm), 20 cm (80-100 cm), 50 cm (100-150cm), 50 cm (150-200cm), 100 cm (200-300 cm), 200 cm (300-500 cm), 300 cm (500-800 cm) and 400 cm (800 to 1200 cm), see also Figure 1 of Decharme et al., 2011. Snow is represented using the ISBA 12-layers explicit snow scheme (Boone and Etchevers, 2001, Decharme et al., 2016).

#### 1600 2.1.2 CTRIP river routing system

The ISBA-TRIP river routing system is ~~able~~ to simulate continental scale hydrological variables based on a set of three prognostic equations. They correspond to (i) the groundwater, (ii) the surface stream water and (iii) the seasonal floodplains. It converts the runoff simulated by ISBA into river discharge. ISBA-CTRIP river-routing network has a spatial resolution of 0.5° x 0.5°  
1605 globally and is coupled daily with ISBA through the OASIS3-LCT coupler (Voldoire et al., 2017). ISBA provides to CTRIP updated fields of runoff, drainage, groundwater and floodplain recharges. In turn, CTRIP provides ISBA with water table depth, floodplain fraction as well as flood potential infiltration so that ISBA can simulate capillarity rise, evaporation and infiltration over flooded areas. A comprehensive overview of ISBA-CTRIP is available in Decharme et al., (2019).

#### 1610 2.1.3 Data assimilation

The SEKF used in LDAS-Monde is a 2-step sequential approach in which a forecast step is followed by an analysis step. The forecast step propagates the initial state of the model (being a short term forecast from the ISBA LSM) and then, the analysis step corrects this forecast by assimilating observations. ~~Flow dependency between the model control variables and the observations are generated using finite differences from perturbed simulations~~  
1615 ~~The flow-dependency (dynamic link) between the prognostic variables and the observations is ensured in the SEKF through the observation operator Jacobians, which propagate information from the observations to the analysis via finite-difference computations (de Rosnay et al., 2013).~~ The analysis involves the computation of a Jacobian matrix having as many rows as assimilated observation types (here two:  
1620 SSM and LAI) and as many columns as model control variables requested (here eight ~~soil layer: soil moisture from the second to the eight layers of soil~~, 1-100cm, and LAI). ~~In A~~ Additionally to a control run, computing the Jacobian matrix requires perturbed runs, one for each control variable. ~~The eight control variables are directly updated using their sensitivity to observed variables (i.e.~~

1625 defined by the Jacobians). Other variables are indirectly modified through biophysical processes  
and feedbacks from the model-. Several studies (e.g. Draper et al., 2009; Rüdiger et al., 2010) have  
demonstrated that small perturbations lead to a good approximation of this linear behaviour,  
provided that computational round-off error is not significant. Typically, for those runs, the initial  
state of the control variable is perturbed by about 0.1% (see Albergel et al., 2017; Rüdiger et al.,  
2010). The length of the LDAS-Monde assimilation window is 24-hours. A mean volumetric  
1630 standard deviation error is specified proportional to the soil moisture range (the difference between  
the volumetric field capacity and the wilting point, calculated as a function of the soil type, as given  
by Noilhan et Mahfouf, 1996) and scaled by a factor 0.04 for SSM in its model equivalent (the  
second layer of soil between 1 and 4 cm), scaled with and 0.02 for deeper layers (~~layers of soil~~ layer  
3 to 8, 4-100cm). The observational SSM error follows the same rule scaled by 0.05 and is  
1635 consistent with errors typically expected for remotely sensed SSM (e.g., de Jeu et al., 2008, Gruber  
et al, 2016). Soil moisture errors for both the model and the observations are assumed to be  
proportional to the soil moisture range (being defined as the difference between the volumetric field  
capacity and the wilting point, calculated as a function of the soil type, as given by Noilhan et  
Mahfouf, 1996). ~~The standard deviation of errors for the observed LAI is assumed to be 20% and a~~  
~~similar assumption is made for the standard deviation of errors of the modelled LAI values higher~~  
1640 ~~than  $2 \text{ m}^2\text{m}^{-2}$ . For modelled LAI values lower than  $2 \text{ m}^2\text{m}^{-2}$ , a constant error of  $0.4 \text{ m}^2\text{m}^{-2}$  is~~  
~~assumed (Barbu et al., 2011). More details can be found in Albergel et al, 2017 or Tall et al.,~~  
~~2019.~~ Based on previous results from Jarlan et al., 2008, Rüdiger et al., 2010, Barbu et al., 2011,  
observed and modelled LAI standard deviation errors are set to 20 % of the LAI value itself for  
1645 values higher than  $2 \text{ m}^2\text{m}^{-2}$ . For LAI values lower than  $2 \text{ m}^2\text{m}^{-2}$ , a fixed value of  $0.04 \text{ m}^2\text{m}^{-2}$  has  
been used. More detailed can be found in Barbu et al., 2011 (section 2.3 on data assimilation  
scheme and figure 2).

## 2.2 Atmospheric forcing

The lowest model level (about 10-meters above ground level) of air temperature, wind speed,  
1650 specific humidity and pressure and the downwelling fluxes of shortwave, ~~and~~ longwave radiations  
as well as precipitations (partitioned in solid and liquid phases) are needed to force LDAS-Monde.  
In this study, LDAS-Monde is driven by several near-surface meteorological fields from ECMWF,  
its most recent atmospheric reanalysis (ERA5), ~~as well as or~~ its high resolution operational weather  
analysis and forecasts (HRES). ERA5 (Hersbach et al., 2018, 2019 submitted) is the ~~fifth generation~~  
1655 ~~of European reanalyses produced by the ECMWF~~ fifth generation of global reanalyses produced by  
ECWME. This atmospheric reanalysis is a key element of the Copernicus Climate Change Service

(C3S, ~~EU-funded~~) and is available from 1979 onward (data is released about 2 months behind real time). ERA5 has hourly output analysis, 31 km horizontal dimension and 137 levels in the vertical dimension resolution. Several studies have validated the ERA5 datasets, for example ~~Although being quite new, ERA5 quality has already been evaluated in the scientific literature~~. Urraca et al. (2018) have compared incoming solar radiation from both ERA5 and the ~~former~~ ERA-interim reanalysis (Dee et al., 2011) at a global scale and found evidence that ERA5 outperforms ERA-Interim. In another study, Beck et al. (2019) have highlighted the good performance of ERA5 precipitation with respect to a set of 26 gridded (sub-daily) precipitation data sources by comparing them to Stage-IV gauge-radar data over the CONUS domain (CONTinental United States of America). Tall et al. (2019) have used in situ measurements of precipitation at more than 100 stations spanning all over Burkina-Faso in western Africa as well as incoming solar radiation from 4 in situ stations to evaluate the quality of ERA5 over ERA-Interim also with positive outcomes for ERA5 as well. They have also evaluated both reanalysis datasets through their impact on the representation of LSVs when used to force the ISBA LSM, again demonstrating a clear advantage for ERA5. Similar work has been done by Albergel et al. (2018a), over North America, ~~they~~ this study found enhanced performances in the representation of evaporation, snow depth, soil moisture as well as river discharge when the ISBA\_-LSM was forced by ERA5 compared to ERA-Interim. At the time of the study, ERA5 underlying model and data assimilation system (Cycle 41r2) are very similar to that of the operational weather forecast, HRES, which has production cycles ranging from 41r2 to 45r1 during the study period (it is 46r1 from June 2019, more information at <https://www.ecmwf.int/en/forecasts/documentation-and-support/changes-ecmwf-model>, last accessed July 2019). The main difference between ERA5 and HRES over the considered period is the horizontal resolution, 9 km in HRES and 31 km in ERA5. ~~The a~~ Atmospheric forcing is interpolated from the native grids of ERA5 and HRES to regular grids of  $0.25^\circ \times 0.25^\circ$  and  $0.1^\circ \times 0.1^\circ$ , respectively, using a bilinear interpolation from the native ~~reanalysis~~ grid to the regular grid. The four neighbouring cells in the source grid fitting latitude and longitude were linearly interpolated. ERA5 and HRES were used in Albergel et al. (2019) to force LDAS-Monde in order to study the impact of the 2018 summer heatwave in Europe. Authors have highlighted that the HRES configuration exhibits better monitoring skills than the coarser resolution ERA5 configuration. From the forecast initialized at 00:00 UTC, HRES is also available with a 10-day lead time, but with changes in the temporal resolution. HRES forecast step frequency is hourly up to time step 90 (i.e. day 3), 3-hourly from time-step 90 to 144 (i.e. day 6) and 6-hourly from time-step 144 to 240 (i.e. day 10). In this study, for forecast experiments (see section 2.4 for details on the experimental setup) HRES forecasts with a 10-day lead time are used to initialize forecasts of the LSVs from

LDAS\_HRES open-loop and analysis configurations in order to evaluate the impact of the initialisation on the forecast of LSVs. The original 3-hourly time steps are used up to day 6 (time step 144), the 6-hourly time steps from day 6 to 10 are interpolated to 3-hourly frequency to avoid discontinuities.

### 1695 2.3 Assimilated satellite Earth Observations

Two types of satellite derived variables are assimilated in LDAS-Monde, ASCAT Soil Wetness Index (SWI) and LAI GEOV1. They are both freely available through the Copernicus Global Land Service (CGLS, <https://land.copernicus.eu/global/index.html>, last accessed June 2019). They are illustrated by Figure 1.

1700 ASCAT stands for Advanced Scatterometer, it is an active C-band microwave sensor that is onboard the European MetOp polar orbiting satellites (METOP-A, from 2006, B from 2012 and also C from 2018). From ASCAT radar backscatter coefficients, it is possible to derive information on SSM following a change detection approach (Wagner et al., 1999, Bartalis et al., 2007). The recursive form of an exponential filter (Albergel et al., 2008), is then applied to estimate the Soil Wetness Index (SWI) using a timescale parameter, T (varying between 1 day and 100 days) and ranging between 0 (dry) and 100 (wet). T is a surrogate parameter for all the processes potentially affecting the temporal dynamics of soil moisture (like, soil hydraulic properties and thickness of the soil layer, evaporation, run-off and vertical gradient of soil properties such as texture and density). In this study, CGLS SWI-001 (i.e. produced with a T-value of 1 day) is used as a proxy of SSM (Kidd et al., 2013). Grid points with an average altitude exceeding 1500 m above sea level as well as those with more than 15 % of urban land cover were rejected as those conditions are known to affect the retrieval of SSM. Prior to the assimilation, SSM has to be converted from the observation space to the model space. ~~This is done through a linear rescaling as proposed by Scipal et al. (2007), where the observations mean and variance are matched to the modelled soil moisture mean and variance from the second layer of soil (1-4 cm depth). This rescaling known as Cumulative Distribution Function (CDF) matching is run at seasonal scale using a 3-month moving window as suggested by Draper et al., (2011), Barbu et al., (2014)~~ This is done through a linear rescaling as proposed by Scipal et al. (2007), where the mean and variance of observations are matched to the mean and variance of the modelled soil moisture from the second layer of soil (1-4 cm depth). This rescaling gives in practice very similar results to CDF (cumulative distribution function) matching. The linear rescaling is performed on a seasonal basis (with a 3-month moving window) as suggested by Draper et al., (2011), Barbu et al., (2014). As in Albergel et al., 2018a, 2018b, pixels whose average

altitude exceeds 1500 m above sea level as well as pixels with urban land cover fractions larger than 15% were discarded as those conditions may affect the retrieval of soil moisture from space.

1725 The LAI GEOV1 observations are based on data from from both SPOT-VGT and then PROBA-V  
satellites. They span from 1999 to present, have a 1km x 1km spatial resolution and are produced  
daily according to the methodology developed by Baret et al. (2013). As in previous studies (e.g,  
Barbu et al., 2014, Albergel et al., 2019), observations are interpolated by an arithmetic average to  
1730 the model grid points ( $0.25^\circ$  or  $0.10^\circ$  in this study), if at least 50 % of the model grid points are  
observed (i.e. half the maximum amount). LAI GEOV1 observations have a temporal frequency of  
10 days at best (in the presence of clouds, no observation are available). LAI data are masked in the  
presence of snow from the open-loop experiment.

## 2.4 Experimental setup

LDAS-Monde is first run at a global scale, at  $0.25^\circ \times 0.25^\circ$  spatial resolution, forced by ERA5  
1735 atmospheric reanalysis and assimilating SSM and LAI EOs from 2010 to 2018 (LDAS\_ERA5  
hereafter). LDAS-ERA5 was spun-up by running year 2010 twenty times. LDAS\_ERA5 analysis as  
well as its model counterpart (open-loop, i.e. no data assimilation) are presented and evaluated in  
this study.

~~This 9-yr global reanalysis was then used to provide a climatology for estimating anomalies of the  
1740 land surface conditions. This 9-yr global reanalysis was then used to provide a monthly climatology  
for estimating anomalies of the land surface conditions. For each month (and variable considered)  
of 2018 we have removed the monthly mean and scaled by the monthly standard deviation of the  
2010-2018 period.~~ Significant anomalies were used to trigger more detailed monitoring as well as  
forecasting activities for a region of interest. 19 regions across the globe known for being potential  
1745 hot spots for droughts and heat waves were selected. They are listed in Table I and presented in  
Figure 2. Monthly anomalies of LDAS\_ERA5 analysis of SSM and LAI for those 19 regions are  
assessed for 2018 (with respect to the 2010-2018 period) and regions presenting significant level of  
anomalies were selected and further investigated. For those regionthem, LDAS-Monde has been  
driven by HRES atmospheric analysis leading to a  $0.1^\circ \times 0.1^\circ$  reanalysis of the LSVs from April  
1750 2016 to December 2018 (LDAS\_HRES herafter). HRES is available at a  $0.1^\circ \times 0.1^\circ$  resolution only  
from April 2016. April to December 2016 is used as a short period for spinup and results are  
presented for the period 2017-2018. Although a 9-month spinup period can be seen as rather short,  
evaluating LDAS-HRES on either 2017-2018 or 2018 (using instead a 21-month spinup) leads to  
similar results on surface soil moisture and LAI (not shown). While the system is not fully spun-up,  
1755 it can be considered as representative of the system response to data assimilation. ~~The period 2017-~~

2018 is presented, HRES is available at this spatial resolution from April 2016, only, and the time period from April to December 2016 is used as a short spinup. LDAS\_HRES complements the coarser spatial resolution LDAS\_ERA5. HRES forecasts with a 10 day lead time are also used, and initialised by either LDAS\_HRES open-loop or analysis (LDAS\_Fc hereafter) in order to assess the impact of the initialisation on the forecast. A summary of the experimental setup is given in Table II.

## 2.5 Evaluation datasets and metrics

This study uses several satellite-derived estimates of EOs as well as in situ measurement data. LDAS\_ERA5 analysis impact is assessed with respect to the open-loop model run (i.e. no assimilation). The two assimilated datasets, CGLS SSM and LAI, were used to verify to which extent the assimilation system was able to ~~produce analyses closer~~ correctly integrate to them (i.e. suggesting a healthy behaviour from the data assimilation system). Then several independent spatially distributed datasets independent from both experiments: (namely) evapotranspiration from the GLEAM project (Miralles et al., 2011, Martens et al., 2017, version 3b entirely satellite driven), Gross Primary Production (GPP) from the FLUXCOM project (Tramontana et al., 2016, Jung et al., 2017), Sun Induced Fluorescence (SIF) from the GOME-2 (Global Ozone Monitoring Experiment-2) scanning spectrometer (Munro et al., 2006, Joiner et al., 2016) and snow cover data from the Interactive Multi-sensor Snow and Ice Mapping System (or IMS, <https://www.natice.noaa.gov/ims/>) were used in the evaluation process. The IMS snow cover product combines ground observations and satellite data from microwave and visible sensors (using geostationary and polar orbiting satellites) to provide snow cover information in all weather conditions. The IMS product is available daily for the northern hemisphere.

~~along with several river discharge observations (see Table S1) and evapotranspiration from FLUXNET-2015 synthesis data set (<http://fluxnet.fluxdata.org/data/fluxnet2015-dataset/>, last access: June 2019).~~ also, Ground-based measurements of soil moisture from the International Soil Moisture Network (ISMN, Dorigo et al., 2011, 2015) were used. In situ measurements of surface soil moisture from 19 networks across 14 countries available from the ISMN are also used to evaluate the performance of the soil moisture analysis. They represent 782 stations with at least 2 years of daily data over 2010-2018. Sensors at 5 cm depth (SSM) are compared with soil moisture from LDAS\_ERA5 third layer of soil (4-10 cm), sensors a 20 cm with the forth layer of soil (10-20 cm, 685 stations from 10 networks). Beside 11 stations located in 4 countries of Western Africa (Benin, Mali, Sénégal and Niger) and 21 stations in Australia, most of the station are located in North America and Europe, see Table S3.

1790 Most of these ground stations for all types of in situ observations are located in Europe and North America and they were already have been used in previous studies (e.g. Albergel et al., 2017, 2018a,b, Leroux et al., 20189) to assess the LDAS-Monde quality. Therefore, the LDAS-Monde evaluation using ground measurements is discussed in the result section while figures are reported as supplementary materials of this study. Evaluation datasets are listed in Table III along with the metrics used (correlation, Root Mean Square Differences -RMSD- and unbiased RMSD -ubRMSD- and bias). For in situ datasets, a Normalized Information Contribution (NIC, Eq.(1)) measure is applied to the correlation values to quantify the improvement or degradation due to the specific configuration. For global estimates, Normalized RMSD ( $N_{RMSD}$ , Eq.(2)) was used, also. Finally, for surface soil moisture, R was calculated for both absolute and anomaly time-series in order to remove the strong impact from the SSM seasonal cycle on this specific metric (see e.g. Albergel et al., 2018a, 2018b).

$$NIC_R = \frac{R_{[Analysis]} - R_{[Model]}}{1 - R_{[Model]}} \times 100 \quad \text{Eq.(1)}$$

$$N_{RMSD} = \frac{RMSD_{[Analysis]} - RMSD_{[Model]}}{RMSD_{[Model]}} \times 100 \quad \text{Eq.(2)}$$

1805 NIC scores were classified according to three categories: (i) negative impact from the analysis with respect to the open-loop with values smaller than -3 %, (ii) positive impact from the analysis with respect to the open-loop with values greater than +3 % and (iii) neutral impact from the analysis with respect to the open-loop with values between -3 % and 3 %.

The Nash-Sutcliffe Efficiency score (NSE, Eq.(32), Nash and Sutcliffe, 1970) is used to evaluate LDAS\_ERA5 experiments ability to represent the monthly discharge dynamics.

$$NSE = 1 - \frac{\sum_{mt=1}^T (Q_s^{mt} - Q_o^{mt})^2}{\sum_{mt=1}^t (Q_s^{mt} - \overline{Q_s^{mt}})^2} \quad \text{Eq.(32)}$$

1810 where  $Q_s^{mt}$  is the monthly river discharge from LDAS\_ERA5 (analysis or open-loop) at month  $mt$ , and  $Q_o^{mt}$  is the observed river discharge at month  $mt$ . NSE can vary between  $-\infty$  and 1. An exact match between model predictions and observed data is defined as a value of 1, whereas a value of 0 means that the model predictions have the same accuracy as the mean of the observed data. Finally negative values represent when the observed mean is a better predictor than the model simulation.

1815 NIC presented in Eq.(1) has also been applied to NSE scores to assess the added value of LDAS\_ERA5 analysis over its open-loop counterpart. Stations with NSE values lesser that -2 were discarded. Similar threshold has already been used in previous studies evaluating LDAS-Monde



1820 (e.g. Albergel et al., 2017, 2018a). Many processes, most of them linked to water management such as the presence of dams and reservoirs, irrigation, water uptake in urban areas, are not yet represented in ISBA leading to a poor representation of river discharges. As previous evaluations studies have suggested a neutral to positive impact from the assimilation, only, it has been decided to focus on stations with reasonable NSE values.

1825 As for SIF, in ISBA the fluorescence is not simulated directly, however photosynthesis activity is simulated through the calculation of the GPP, which is driven by plant growth and mortality in the model. Modelled GPP values are expressed in  $\text{g(C)} \cdot \text{m}^{-2} \cdot \text{day}^{-1}$ , while SIF is an energy flux emitted by the vegetation ( $\text{mW} \cdot \text{m}^{-2} \cdot \text{sr}^{-1} \cdot \text{nm}^{-1}$ ). Hence, GPP and SIF cannot be directly compared as they do not represent the same physical quantities. However, several studies (e.g. Zhang et al., 2016, Sun et al., 2017, Leroux et al., 2018) have found that their time dynamics investigated, highlighting the potential of SIF products to be used as a validation support for GPP models.

## 1830 3 Results

### 3.1 Global assessment of LDAS\_ERA5

#### 3.1.1 Gridded datasets

Figure 3 presents mean RMSD values between the observations and LDAS\_ERA5 for the open-loop (Figure 3a), and for the analysis (Figure 3b) for LAI over 2010-2018. Because LAI observations are ingested into the model, the assimilation reduces the LAI RMSD values almost everywhere. It can be noted that rather large LAI RMSD values ( $> 1.5 \text{ m}^2\text{m}^{-2}$ ) can remain in some areas after the assimilation, especially in densely forested areas. Figure 4 illustrates latitudinal plots of LAI, SSM, GPP and evapotranspiration for LDAS\_ERA5 before assimilation (the open-loop) and after assimilation (the analysis) along with observations. The number of points considered per latitudinal stripes of  $0.25^\circ$  is represented, also. From Figure 4a it is possible to appreciate the positive impact of the analysis compared to the open-loop, with the former being closer to the observations. Improvement from the analysis occurs from nearly  $80^\circ\text{North}$  to about  $55^\circ\text{South}$ , areas around the equator are particularly improved. A smaller impact than for LAI is obtained for SSM, GPP and EVAP, hardly visible at this scale. The mean latitudinal results show a consistent difference in terms of GPP and Evapotranspiration between the LDAS\_ERA5 and the observational products. These differences are systematic with higher values in tropical regions. Figure 5 represents latitudinal plots of score differences (correlations and normalized RMSD) for LAI, SSM, GPP, EVAP and SIF (Figure 5i, correlation only). Score differences are computed as follow, analysis minus open-loop using monthly averages over 2010-2018 for LAI and SSM, 2010-2013

1850 for GPP, 2010-2016 for EVAP and 2010-2015 for SIF. For SIF only differences in correlation are represented as it is used to evaluate GPP variability as in Leroux et al., 2018. For each panel of Figure 5, the vertical dashed line represents the 0-value. Therefore, for plots of correlation differences, positive values indicate an improvement from the analysis with respect to the open-loop simulation. Similarly, for plots of RMSD differences negative values indicate an improvement from the analysis with respect to the open-loop simulation. LAI and SSM being assimilated variables, the analysis leads to a clear improvement in both correlation and RMSD. Such improvement is expected and reflects the healthy behaviour of the assimilation system. Both variables are improved at almost all latitudes with the exception around 45°S for LAI correlation values (very few land points). For SSM a noticeable improvement in both correlation and RMSD is found around 20°N corresponding mainly to an improvement in the Sahara desert (not shown). Being linked to LAI, GPP is also improved across almost all latitudes (to a lesser extend than LAI) with a particularly positive impact below 20°N. As seen on Figure 5 d) and i), there is little impact on variable EVAP which can be considered negligible. It highlights the difficulty of land surface data assimilation to impact model fluxes by modifying model states.

1860 ~~For SSM a noticeable improvement in both correlation and RMSD is found around 20°N corresponding mainly to an improvement in the Sahara desert (not shown). GPP is also improved across almost all latitude with a particularly positive impact below 20°N which is also true for EVAP. This variable is less impacted by the analysis and some parts of the world show a decrease in e.g. RMSD values.~~ Panels of Figure 6 illustrate histograms of score differences (correlation and RMSD, analysis minus open-loop) for LAI, SSM, GPP, EVAP and SIF. The Number of available data as well as the percentage of positive and negative values are reported. For correlations ( $N_{RMSD}$ ) differences, positive (negative) values indicate an improvement from the analysis over the open-loop. It complements Figure 5. Regarding LAI the analysis improves 96.9% of the grid points for correlations and 99.9% for  $N_{RMSD}$ . As for SSM, correlation values are improved for 92.8% of the grid points, it is 92.4% for  $R_{MSD}$ . When using independent datasets such as GPP and SIF, one may also notice an improvement from the analysis, correlation ( $N_{RMSD}$ ) are better for 81.1% (74.1%), 79.7% (SIF  $N_{RMSD}$  N/A) of the grid points. Results using the GLEAM dataset for evapotranspiration are more contrasted with 63.6% (48.9%) of the grid points showing an improvement from the analysis and it is worth mentioning that 24.9% (39.6%) of the grid point shows a ~~degradation~~decrease in skill. However GLEAM only estimates (root-zone) soil moisture and terrestrial evaporation, while ISBA in LDAS\_ERA5 is a physically-based land surface model, accounting for more processes linked to vegetation

1870 However GLEAM is an evaporation model designed to be driven by remote sensing observations only. GLEAM only estimates (root-zone) soil moisture and terrestrial evaporation while the CO2-

1880

1885 responsive version of ISBA in LDAS\_ERA5 is a physically-based land surface model, accounting  
for more processes linked to vegetation (see section 2.1.1). It has to be noted that the auxiliary  
dataset used to e.g. represent the different land cover types are different also. Within GLEAM, the  
land cover types fractions are sourced from the Global Vegetation Continuous Fields product  
(MOD44B), based on observations from the Moderate Resolution Image Spectroradiometer  
(MODIS). Four land cover types are considered, bare soil, low vegetation (e.g. grass), tall  
1890 vegetation (e.g. trees), and openwater (e.g. lakes). In ISBA the 12 land cover types fraction depart  
from prevalent land cover products such as CLC2000 (Corine Land Cover) and GLC2000 (Global  
Land Cover). It can potentially impact the distribution of the terrestrial evaporation between  
GLEAM and ISBA. Further work at CNRM will focus on understanding the differences between  
ISBA and GLEAM, in particular investigating the sub-components of terrestrial evaporation.

1895 Finally, Figure [S1](#) and Figure [S2](#) illustrate snow cover evaluation. LDAS\_ERA5 snow cover was  
evaluated against the IMS snow cover (as e.g. in Orsolini et al., 2019). ~~The IMS snow cover product~~  
~~combines ground observations and satellite data from microwave and visible sensors (using~~  
~~geostationary and polar orbiting satellites) to provide snow cover information in all weather~~  
~~conditions. The IMS product is available daily for the northern hemisphere.~~ Figure [S1](#) shows the  
1900 averaged northern hemisphere snow cover fraction for the 2010-2018 period, ~~and is~~ It is  
complemented by all panels of Figure [S2](#) showing (i) maps of IMS snow cover (top row) for 3  
seasons, September-October-November (SON), December-January-February (DJF) and March-  
April-May (MAM), respectively, (ii) maps of snow cover from LDAS\_ERA5 open-loop (second  
row), (iii) maps of snow cover differences between the open-loop and IMS data and (iv) maps of  
1905 snow cover differences between the analysis and the open-loop. LDAS\_ERA5 open-loop compares  
very well with the IMS snow-cover data in the accumulation season from September to February  
(Figure [S2](#) and panels d) to l) of Figure [S1](#)), only with an overestimation over the Tibetan Plateau.  
The ~~latter~~ issue over Tibet ~~from in~~ ERA5 is not new, and consistent with previous studies like  
Orsolini et al., 2019. An early melt in ~~s~~Spring compared to observations is noted in LDAS\_ERA5  
1910 and could be related with the snow cover parametrization in ISBA. As expected, the analysis has an  
almost neutral impact on snow as both SSM and LAI observations are filtered out from frozen/snow  
condition and as there is no snow data assimilation in LDAS\_ERA5 (Figure [S2](#) and panels (j), (k)  
and (l) of Figure [S1](#)). This clearly shows, however an area of potential improvement of data  
assimilation within LDAS-Monde using satellite data such as the IMS one (as in e.g. de Rosnay et  
1915 al., 2014).

### 3.1.2 Ground-based datasets

LDAS\_ERA5 analysis and open-loop are also evaluated using in situ measurements of evapotranspiration, river discharge and surface soil moisture across the world. Daily in situ measurements of evapotranspiration from the ~~Fluxnet~~FLUXNET-2015 synthesis data set (<http://fluxnet.fluxdata.org/>, last accessed June 2019) are first used in this study. ~~Stations with at least two years of data (after 2010) are retained leading to a pool of 85 stations available for this evaluation (note that none of these stations include 2015), they are listed in Table S2. The~~ LDAS\_ERA5 ability to represent evapotranspiration is evaluated using correlation (R), RMSD and ubRMSD as well as bias (LDAS\_ERA5 minus observations) using the 85 selected FLUXNET-2015 stations. Median R, RMSD, ubRMSD and bias for LDAS\_ERA5 analysis (open-loop) are 0.73 (0.72), 28.74 (29.60) ~~W~~w.m<sup>-2</sup>, 27.37 (26.92) ~~w~~W.m<sup>-2</sup> and 4.64 (4.40) w.m<sup>-2</sup>, respectively. ~~If t~~These numbers depict a small advantage of the analysis over the open-loop configuration, it is worth mentioning that differences are rather small and likely to fall within the uncertainty of the in situ measurement.

Figure S31(a) represents the added value of the analysis based on NIC<sub>R</sub> (Eq.(1)), large blue circles represent a positive impact from the analysis (20 stations) at NIC<sub>R</sub> greater than +3 (i.e. R values are better when the analysis is used than when the model is used) while large red circles represent a degradation from the analysis (5 stations) at NIC<sub>R</sub> smaller than -3. Stations with a rather neutral impact (60 stations) at NIC<sub>R</sub> between [-3, +3] are not reported for sake of clarity. Figure S31 (b), (c), (d) and (e) are scatter-plots of R, ubRMSD, absolute bias and RMSD between LDAS\_ERA5 open-loop and the 85 stations from the Fluxnet2015 (y-axis) against LDAS\_ERA5 analysis and the same pool of stations (x-axis). 56 stations (out of 85) have better R values considering the analysis. They are 41 for ubRMSD, 47 for RMSD and 44 for absolute bias.

~~Over 2010-2017, river discharge from LDAS\_ERA5 analysis and open-loop runs were compared to daily streamflow data from 7 large networks across the world (see Table S1). As in Albergel et al., 2018a, data were selected for sub-basins with rather large drainage areas (10,000 km<sup>2</sup> or greater) due to the low resolution of CTRIP (0.5 x 0.5°) and with observation time series of 4 years or more. Results on river discharge are illustrated by Figures S42 and S53. Figure S42 represents NSE scores and as NSE values below -2 were discarded, it leads to a subset of 982 stations available. Most of them are located in North America and Europe while a few are available in South America and Africa. Figure S42 is complemented by Figure S53. Panel a) of Figure S53 represents the NIC scores applied to NSE scores and emphasizes the added value of LDAS\_ERA5 analysis over the open-loop. 74% of this subset of stations presents a rather neutral impact from the analysis (at NIC ranging between -3 and +3) while 26% (254 stations) presents an impact greater or smaller than 3%.~~

When the analysis impacts the representation of river discharge, this impact tends to be positive

with 74% (189 stations) having a NIC score greater than 3% while only 26% (65 stations) presents NIC score smaller than -3%. These results are supported by panels (b) and (c) of Figure S53, also (density of NSE scores for LDAS\_ERA5 analysis and open-loop, scatter-plot of NSE scores for LDAS\_ERA5 analysis and open-loop, respectively).

1955 ~~at global scale ((a) panel) and with a zoom over the continental USA ((b) panel). 4 Figure S by 0.67~~  
~~(it is 0.66 for the open-loop) with averaged-network values going up to 0.88 (SOILSCAPE network,~~  
~~49 stations in the USA) and always higher than 0.55 except for one network, ARM (10 stations in~~  
~~the USA) presenting an averaged R value of 0.29. Averaged ubRMSD and bias (LDAS\_ERA5~~  
~~minus in situ) are 0.058 m<sup>3</sup>m<sup>-3</sup> and 0.079 m<sup>3</sup>m<sup>-3</sup> for the analysis, 0.059 m<sup>3</sup>m<sup>-3</sup> and 0.078 m<sup>3</sup>m<sup>-3</sup> for the~~  
1960 ~~open-loop, respectively. Results for each network are summarized in Table S2. NIC (Eq.1) has also~~  
~~been applied to R values, 64% of the pool of stations present a neutral impact from the analysis (at~~  
~~NIC ranging between -3 and +3), 12% present a negative impact (at NIC < -3) and 24% present a~~  
~~positive impact at (NIC > +3). NIC scores are also presented is pool of stations, averaged statistical~~  
~~metrics (ubRMSD, R and bias) are similar for both LDAS\_ERA5 analysis and open-loop even if~~  
1965 ~~local differences exist. For the analysis, averaged R values is Using th~~  
~~In situ measurements of~~  
~~surface soil moisture from 20 networks across 14 countries available from the ISMN are also used~~  
~~to evaluate the performance of SSM analysis. They represent more than 900 stations with at least 2~~  
~~years of daily data over 2010-2018. Sensors at 5 cm depth are compared with soil moisture from~~  
~~LDAS\_ERA5 third layer of soil (4-10 cm). Beside 11 stations located in 4 countries of Western~~  
1970 ~~Africa (Benin, Mali, Sénégal and Niger) and 19 stations in Australia, most of the station are located~~  
~~in North America and Europe, see Table S3. The statistical scores for soil moisture from~~  
~~LDAS\_ERA5 open-loop and analysis (third and fourth layers of soil, 4-10 cm depth, 10-20 cm~~  
~~depth, respectively) over 2010-2018 when compared with ground measurements from the ISMN (5~~  
~~cm depth and 20 cm depth) are presented in Table S2 for each individual network. Averaged~~  
1975 ~~statistical metrics (ubRMSD, R, R<sub>anomaly</sub> and bias) are similar for both LDAS\_ERA5 analysis and~~  
~~open-loop even if local differences exist. For the analysis, averaged R (R<sub>anomaly</sub>) values along with its~~  
~~95% Confidence Interval (CI) using in situ measurements at 5 cm (782 stations from 19 networks)~~  
~~are 0.68±0.03 (0.53±0.04) (0.67±0.03(0.53±0.04) for the open-loop) with averaged-network values~~  
~~going up to 0.88±0.01 (0.58±0.04) for the analysis (SOILSCAPE network, 49 stations in the USA)~~  
1980 ~~and always higher than 0.55 except for one network, ARM (10 stations in the USA) presenting an~~  
~~averaged R value of 0.29±0.05. Averaged ubRMSD and bias (LDAS\_ERA5 minus in situ) are 0.060~~  
~~m<sup>3</sup>m<sup>-3</sup> and 0.077 m<sup>3</sup>m<sup>-3</sup> for the analysis, 0.060 m<sup>3</sup>m<sup>-3</sup> and 0.076 m<sup>3</sup>m<sup>-3</sup> for the open-loop,~~  
~~respectively. NIC (Eq.1) has also been applied to R values, 65% of the pool of stations present a~~  
~~neutral impact from the analysis (511 stations at NIC ranging between -3 and +3), 12% present a~~

1985 negative impact (91 stations at NIC < -3) and 23% present a positive impact at (180 stations at NIC > +3).

1990 The number of stations where R differences between the analysis and the open-loop are significant (i.e. their 95% CI are not overlapping) is 186 out of 782 (about 26%). There is an improvement from the analysis w.r.t. the open-loop for 128 stations (out of 186, i.e. about 69%) and a degradation for 58 stations (about 31%). Figure 7 illustrates R differences between the analysis and the open-loop runs. When differences (analysis minus open-loop) are not significant stations are represented by a small dot. When they are significant, large circles have been used, blue for positive differences (an improvement from the analysis) and red for negative differences (a degradation from the analysis). For most of the stations where a significant difference is obtained, it represent an improvement from the analysis.

1995 Averaged analysis R (95%CI), bias and ubRMSD for the fourth layer of soil (685 stations from 10 networks) are  $0.65 \pm 0.03$ ,  $0.049 \text{ m}^3\text{m}^{-3}$  and  $0.055 \text{ m}^3\text{m}^{-3}$ , respectively. For the open-loop, they are  $0.64 \pm 0.03$ ,  $0.048 \text{ m}^3\text{m}^{-3}$  and  $0.056 \text{ m}^3\text{m}^{-3}$ , respectively. For soil moisture at that depth, about 60% of the stations present a neutral impact from the analysis (410 stations at NIC ranging between -3 and +3), 28% a positive impact (189 stations at NIC > +3) and 12% a negative impact (86 stations at NIC < -3). Although differences between the open-loop run and the analysis are rather small, these results underline the added value of the analysis with respect to the model run. Figure S6 represents the distribution of the scores values for LDAS\_ERA5 open-loop and analysis using boxplots centred on the median value. They look very similar and from Figure S6, it is difficult to see either improvement or degradation from the analysis.

2000 For evapotranspiration, river discharge and surface soil moisture ~~it can be stated that~~ there is an slight advantage ~~forrom~~ LDAS\_ERA5 analysis with respect to its open-loop counterpart. Even if the distribution of the averaged statistical metrics can be rather similar for both (particularly true for surface soil moisture evaluation), there are significant regional differences for some sites, which shows the added value of the analysis with respect to the open-loop.

### 3.2 Monitoring and forecasts for areas under severe/extreme conditions

2015 For each individual region presented in Table I and Figure 22, monthly anomalies (scaled by the standard deviation) of analysed SSM (second layer of soil, 1-4cm) and LAI for 2018 were assessed with respect to the 2010-2018 period. The anomalies (see Figure 8) highlight three regions, two presenting strong negative anomalies for both SSM and LAI for almost all 2018 (north western Europe, WEUR, and the Murray-Darling basin, MUDA, in south eastern Australia) and one presenting strong positive anomalies of SSM and LAI in Eastern Africa (EAFR). WEUR and

MUDA regions were affected by a severe heatwave and a drought in 2018 impacting LSVs analysed by LDAS\_ERA5. According to Figure 8, monthly anomalies of SSM and LAI for MUDA are negative through ~~all the year~~ the whole 2018 with 7 and 6 months presenting LAI and SSM anomalies below -1 standard deviation (stdev), respectively. WEUR has negative SSM anomalies from May to December 2018 with values going below -2 stdev. LAI was severely impacted as well with July to October 2018 presenting negative anomalies below -2 stdev. For WEUR, 5 months present LAI and SSM anomalies below -1 stdev. EAFR ~~has~~ experiences 3 and 7 months with positive anomalies for SSM and LAI in 2018 above 1 stdev (8 and 7 months consecutively present positive anomalies for SSM and LAI respectively).

According to the National Oceanic and Atmospheric Administration (NOAA), Europe experienced its warmest summer since continental records began in 1910 at +2.16°C (Global Climate Report, <https://www.ncdc.noaa.gov/sotc/global/> last accessed April 2019). In Europe, temperature for the whole summer 2018 was above climatology. The summer 2018 heatwave in Europe was already reported in the scientific literature (e.g. Magnusson et al., 2018, Albergel et al., 2019, Blyverket et al., 2019). In its 70<sup>th</sup> Special Climate Statement, the Australian Bureau of Meteorology (BoM) has reported a very hot and dry summer 2018 in eastern Australia (BoM, 2019). Like much of Australia, the Murray Darling Basin has experienced a remarkably dry and hot weather during 2018 (~~<http://www.bom.gov.au/state-of-the-climate/>, last visited: April 2019~~). The annual maximum temperature for the Murray Darling Basin as a whole was more than two degrees above average during 2018. The northern Murray–Darling Basin in particular was severely affected with inflows to all catchments persistently well below average (~~<http://www.bom.gov.au/state-of-the-climate/>, last visited: April 2019~~). Finally, the East Africa Seasonal Monitor based on the Famine Early Warning System Network (FEWS) confirms above-average rainfall amounts as well as significantly greener than normal vegetation conditions (e.g., <https://reliefweb.int/report/somalia/east-africa-seasonal-monitor-july-27-2018>, last visited: April 2019). As this study focuses on monitoring and forecasting the impact of severe conditions on LSVs, WEUR and MUDA are selected for further investigation.

### 3.2.1 Case studies for assessing LDAS-Monde medium resolutions (0.25° x 0.25°) experiments

Figure 9 illustrates seasonal cycles of observed LAI (Figure 9a) and SWI (Figure 9e), LDAS\_ERA5 analysis and open-loop LAI (Figure 9b) and SWI (Figure 9f) for the WEUR domain. The last year (2018) is compared to an average of the previous years (2010-2017). From Figure 9a one may see the heatwave impact with a sharp drop in observed LAI values from June to November 2018 (solid green line). Such low LAI values have never been observed ~~over the eight previous years~~ s (dashed green line for the 2010-2017 averaged along with the 2010-2017 minimum and maximum

observations in shaded green). A similar behaviour is also visible in the ASCAT SWI dataset in Figure 9e with the lowest values ever reached in this 2010-2018 period. Over WEUR, LDAS\_ERA5 open-loop overestimates LAI in the second part of the year as already highlighted by several studies (e.g. Albergel et al., 2017, 2019). LDAS\_ERA5 analysis has a positive impact, reducing LAI values, as seen on Figure 9b (LAI open-loop in blue, analysis in red) and on Figure 9c representing RMSD seasonal cycles. LDAS\_ERA5 analysis also leads to an improvement in correlations for LAI (see Figure 9d). Similar conclusions can be drawn for SSM (Figure 9e to h). Note that for data assimilation and statistical scores, ASCAT SWI estimates were converted into the model space, in  $\text{m}^3\text{m}^{-3}$ , as detailed in section 2.3. Finally looking at the MUDA area (panels of Figure 10) ~~one may appreciate~~ similar positive impact from the analysis over the open-loop simulation is obtained. Almost all month of 2018 presents the lowest anomaly values for both SSM and LAI. For both MUDA and WEUR the smaller differences between LDAS\_ERA5 analysis and open-loop in 2018 than in 2010-2017 (Figure 9 b and f, Figure 10 b and f) also suggest that both extreme events were well captured in the atmospheric forcing used to drive LDAS\_ERA5 while the statistical scores presented in Figure 9 c, d, g, h as well as in Figure 10 c, d, g, h also suggest an improvement from the analysis over the open-loop simulation.

### 3.2.2 Case studies for assessing LDAS-Monde high resolutions ( $0.1^\circ \times 0.1^\circ$ ) experiments

For these two specific areas, LDAS-Monde was also run forced by HRES (LDAS\_HRES) at  $0.1^\circ \times 0.1^\circ$  spatial resolution over April 2016 to December 2018. Additionally to LDAS\_HRES analysis, forecast experiments with a lead time of 4-days and 8-days, initialised by either LDAS\_HRES analysis or open-loop are presented for 2017-2018 (for SSM and LAI) in order to assess the impact of the initial conditions on the forecast of LSVs.

Upper panels of Figure 11 and Figure 12, illustrate seasonal RMSD (Figure 11a, 12a) and correlation (Figure 11b, 12b) values between SSM from the second layer of soil (1–4 cm) from LDAS-Monde forced by HRES (LDAS\_HRES, open-loop and analysis) and ASCAT SSM estimates over 2017-2018. Scores between SSM from the second layer of soil of LDAS\_HRES 4-day forecast (LDAS\_fc4, initialised by either the open-loop or analysis) and 8-day forecast (LDAS\_fc8, initialised by either the open-loop or analysis) and ASCAT SSM estimates are reported, also. From the upper panels of those figures one may notice a small improvement from the analysis (solid red line) over the open-loop simulation (solid blue line), slightly decreasing RMSD values and increasing correlations values. However no improvement (nor degradation) is visible from the 4-d and 8-d forecasts experiments initialised by LDAS\_HRES analysis over those initialised by LDAS\_HRES open-loop, they display very similar scores. LDAS\_HRES SSM is of better quality than LDAS\_fc4 and LDAS\_fc8. ~~Note however that for the MUDA area, a 4-d forecast~~



of surface soil moisture initialised by the analysis is of better quality than a 4-d forecast initialised by the open-loop. Note however that for the MUDA area, there is a small positive impact of the initialisation on the 4-d and 8-d forecast of surface soil moisture (blue areas on Figure 13 c) and d)). Those results suggest that this fast evolving model variable (SSM between 1 cm and 4 cm depth) is more sensitive to relies more on the atmospheric forcing than to initial conditions (at least within the forecast range presented in this study) and it can be assumed that the 4-day and 8-day atmospheric forecast from HRES is of poorer lower quality than the first day 24-h analysis. Results for LAI are different than for SSM (lower panels of Figure 11 and Figure 12). Firstly, there is a large improvement from the analysis (solid red line) over the open-loop (solid blue line), particularly in the LAI decaying phase (Boreal and Austral autumns mainly). Secondly, LDAS\_HRES open-loop (solid blue line), LDAS\_fc4 (dotdashed blue line) and LDAS\_fc8 (dashed blue line) initialised by LDAS\_HRES open-loop present very similar skills, so do LDAS\_fc4 and LDAS\_fc8 initialised by LDAS\_HRES analysis (dotdashed and dashed red lines, respectively). They outperform however skills of LDAS\_HRES open-loop, LDAS\_fc4 and LDAS\_fc8 initialised by LDAS\_HRES open-loop. This suggests that LAI is more sensitive to relies more on its initial conditions than to the atmospheric forcing (at least within the forecast range presented in this study) and that forecasting -LAI is also a matter of initial conditions. This is true for these two contrasted areas, WEUR and MUDA.

These results are corroborated by Figures 13 (for WEUR) and 14 (for MUDA), top rows illustrate SSM and bottom rows LAI. Figures 13(a) and 14(a) show RMSD values between LDAS\_HRES open-loop SSM (1-4 cm) and ASCAT SSM over 2017-2018 for the WEUR and MUDA domains, respectively. Due to the CDF matching seasonal linear rescaling applied to ASCAT estimates, RMSD values are rather small. For the WEUR (MUDA) domain they range from 0 to 0.048 m<sup>3</sup>m<sup>-3</sup> (0 to 0.040 m<sup>3</sup>m<sup>-3</sup>). Figures 13(b) and 14(b) represent maps of RMSD differences between LDAS\_HRES analysis (open-loop) and ASCAT SSM estimates over 2017-2018 for the WEUR and MUDA domains, as well. Both maps are dominated by negative values (in blue) indicating that RMSD values are smaller (better) when using LDAS\_HRES analysis than when using LDAS\_HRES open-loop. It is also worth-mentioning that no positive differences (i.e. a degradation from the analysis) are present in those maps. RMSD differences for the WEUR domain range from -0.004 m<sup>3</sup>m<sup>-3</sup> to 0.004 m<sup>3</sup>m<sup>-3</sup> meaning that the analysis is improving them by about 8 %. For the MUDA domain, they are improved by about 15%. Figures 13(c), (d) 14(c),(d) are also maps of RMSD differences, they consider forecast experiments (LDAS\_fc4, LDAS\_fc8). It appears that for both domains, the impact from the initialisation is rather small with few coloured areas, strengthening previous results suggesting that to forecast SSM variable, forcing quality is more

2120 important than initial conditions. It is different for LAI, RMSD values for LDAS\_HRES open-loop  
are ranging between 0 and 1.6 m<sup>2</sup>m<sup>-2</sup> over WEUR, 0 and 1 m<sup>2</sup>m<sup>-2</sup> over MUDA (Figures 13(e) and  
14(e)). RMSD values are improved by up to 37 % over WEUR and up to 60% over MUDA by the  
analysis (Figures 13(f) and 14(f)). Improvement from the analysis over the open-loop experiment is  
consistent through all the WEUR domain while it is mainly the south eastern part of the MUDA  
2125 domain that is improved (the north western part has low RMSD values as the open-loop).

Similarly to Figures 13(a, b, c, d) panels of Figure 15 illustrates the impact of the analysis on SSM  
using correlations. This time, ASCAT SWI (i.e. no rescaling) has been used. Figure 15 (top panels)  
shows map of R values based on absolute values while Figure 15 (bottom panels) shows R values  
on anomalies (short term variability) as defined in Albergel et al., 2018a. Figure 15 (a) and (e)  
2130 represents R values and anomaly R values for LDAS HRES, respectively. As expected R values are  
higher than anomaly R values. Maps of differences (panels b and f) of Figure 15 suggest that after  
assimilation, both scores are improved rather equally. While the 4 day and 8-day forecast still show  
an improvement from the initial condition on R values (panels c and d of Figure 15 dominated by  
positive differences, analysis minus open-loop), maps of anomaly R values forecast do not display  
2135 any negative or positive impact (panels g and h of Figure 15).

Top panels of Figure 16 illustrate the impact of the analysis on drainage monitoring and forecast  
over WEUR. Fig. 16 a) represents drainage from LDAS HRES open-loop varying between 0 and 1  
kg.m<sup>-2</sup>.day<sup>-1</sup>, as seen in Fig.16 b) (drainage difference between LDAS HRES analysis and open-  
loop) analysis impact is rather small, about ±3% and more pronounced in areas where the analysis  
2140 has affected LAI more (see panels f, g) and h) of Figure 13). As seen on panels c) and d), there is  
also an impact from the initialisation in areas were the analysis was more effectively correcting  
LAI. Bottom panels of Figure 16 illustrate similar impact on runoff. As for drainage, this variable is  
affected by the analysis. Initial conditions have an impact on its forecast, also. Although we did not  
present a quality assessment of those two variables, our findings on river discharge analysis impact,  
2145 but also those from Albergel et al., 2017, 2018a, suggest a neutral to positive impact, propagated  
from the analysis of SSM and LAI to river discharge through variables such as drainage and runoff.

#### 4 Discussion and conclusion

This study has demonstrated that combining a LSM, satellite EOs and atmospheric forcing through  
LDAS-Monde has a great potential to represent the impact of extreme weather (heatwaves and  
2150 droughts) on land surface conditions. LDAS-Monde is now ready for use in various applications  
such as (i) reanalyses of land Essential Climate Variables (ECVs), (ii) monitoring of water  
resources, drought and vegetation, and (iii) detection of severe conditions over land and

initialisation of LSVs forecast. It has been applied in this study to past events of 2018 with respect to a short period of time (2010-2018) as a demonstrator but will be extended to longer time period.

2155 LDAS-Monde operational use in near real time has the capacity to serve as an emergency monitoring system for the LSVs. Using atmospheric reanalysis like ERA5 ~~to~~ force LDAS-Monde guarantees a high level of consistency because of its ~~fixed~~~~frozen~~ configuration (no changes in spatial and vertical resolutions, data assimilation and parameterizations). The ERA5 coarse spatial resolution makes it affordable to run long term and; large scale LDAS-Monde experiments.

2160 With ERA5 available ~~now back to~~~~from~~ 1979 and now covering near real-time needs with ~~its~~~~the~~ ERA5T version (<https://climate.copernicus.eu/climate-reanalysis>), an LDAS\_ERA5 configuration would be able to provide a long term and; near real time coarse resolution (0.25° x 0.25°) climatology as reference for anomalies of the land surface conditions. Significant anomalies could then be used to trigger more focussed “on-demand” simulations for regions experiencing extreme

2165 conditions~~weather~~. In that case LDAS-Monde could be run forced by e.g. ECMWF operational high resolution product (0.10° x 0.10°) in monitoring and forecast (up to 10-d ahead) modes, as was presented here for two regions in North Western Europe and South Eastern Australia. In term of RMSD, oOur results showed a very small impact of initial conditions on the forecasts of SSM. This was expected due to the reduced memory of the top soil surface (~~0-1-4~~ cm), which is dominated by meteorological variability. However, the LAI initialisation had significant impact on the LAI forecast skill. This was also expected due to the memory of vegetation evolution. For SSM, the assimilation is done after a rescaling to the model climatology (see section 2.3), which removes bias. For LAI, however this is not the case and the assimilation process removes bias in the modelled LAI (w.r.t. the observation). This technical difference between SSM and LAI assimilation,

2175 combined with the longer memory of LAI compared to SSM, contributes to the results presented in this section. Despite the expected behaviour of these two LSVs in forecasting, our results show that LDAS-Monde system is capable of propagating the initial LAI conditions, which is relevant not only for LSV medium-range forecasting but with potential for longer lead-times. The strong impact of LAI initialisation on the forecast does not seem to propagate to surface soil moisture and further

2180 studies are necessary to test the impact of initial conditions to more variables from LDAS-Monde (including soil moisture in deeper layers and; evapotranspiration). Another possibility would be to force LDAS-Monde using ECMWF ensemble forecasts, although the ensemble system has coarser spatial-resolution (~0.20° x 0.20°), it offers a 15-day forecast and a 51 member ensemble, which can introduce forcing uncertainty into the LSVs. The maximum range of the soil and vegetation

2185 forecast could even reach up to six months if using seasonal atmospheric forecasts as forcing.

LDAS-Monde has well identified areas of developments that can further improve the representation of LSVs. For instance, it does not consider snow data assimilation yet and it has been shown in this study that ~~if~~ the snow accumulation seems to be represented correctly in the system, it suffers from a ~~toon~~ early snow-melt in spring. To overcome this issue, two possibilities will be explored. Firstly

2190 using a recently developed ISBA parametrisation, MEB for Multiple Energy Budget which is known to lead to a better representation of the snowpack (Boone et al., 2017), in particular in the densely forested areas of the Northern Hemisphere where large differences between LDAS-Monde and the IMS snow cover were found in spring (Figure S2(i), Aaron Boone CNRM, personal communication June 2019) and (ii) adapting the current data assimilation scheme of LDAS-Monde

2195 to permit assimilation the IMS snow cover data (as done e.g. at ECMWF, de Rosnay et al., 2014). The ~~c~~Current SEKF data assimilation scheme is also being revisited. Even though it has provided good results, one of its limitations is the computation of a Jacobian matrix which requires one model run for each control variable, requiring significant computational resources with increased number of control variables. That is why more flexible Ensemble based approaches like the

2200 Ensemble Square Root Filter (EnSRF) have recently been implemented (Fairbain et al., 2015, Bonan et al., 2020+9). Bonan et al., 2020+9 have evaluated performances from the EnSRF and the SEKF over the Euro-Mediterranean area. Both data assimilation schemes have a similar behaviour for LAI while for SSM, EnSRF estimates tend to be closer to observations than those from the SEKF. They have also conducted an independent evaluation of both assimilation approaches using

2205 satellite estimates of evapotranspiration and GPP as well as measures of river discharges from gauging stations. They have found that the EnSRF leads to a systematic (moderate) improvement for evapotranspiration and GPP and a highly positive impact on river discharges, while the SEKF lead to more contrasting performance. As for applications in hydrology, the  $0.5^\circ \times 0.5^\circ$  spatial resolution TRIP river network is currently being improved to  $1/12^\circ \times 1/12^\circ$  globally.

2210 CNRM is also investigating the direct assimilation of ASCAT radar backscatter (Shamambo et al., 2019), it is supposed to tackle the way vegetation is accounted for in the change detection approach used to retrieve SSM with an improved representation of its effect. Assimilating ASCAT radar backscatter also raises the question of how to specify observation, background, and model error covariance matrices, so far mainly relying on soil properties (see section 2.1.3 on data assimilation).

2215 The last decade has seen the development of techniques to estimate those matrices. Approaches based on Desroziers diagnostics (Desroziers et al., 2005) are affordable for land data assimilation systems from a computational point of view and could provide insightful information on the various sources of the data assimilation system

2220 | Also, the added value of LDAS-Monde compared to already existing datasets has to be evaluated  
| and current work at Météo-France is investigating its quality against state of the art reanalyses such  
| as those from NASA at either global scale (GLDAS, [Rodell et al., 2004](#), MERRA-2, The Modern-  
Era Retrospective Analysis for Research and Applications, Version 2, Reichle et al., 2017, Draper et  
al., 2018) or regional scale (NCALDAS over the continental USA, FLDAS over Africa). Finally,  
2225 | first attempts to go to higher spatial resolution over smaller areas like the AROME domain  
| (Applications de la Recherche à l'Opérationnel à Méso-Echelle, [https://www.umr-cnrm.fr/spip.php?  
| article120](https://www.umr-cnrm.fr/spip.php?article120), last accessed July 2019) of Météo-France (centred over France) at kilometre scale and  
assimilating kilometric and sub-kilometric scale satellite retrieval of SSM and LAI (from CGLS)  
are very promising.

2230

**Code availability.** LDAS-Monde is a part of the ISBA land surface model and is available as open  
source via the surface modelling platform called SURFEX. SURFEX can be downloaded freely at  
<http://www.umr-cnrm.fr/surfex/> using a CECILL-C Licence (a French equivalent to the L-GPL  
licence; [http://www.cecill.info/licences/Licence\\_CeCILL-C\\_V1-en.txt](http://www.cecill.info/licences/Licence_CeCILL-C_V1-en.txt)). It is updated at a relatively  
2235 | low frequency (every 3 to 6 months). If more frequent updates are needed, or if what is required is  
not in Open-SURFEX (DrHOOK, FA/LFI formats, GAUSSIAN grid), you are invited to follow the  
procedure to get a SVN account and to access real-time modifications of the code (see the  
instructions at the first link). The developments presented in this study stemmed on SURFEX  
version 8.1. LDAS-Monde technical documentation and contact point are freely available at: [https://  
| opensource.umr-cnrm.fr/projects/openldasmonde/files](https://<br/>2240 | opensource.umr-cnrm.fr/projects/openldasmonde/files)

**Data availability:** upon request by contacting the corresponding author.

**Author Contributions:** Conceptualization, CA, JCC.; Investigation, CA, YZ, SM, NRF;  
Methodology, CA; Writing—original draft, CA; Writing—review and editing, All

2245 | **Funding:** This research was funded by IRT Antoine de Saint-Exupéry Foundation, grant number  
CDT-R056-L00-T00 (POMME-V project), the Climate Change Initiative Programme Extension,  
Phase 1 - Climate Modeling User Group ESA/contract No [4000125156](#)/18/I-NB

**Acknowledgments:** Results were generated using the Copernicus Climate Change Service Information, 2017. The Authors would like to thanks the Copernicus Global Land Service for providing the satellite derived Leaf Area Index and Surface Soil Moisture.

**Conflicts of Interest:** The authors declare no conflict of interest

2255 **References**

- Albergel, C.; Rüdiger, C.; Pellarin, T.; Calvet, J.-C.; Fritz, N.; Froissard, F.; Suquia, D.; Petitpa, A.; Pignatelli, B.; Martin, E. From near-surface to root-zone soil moisture using an exponential filter: An assessment of the method based on in-situ observations and model simulations. *Hydrol. Earth Syst. Sci.*, 12, 1323–1337, 2008.
- 2260 Albergel, C., Munier, S., Leroux, D. J., Dewaele, H., Fairbairn, D., Barbu, A. L., Gelati, E., Dorigo, W., Faroux, S., Meurey, C., Le Moigne, P., Decharme, B., Mahfouf, J.-F., and Calvet, J.-C.: Sequential assimilation of satellite-derived vegetation and soil moisture products using SURFEX\_v8.0: LDAS-Monde assessment over the Euro-Mediterranean area, *Geosci. Model Dev.*, 10, 3889–3912, <https://doi.org/10.5194/gmd-10-3889-2017>, 2017.
- 2265 Albergel, C.; Munier, S.; Bocher, A.; Bonan, B.; Zheng, Y.; Draper, C.; Leroux, D.J.; Calvet, J.-C. LDAS-Monde Sequential Assimilation of Satellite Derived Observations Applied to the Contiguous US: An ERA5 Driven Reanalysis of the Land Surface Variables. *Remote Sens.*, 10, 1627, 2018a
- Albergel, C.; Dutra, E.; Munier, S.; Calvet, J.-C.; Munoz-Sabater, J.; de Rosnay, P.; Balsamo, G. ERA-5 and ERA-Interim driven ISBA land surface model simulations: Which one performs better? *Hydrol. Earth Syst. Sci.*, 22, 3515–3532, 2018b.
- 2270 Albergel, C.; Dutra, E.; Bonan, B.; Zheng, Y.; Munier, S.; Balsamo, G.; de Rosnay, P.; Muñoz-Sabater, J.; Calvet, J.-C. Monitoring and Forecasting the Impact of the 2018 Summer Heatwave on Vegetation. *Remote Sens.*, 11, 520, 2019.
- Balsamo, G., Albergel, C., Beljaars, A., Boussetta, S., Brun, E., Cloke, H., Dee, D., Dutra, E., Muñoz-Sabater, J., Pappenberger, F., de Rosnay, P., Stockdale, T., and Vitart, F.: ERA-Interim/Land: a global land surface reanalysis data set, *Hydrol. Earth Syst. Sci.*, 19, 389–407, <https://doi.org/10.5194/hess-19-389-2015>, 2015.
- 2275 Balsamo, G.; Agusti-Panareda, A.; Albergel, C.; Arduini, G.; Beljaars, A.; Bidlot, J.; Bousserez, N.; Boussetta, S.; Brown, A.; Buizza, R.; Buontempo, C.; Chevallier, F.; Choulga, M.; Cloke, H.; Cronin, M.F.; Dahoui, M.; De Rosnay, P.; Dirmeyer, P.A.; Dutra, M.D.E.; Ek, M.B.; Gentine, P.; Hewitt, H.; Keeley, S.P.E.; Kerr, Y.; Kumar, S.; Lupu, C.; Mahfouf, J.-F.; McNorton, J.; Mecklenburg, S.; Mogensen, K.; Muñoz-Sabater, J.; Orth, R.; Rabier, F.; Reichle, R.; Ruston, B.; Pappenberger, F.; Sandu, I.; Seneviratne, S.I.; Tietsche, S.; Trigo, I.F.; Uijlenhoet, R.; Wedi, N.; Woolway, R.I.; Zeng, X. Satellite and In Situ Observations for Advancing Global Earth Surface Modelling: A Review. *Remote Sens.*, 10(12), 2038; <https://doi.org/10.3390/rs10122038>, 2018.
- 2280 Bamzai, A.; Shukla, J. Relation between Eurasian snow cover, snow depth and the Indian summer monsoon: An observational study. *J. Clim.*, 12, 3117–3132, 1999.
- 2290 Barbu, A.L.; Calvet, J.-C.; Mahfouf, J.-F.; Albergel, C.; Lafont, S. Assimilation of Soil Wetness Index and Leaf Area Index into the ISBA-A-gs land surface model: Grassland case study. *Biogeosciences*, 8, 1971–1986., 2011.
- Barbu, A. L., Calvet, J.-C., Mahfouf, J.-F., and Lafont, S.: Integrating ASCAT surface soil moisture and GEOV1 leaf area index into the SURFEX modelling platform: a land data assimilation application over France, *Hydrol. Earth Syst. Sci.*, 18, 173–192, <https://doi.org/10.5194/hess-18-173-2014>, 2014.
- 2295 Barella-Ortiz, A. and Quintana-Seguí, P.: Evaluation of drought representation and propagation in Regional Climate Model simulations over Spain, *Hydrol. Earth Syst. Sci. Discuss.*, <https://doi.org/10.5194/hess-2018-603>, in review, 2018.

- 2300 Baret, F.; Weiss, M.; Lacaze, R.; Camacho, F.; Makhmarad, H.; Pacholczyk, P.; Smetse, B. GEOV1: LAI, FAPAR essential climate variables and FCOVER global time series capitalizing over existing products, Part 1: Principles of development and production. *Remote Sens. Environ.*, 137, 299–309, doi:10.1016/j.rse.2012.12.027, 2013.
- 2305 Bartalis, Z.; Wagner, W.; Naeimi, V.; Hasenauer, S.; Scipal, K.; Bonekamp, H.; Figa, J.; Anderson, C.: Initial soil moisture retrievals from the METOP-A advanced Scatterometer (ASCAT). *Geophys. Res. Lett.*, 34, L20401, doi: 10.1029/2007GL031088., 2007.
- Bauer, P.; Thorpe, A.; Brunet, G. The quiet revolution of numerical weather prediction. *Nature*, 525, 47–55, doi:10.1038/nature14956, 2015.
- 2310 Beck, H. E., Pan, M., Roy, T., Weedon, G. P., Pappenberger, F., van Dijk, A. I. J. M., Huffman, G. J., Adler, R. F., and Wood, E. F.: Daily evaluation of 26 precipitation datasets using Stage-IV gauge-radar data for the CONUS, *Hydrol. Earth Syst. Sci.*, 23, 207–224, <https://doi.org/10.5194/hess-23-207-2019>, 2019.
- 2315 Bell, J. E., M. A. Palecki, C. B. Baker, W. G. Collins, J. H. Lawrimore, R. D. Leeper, M. E. Hall, J. Kochendorfer, T. P. Meyers, T. Wilson, and H. J. Diamond.: U.S. Climate Reference Network soil moisture and temperature observations. *J. Hydrometeorol.*, 14, 977–988. doi: 10.1175/JHM-D-12-0146.1, 2013.
- Bierkens, M.; van Beek, L. Seasonal predictability of European discharge: Nao and hydrological response time. *J. Hydrometeorol*, 10, 953–968, 2009.
- Blyverket, J.; Hamer, P.D.; Schneider, P.; Albergel, C.; Lahoz, W.A. Monitoring Soil Moisture Drought over Northern High Latitudes from Space. *Remote Sens.*, 11, 1200, 2019.
- 2320 Bonan, B., Albergel, C., Zheng, Y., Barbu, A. L., Fairbairn, D., Munier, S., and Calvet, J.-C.: An Ensemble Square Root Filter for the joint assimilation of surface soil moisture and leaf area index within LDAS-Monde: application over the Euro-Mediterranean region, *Hydrol. Earth Syst. Sci. Discuss.*, <https://doi.org/10.5194/hess-2019-391>, [accepted in review](#), 2020+19.
- 2325 Boone, A.; Masson, V.; Meyers, T.; Noilhan, J. The influence of the inclusion of soil freezing on simulations by a soil-vegetation-atmosphere transfer scheme. *J. Appl. Meteorol.*, 39, 1544–1569, 2000.
- Boone, A. and Etchevers, P.: An intercomparison of three snow schemes of varying complexity coupled to the same land-surface model: local scale evaluation at an Alpine site, *J. Hydrometeorol.*, 2, 374–394, 2001.
- 2330 Boone, A., Samuelsson, P., Gollvik, S., Napoly, A., Jarlan, L., Brun, E., and Decharme, B.: The interactions between soil–biosphere–atmosphere land surface model with a multi-energy balance (ISBA-MEB) option in SURFEXv8 – Part 1: Model description, *Geosci. Model Dev.*, 10, 843–872, <https://doi.org/10.5194/gmd-10-843-2017>, 2017.
- 2335 Bruce, J.P., Natural disaster reduction and global change. *Bulletin of the American Meteorological Society*, 75(10): 1831–1835, 1994.
- Bureau of Meteorology Special Climate Statement 70: Drought conditions in eastern Australia and impact on water resources in the Murray–Darling Basin, Issued 9 April 2019, <http://www.bom.gov.au/climate/current/statements/scs70.pdf>, 2019.
- 2340 Calvet, J.-C.; Noilhan, J.; Roujean, J.-L.; Bessemoulin, P.; Cabelguenne, M.; Olioso, A.; Wigneron, J.-P. An interactive vegetation SVAT model tested against data from six 780 contrasting sites. *Agric. For. Meteorol*, 92, 73–95, 1998.
- Calvet, J.-C.; Rivalland, V.; Picon-Cochard, C.; Guehl, J.-M. Modelling forest transpiration and CO2 fluxes—Response to soil moisture stress. *Agric. For. Meteorol*, 124, 143–156, 2004.



- 2345 Cook, E.R., Seager, R., Cane, M.A. and Stahle, D.W., North American drought: reconstructions, causes, and consequences. *Earth Science Reviews*, 81(1): 93–134, 2007.
- de Jeu, R.A.; Wagner, W.; Holmes, T.R.H.; Dolman, A.J.; Van De Giesen, N.C.; Friesen, J. Global soil moisture patterns observed by space borne microwave radiometers and scatterometers. *Surv. Geophys.*, 29, 399–420, 2008.
- 2350 de Rosnay, P. A simplified Extended Kalman Filter for the global operational soil moisture analysis at ECMWF. *Q. J. R. Meteorol. Soc.*, 139, 1199–1213, doi: [10.1002/qj.2023](https://doi.org/10.1002/qj.2023), 2013.
- de Rosnay, P.; Balsamo, G.; Albergel, C.; Muñoz-Sabater, J.; Isaksen, L. Initialisation of land surface variables for numerical weather prediction. *Surv. Geophys.*, 35, 607–621, doi: [10.1007/s10712-012-9207-x](https://doi.org/10.1007/s10712-012-9207-x), 2014.
- 2355 [Desroziers, G.; Berre, L.; Chapnik, B.; Poli, P. Diagnosis of observation, background and analysis-error statistics in observation space. \*Q. J. Roy. Meteor. Soc.\*, 131, 3385–3396, 2005.](https://doi.org/10.1002/qj.2023)
- Di Napoli, C., F. Pappenberger, and H.L. Cloke: Verification of Heat Stress Thresholds for a Health-Based Heat-Wave Definition. *J. Appl. Meteor. Climatol.*, 58, 1177–1194, <https://doi.org/10.1175/JAMC-D-18-0246.1>, 2019.
- 2360 Decharme, B., Boone, A., Delire, C., and Noilhan, J.: Local evaluation of the Interaction between soil biosphere atmosphere soil multilayer diffusion scheme using four pedotransfer functions, *J. Geophys. Res.*, 116, D20126, <https://doi.org/10.1029/2011JD016002>, 2011.
- Decharme, B.; Martin, E.; Faroux, S. Reconciling soil thermal and hydrological lower boundary conditions in land surface models. *J. Geophys. Res. Atmos.*, 118, 7819–7834, 2013.
- 2365 Decharme, B., Brun, E., Boone, A., Delire, C., Le Moigne, P., and Morin, S.: Impacts of snow and organic soils parameterization on northern Eurasian soil temperature profiles simulated by the ISBA land surface model, *The Cryosphere*, 10, 853–877, <https://doi.org/10.5194/tc-10-853-2016>, 2016.
- Decharme, B., Delire, C., Minvielle, M., Colin, J., Vergnes, J.-P., Alias, A., Saint-Martin, D., Séférian, R., Sénési, S. and Voldoire, A.: Recent changes in the ISBA-CTRIP Land Surface System for use in the CNRM-CM6 climate model and in global off-line hydrological applications, *J. Adv. Model Earth Sy.*, 11, 1207-1252, [10.1029/2018MS001545](https://doi.org/10.1029/2018MS001545), 2019.
- 2370 Dee, D.P.; Uppala, S.M.; Simmons, A.J.; Berrisford, P.; Poli, P.; Kobayashi, S.; Andrae, U.; Balmaseda, M.A.; Balsamo, G.; Bauer, D.P. The ERA-Interim reanalysis: Configuration and performance of the data assimilation system. *Q. J. R. Meteorol. Soc.*, 137, 553–597, 2011.
- 2375 Dirmeyer, P. A., Gao, X., Zhao, M., Guo, Z., Oki, T., and Hanasaki N.: The Second Global Soil Wetness Project (GSWP-2): Multi-model analysis and implications for our perception of the land surface, *B. Am. Meteorol. Soc.*, 87, 1381–1397, <https://doi.org/10.1175/BAMS-87-10-1381>, 2006.
- 2380 Dorigo, W. A., Wagner, W., Hohensinn, R., Hahn, S., Paulik, C., Xaver, A., Gruber, A., Drusch, M., Mecklenburg, S., van Oevelen, P., Robock, A., and Jackson, T.: The International Soil Moisture Network: a data hosting facility for global in situ soil moisture measurements, *Hydrol. Earth Syst. Sci.*, 15, 1675-1698, <https://doi.org/10.5194/hess-15-1675-2011>, 2011.
- Dorigo, W.A., A. Gruber, R.A.M. De Jeu, W. Wagner, T. Stacke, A. Loew, C. Albergel, L. Brocca, D. Chung, R.M. Parinussa and R. Kidd: Evaluation of the ESA CCI soil moisture product using ground-based observations, *Remote Sensing of Environment*, <http://dx.doi.org/10.1016/j.rse.2014.07.023>, 2015.
- 2385 [Draper, C. S., Mahfouf, J.-F., and Walker, J. P.: An EKF assimilation of AMSR-E soil moisture into the ISBA land surface scheme, \*J. Geophys. Res.\*, 114, D20104, <https://doi.org/10.1029/2008JD011650>, 2009.](https://doi.org/10.1029/2008JD011650)

- 2390 | Draper, C.; Mahfouf, J.-F.; Calvet, J.-C.; Martin, E.; Wagner, W. Assimilation of ASCAT near-surface soil moisture into the SIM hydrological model over France. *Hydrol. Earth Syst. Sci.*, 15, 3829–3841, 2011.
- | Draper, C. S., R. H. Reichle, and R. D. Koster, Assessment of MERRA-2 Land Surface Energy Flux Estimates, *Journal of Climate*, 31, 671-691, doi:10.1175/JCLI-D-17-0121.1, 2018.
- 2395 | Faroux, S.; Kaptué Tchuenté, A.T.; Roujean, J.-L.; Masson, V.; Martin, E.; Moigne, P.L. ECOCLIMAP-II/Europe: A twofold database of ecosystems and surface parameters at 1 km resolution based on satellite information for use in land surface, meteorological and climate models. *Geosci. Model Dev.*, 6, 563–582, 2013.
- 2400 | Fairbairn, D., Barbu, A. L., Mahfouf, J.-F., Calvet, J.-C. and Gelati, E.: Comparing the ensemble and extended Kalman filters for in situ soil moisture assimilation with contrasting conditions, *Hydrol. Earth Syst. Sci.*, 19, 4811–4830, doi: [10.5194/hess-19-4811-2015](https://doi.org/10.5194/hess-19-4811-2015), 2015.
- | Fairbairn, D.; Barbu, A.L.; Napoly, A.; Albergel, C.; Mahfouf, J.-F.; Calvet, J.-C. The effect of satellite-derived surface soil moisture and leaf area index land data assimilation on streamflow simulations over France. *Hydrol. Earth Syst. Sci.*, 21, 2015–2033, 2017.
- 2405 | Fox, A.M.; Hoar, T.J.; Anderson, J.L.; Arellano, A.F.; Smith, W.K.; Litvak, M.E.; MacBean, N.; Schimel, D.S.; Moore, D.J.P. Evaluation of a Data Assimilation System for Land Surface Models using CLM4.5. *J. Adv. Model. Earth Syst.*, 10, 2471–2494, 2018.
- | Gibelin, A.-L.; Calvet, J.-C.; Roujean, J.-L.; Jarlan, L.; Los, S.O. Ability of the land surface model ISBA-A-gs to simulate leaf area index at global scale: Comparison with satellite products. *J. Geophys. Res.*, 111, 1–16, 2006.
- 2410 | Gruber, A.; Su, C.-H.; Zwieback, S.; Crow, W.; Dorigo, W.; Wagner, W. Recent advances in (soil moisture) triple collocation analysis. *Int. J. Appl. Earth Obs. Geoinf.*, 45, 200–211, 2016.
- 2415 | Hersbach, H., de Rosnay, P. Bell, B., Schepers, D., Simmons, S., Soci, S., Abdalla, S., Alonso Balmaseda, M., Balsamo, G., Bechtold, P., Berrisford, P., Bidlot, J., de Boissésou, E., Bonavita, M., Browne, P., Buizza, R., Dahlgren, P., Dee, D., Dragani, R., Diamantakis, M., Flemming, J., Forbes, R., Geer, A., Haiden, T., Hólm, E., Haimberger, L., Hogan, R., Horányi, A., Janisková, M., Laloyaux, P., Lopez, P., Muñoz-Sabater, J., Peubey, C., Radu, R., Richardson, D., Thépaut, J.-N., Vitart, F., Yang, X., Zsótér, E. and Zuo H. Operational global reanalysis: Progress, future directions and synergies with NWP. *ERA Rep. Ser.*, 27, 65., 2018.
- 2420 | Hersbach, H., B. Bell, P. Berrisford, S. Hirahara, A. Horanyi, J. Muñoz-Sabater, J. Nicolas, C. Peubey, R. Radu, D. Schepers, A. Simmons, C. Soci, S. Abdalla, X. Abellan, G. Balsamo, P. Bechtold, G. Biavati, J. Bidlot, M. Bonavita, G. De Chiara, P. Dahlgren, D. Dee, M. Diamantakis, R. Dragani, J. Flemming, R. Forbes, M. Fuentes, A. Geer, L. Haimberger, S. Healy, R. J. Hogan, E. Holm, M. Janiskova, S. Keeley, P. Laloyaux, P. Lopez, G. Radnoti, P. de Rosnay, I. Rozum, F. Vamborg, S. Villaume, J.-N. Thépaut: The ERA5 Global Reanalysis, *QJRMS*, submitted, 2019
- 2425 | IPCC: Managing the Risks of Extreme Events and Disasters to Advance Climate Change Adaptation. A Special Report of Working Groups I and II of the Intergovernmental Panel on Climate Change . Cambridge University Press, Cambridge, UK, and New York, NY, USA, 582 pp, 2012.
- 2430 | IPCC: Climate change 2014: Synthesis Report. Contribution of Working Groups I, II and III to the Fifth Assessment Report of the Intergovernmental Panel on Climate Change [Core Writing Team, R.K. Pachauri and L.A. Meyer (eds.)]. IPCC, Geneva, Switzerland, 151 pp, 2014.

- Jacobs, C.M.J.; van den Hurk, B.J.J.M.; de Bruin, H.A.R. Stomatal behaviour and photosynthetic rate of unstressed grapevines in semi-arid conditions. *Agric. For. Meteorol.* 80, 111–134, 1996.
- 2435 Jarlan, L., Balsamo, G., Lafont, S., Beljaars, A., Calvet, J.-C., and Mougin, E.: Analysis of leaf area index in the ECMWF land surface model and impact on latent heat on carbon fluxes: Application to West Africa, *J. Geophys. Res.*, 113, D24117, doi:10.1029/2007JD009370, 2008.
- Joiner, J.; Yoshida, Y.; Guanter, L.; Middleton, E.M. New methods for the retrieval of chlorophyll red fluorescence from hyperspectral satellite instruments: Simulations and application to GOME-2 and SCIAMACHY. *Atmos. Meas. Tech.* 2016, 9, 3939–3967, 2016.
- 2440 Jung, M., Reichstein, M., Schwalm, C. R., Huntingford, C., Sitch, S., Ahlström, A., Arneft, A., Camps-Valls, G., Ciais, P., Friedlingstein, P., Gans, F., Ichii, K., Jain, A. K., Kato, E., Papale, D., Poulter, B., Raduly, B., Rödenbeck, C., Tramontana, G., Viovy, N., Wang, Y.-P., Weber, U., Zaehle, S., and Zeng, N.: Compensatory water effects link yearly global land CO<sub>2</sub> sink changes to temperature, *Nature*, 541, 516–520, <https://doi.org/10.1038/nature20780>, 2017.
- 2445 Ionita, M., Tallaksen, L. M., Kingston, D. G., Stagge, J. H., Laaha, G., Van Lanen, H. A. J., Scholz, P., Chelcea, S. M., and Haslinger, K.: The European 2015 drought from a climatological perspective, *Hydrol. Earth Syst. Sci.*, 21, 1397-1419, <https://doi.org/10.5194/hess-21-1397-2017>, 2017.
- 2450 Kaminski, T. Assimilating atmospheric data into a terrestrial biosphere model: A case study of the seasonal cycle. *Glob. Biogeochem. Cycles*, 16, 2002.
- Kidd, R.; Makhmara, H.; Paulik, C. GIO GL1 PUM SWI I1.00.pdf., p. 25. Available online: <http://land.copernicus.eu/global/products/SWI/Documents/ProductUserManual> (accessed on 1 June 2019), 2013.
- 2455 Kumar, S.V., B.F. Zaitchik, C.D. Peters-Lidard, M. Rodell, R. Reichle, B. Li, M. Jasinski, D. Mocko, A. Getirana, G. De Lannoy, M.H. Cosh, C.R. Hain, M. Anderson, K.R. Arsenault, Y. Xia, and M. Ek: Assimilation of Gridded GRACE Terrestrial Water Storage Estimates in the North American Land Data Assimilation System. *J. Hydrometeor.*, 17, 1951–1972, <https://doi.org/10.1175/JHM-D-15-0157.1>, 2016
- 2460 Kumar, S.V.; Jasinski, M.; Mocko, D.; Rodell, M.; Borak, J.; Li, B.; Kato Beaudoin, H.; Peters-Lidard, C.D. NCA-LDAS land analysis: Development and performance of a multisensor, multi-variate land data assimilation system for the National Climate Assessment. *J. Hydrometeorol.*, doi:10.1175/JHM-D-17-0125.1., 2018.
- 2465 Kumar, S.V., D.M. Mocko, S. Wang, C.D. Peters-Lidard, and J. Borak, 0: Assimilation of remotely sensed Leaf Area Index into the Noah-MP land surface model: Impacts on water and carbon fluxes and states over the Continental U.S.. *J. Hydrometeorol.*, <https://doi.org/10.1175/JHM-D-18-0237.1>, 2019.
- Koster, R.D.; Mahanama, S.P.P.; Livneh, B.; Lettenmaier, D.P.; Reichle, R.H. Skill in streamflow forecasts derived from large-scale estimates of soil moisture and snow. *Nat. Geosci. Lett.*, 3, 613–616, 2010.
- 2470 Lahoz, W.; De Lannoy; G. Closing the gaps in our knowledge of the hydrological cycle over land: Conceptual problems. *Surv. Geophys.*, 35, 577–606, 2014.
- Leroux, D.J.; Calvet, J.-C.; Munier, S.; Albergel, C. Using Satellite-Derived Vegetation Products to Evaluate LDAS-Monde over the Euro-Mediterranean Area. *Remote Sens.*, 10, 1199, 2014.
- 2475 Luo, L.; Wood, E.F. Monitoring and predicting the 2007 U.S. drought. *Geophysical Research Letters*, 34. doi:10.1029/2007GL031673, 2007.

- Magnusson, L.; Ferranti, L.; Vamborg, F. Forecasting the 2018 European heatwave. *ECMWF Newslett.*, 157, 4, 2018.
- 2480 Mahfouf, J.-F.; Bergaoui, K.; Draper, C.; Bouyssel, F.; Taillefer, F.; Taseva, L. A comparison of two off-line soil analysis schemes for assimilation of screen level observations. *J. Geophys. Res.*, 114, D08105, 2009.
- Martens, B., Miralles, D. G., Lievens, H., van der Schalie, R., de Jeu, R. A. M., Fernández-Prieto, D., Beck, H. E., Dorigo, W. A., and Verhoest, N. E. C.: GLEAM v3: satellite-based land evaporation and root-zone soil moisture, *Geosci. Model Dev.*, 10, 1903–1925, <https://doi.org/10.5194/gmd-10-1903-2017>, 2017.
- 2485 Massari, C.; Camici, S.; Ciabatta, L.; Brocca, L. Exploiting Satellite-Based Surface Soil Moisture for Flood Forecasting in the Mediterranean Area: State Update Versus Rainfall Correction. *Remote Sens.*, 10, 292, 2018.
- 2490 Masson, V., Le Moigne, P., Martin, E., Faroux, S., Alias, A., Alkama, R., Belamari, S., Barbu, A., Boone, A., Bouyssel, F., Brousseau, P., Brun, E., Calvet, J.-C., Carrer, D., Decharme, B., Delire, C., Donier, S., Essaouini, K., Gibelin, A.-L., Giordani, H., Habets, F., Jidane, M., Kerdraon, G., Kourzeneva, E., Lafaysse, M., Lafont, S., Lebeaupin Brossier, C., Lemonsu, A., Mahfouf, J.-F., Marguinaud, P., Mokhtari, M., Morin, S., Pigeon, G., Salgado, R., Seity, Y., Taillefer, F., Tanguy, G., Tulet, P., Vincendon, B., Vionnet, V., and Voldoire, A.: The SURFEXv7.2 land and ocean surface platform for coupled or offline simulation of earth surface variables and fluxes, *Geosci. Model Dev.*, 6, 929–960, <https://doi.org/10.5194/gmd-6-929-2013>, 2013.
- 2495 McNally, A., Arsenault, K., Kumar, S., Shukla, S., Peterson, P., Wang, S., Funk, C., Peters-Lidard, C.P., Verdin, J.P. A land data assimilation system for sub-Saharan Africa food and water security applications. *Sci. Data* 4:170012 <https://doi.org/10.1038/sdata.2017.12>, 2017
- 2500 Mishra, A.K. and Singh, V.P., A review of drought concepts. *Journal of Hydrology*, 391(1): 202–216, 2010.
- Miralles, D.G., De Jeu, R.A.M., Gash, J.H., Holmes, T.R.H., Dolman, A.J., Magnitude and variability of land evaporation and its components at the global scale. *Hydrol. Earth Syst. Sci.* 15 (3), 967–981. <http://dx.doi.org/10.5194/hess-15-967-2011>, 2011.
- 2505 Nash, J. E. and Sutcliffe, V.: River forecasting through conceptual models, *J. Hydrol.*, 10, 282–290, 1970.
- Noilhan, J. and Planton, S.: A simple parameterization of land surface processes for meteorological models. *Mon. Weather Rev.*, 117, 536–549, doi: [10.1175/1520-0493\(1989\)117<0536%3AASPOLS>2.0.CO;3B2](https://doi.org/10.1175/1520-0493(1989)117<0536%3AASPOLS>2.0.CO;3B2), 1989.
- 2510 Noilhan, J.; Mahfouf, J.-F. The ISBA land surface parameterisation scheme. *Glob. Planet. Chang.*, 13, 145–159, 1996
- Muñoz-Sabater, J. , Lawrence, H. , Albergel, C. , de Rosnay, P. , Isaksen, L. , Mecklenburg, S. , Kerr, Y. and Drusch, M., Assimilation of SMOS brightness temperatures in the ECMWF Integrated Forecasting System. *Q J R Meteorol Soc.* Accepted Author Manuscript. doi:[10.1002/qj.3577](https://doi.org/10.1002/qj.3577), 2019.
- 2515 Munro, R.; Eisinger, M.; Anderson, C.; Callies, J.; Corpaccioli, E.; Lang, R.; Lefebvre, A.; Livschitz, Y.; Perez Albinana, A. GOME-2 on MetOp: From In-Orbit Verification to Routine Operations. In *Proceedings of the EUMETSAT Meteorological Satellite Conference*, Helsinki, Finland, 12–16 June 2006.
- Obasi, G.O.P., WMO's role in the international decade for natural disaster reduction. *Bulletin of the American Meteorological Society*, 75(9): 1655–1661, 1994.

- 2520 Orsolini, Y., Wegmann, M., Dutra, E., Liu, B., Balsamo, G., Yang, K., de Rosnay, P., Zhu, C., Wang, W., and Senan, R.: Evaluation of snow depth and snow-cover over the Tibetan Plateau in global reanalyses using in-situ and satellite remote sensing observations, *The Cryosphere Discuss.*, <https://doi.org/10.5194/tc-2019-49>, in review, 2019.
- 2525 Reichle, R.H.; Koster, R.D.; Liu, P.; Mahanama, S.P.P.; Njoku, E.G.; Owe, M. Comparison and assimilation of global soil moisture retrievals from the Advanced Microwave Scanning Radiometer for the Earth Observing System (AMSR-E) and the Scanning Multichannel Microwave Radiometer (SMMR). *J. Geophys. Res.*, 112, D09108, doi:10.1029/2006JD008033, 2007.
- 2530 Reichle, R. H., C. S. Draper, Q. Liu, M. Girotto, S. P. P. Mahanama, R. D. Koster, and G. J. M. De Lannoy, Assessment of MERRA-2 land surface hydrology estimates, *Journal of Climate*, [30, 2937-2960](https://doi.org/10.1175/JCLI-D-16-0720.1), doi:10.1175/JCLI-D-16-0720.1, 2017.
- Reichle, R. H., Liu, Q., Koster, R. D., Crow, W. T., De Lannoy, G. J. M., Kimball, J. S., Ardizzone, J.V., Bosch, D., Colliander, A., Cosh, M., Kolassa, J., Mahanama, S.P., Prueger, J., Starks, P., Walker, J.P., Version 4 of the SMAP Level-4 Soil Moisture Algorithm and Data Product. *Journal of Advances in Modeling Earth Systems*, 11. <https://doi.org/10.1029/2019MS001729>, 2019.
- 2535 Rodell, M.; Houser, P.R.; Jambor, U.; Gottschalck, J.; Mitchell, K.; Meng, C.-J.; Arsenault, K.; Cosgrove, B.; Radakovich, J.; Bosilovich, M.; Entin, J.K., Walker, J.P., Lohmann, D., and Toll, D. The Global Land Data Assimilation System. *Bull. Am. Meteor. Soc.* 85, 381–394, 2004.
- 2540 Rodríguez-Fernández, N.; de Rosnay, P.; Albergel, C.; Richaume, P.; Aires, F.; Prigent, C.; Kerr, Y. SMOS Neural Network Soil Moisture Data Assimilation in a Land Surface Model and Atmospheric Impact. *Remote Sens.*, 11, 1334. <https://doi.org/10.3390/rs11111334>, 2019.
- Rüdiger, C.; Albergel, C.; Mahfouf, J.-F.; Calvet, J.-C.; Walker, J.P. Evaluation of Jacobians for leaf area index data assimilation with an extended Kalman filter. *J. Geophys. Res.* 2010.
- Sawada, Y.; Koike, T. Simultaneous estimation of both hydrological and ecological parameters in an ecohydrological model by assimilating microwave signal. *J. Geophys. Res. Atmos.* 119, 2014.
- 2545 Sawada, Y.; Koike, T.; Walker, J.P. A land data assimilation system for simultaneous simulation of soil moisture and vegetation dynamics. *J. Geophys. Res. Atmos.* 120, 2015.
- 2550 Schellekens, J., Dutra, E., Martínez-de la Torre, A., Balsamo, G., van Dijk, A., Sperna Weiland, F., Minvielle, M., Calvet, J.-C., Decharme, B., Eisner, S., Fink, G., Flörke, M., Peßenteiner, S., van Beek, R., Polcher, J., Beck, H., Orth, R., Calton, B., Burke, S., Dorigo, W., and Weedon, G. P.: A global water resources ensemble of hydrological models: the earth2Observe Tier-1 dataset, *Earth Syst. Sci. Data*, 9, 389-413, <https://doi.org/10.5194/essd-9-389-2017>, 2017.
- Scipal, K.; Drusch, M.; Wagner, W. Assimilation of a ERS scatterometer derived soil moisture index in the ECMWF numerical weather prediction system. *Adv. Water Resour.*, 31, 1101–1112, 2008.
- 2555 Schlosser, A.; Dirmeyer, P. Potential predictability of Eurasian snow cover. *Atmos. Sci. Lett.*, 2, 1–8, 2001.
- [Shamambo, D.C.; Bonan, B.; Calvet, J.-C.; Albergel, C.; Hahn, S. Interpretation of ASCAT Radar Scatterometer Observations Over Land: A Case Study Over Southwestern France. \*Remote Sens.\*, 11, 2842, 2019.](https://doi.org/10.3390/rs11112842)
- 2560 Svoboda, M. Drought Monitor. *Bulletin of the American Meteorological Society*, pp. 1181–1190. doi:10.1175/1520-0477(2002)083<1181:TDM>2.3.CO;2., 2002
- Tall, M.; Albergel, C.; Bonan, B.; Zheng, Y.; Guichard, F.; Dramé, M.S.; Gaye, A.T.; Sintondji, L.O.; Hountondji, F.C.C.; Nikiema, P.M.; Calvet, J.-C. Towards a Long-Term Reanalysis of Land

- Surface Variables over Western Africa: LDAS-Monde Applied over Burkina Faso from 2001 to 2018. *Remote Sens.*, 11, 735, 2019.
- 2565 Tramontana, G., Jung, M., Schwalm, C. R., Ichii, K., Camps-Valls, G., Ráduly, B., Reichstein, M., Arain, M. A., Cescatti, A., Kiely, G., Merbold, L., Serrano-Ortiz, P., Sickert, S., Wolf, S., and Papale, D.: Predicting carbon dioxide and energy fluxes across global FLUXNET sites with regression algorithms, *Biogeosciences*, 13, 4291–4313, <https://doi.org/10.5194/bg-13-4291-2016>, 2016.
- 2570 Urraca, R.; Huld, T.; Gracia-Amillo, A.; Martinez-de-Pison, F.J.; Kaspar, F.; Sanz-Garcia, A. Evaluation of global horizontal irradiance estimates from ERA5 and COSMO-REA6 reanalyses using ground and satellite-based data. *Sol. Energy*, 164, 339–354, 2018.
- Van Loon, A.F.: Hydrological drought explained. *WIREs Water*, 2:359–392, doi:10.1002/wat2.1085, 2015.
- 2575 Voldoire, A., Decharme, B., Pianezze, J., Lebeaupin Brossier, C., Sevault, F., Seyfried, L., Garnier, V., Bielli, S., Valcke, S., Alias, A., Accensi, M., Arduin, F., Bouin, M.-N., Ducrocq, V., Faroux, S., Giordani, H., Léger, F., Marsaleix, P., Rainaud, R., Redelsperger, J.-L., Richard, E., and Riette, S.: SURFEX v8.0 interface with OASIS3-MCT to couple atmosphere with hydrology, ocean, waves and sea-ice models, from coastal to global scales, *Geosci. Model Dev.*, 10, 4207-4227, <https://doi.org/10.5194/gmd-10-4207-2017>, 2017.
- 2580 Wagner, W.; Lemoine, G.; Rott, H. A method for estimating soil moisture from ERS scatterometer and soil data. *Remote Sens. Environ.*, 70, 191–207, 1999.
- Wilhite, D.A., Drought, a global assessment. Natural Hazards and Disasters Series, vol. 1. Routledge, London, UK, 2000.
- 2585 World Meteorological Organization (WMO) and Global Water Partnership (GWP). Benefits of action and costs of inaction: Drought mitigation and preparedness – a literature review (N. Gerber and A. Mirzabaev). Integrated Drought Management Programme (IDMP) Working Paper 1. WMO, Geneva, Switzerland and GWP, Stockholm, Sweden, 2017.
- 2590 Xia, Y., Mitchell, K., Ek, M., Sheffield, J., Cosgrove, B., Wood, E., Luo, L., Alonge, C., Wei, H., Meng, J., Livneh, B., Lettenmaier, D., Koren, V., Duan, Q., Mo, K., Fan, Y. and Mocko, D., Continental-scale water and energy flux analysis and validation for the North American Land Data Assimilation System project phase 2 (NLDAS-2): 1. Intercomparison and application of model products, *J. Geophys. Res.*, 117, D03109, doi:[10.1029/2011JD016048](https://doi.org/10.1029/2011JD016048), 2012.
- 2595 Xia, Y., Mitchell K., Ek M., Cosgrove B., Sheffield J., Luo L., Alonge C., Wei H., Meng J., Livneh B., Duan Q. and Lohmann D.; Continental-scale water and energy flux analysis and validation for North American Land Data Assimilation System project phase 2 (NLDAS-2): 2. Validation of model-simulated streamflow, *J. Geophys. Res.*, 117, D03110, doi:[10.1029/2011JD016051](https://doi.org/10.1029/2011JD016051), 2012.

**Tables**

2600 Table I: Continental hot spots for droughts and heat waves and number of monthly anomalies SSM and LAI below -1 standard deviation (stdev), above 1 stdev in 2018 with respect to the 2010-2018 period.

Region name	abbreviation	LON-W	LON-E	LAT-S	LAT-N	Number of monthly SSM anomalies below -1 (above 1) stdev	Number of monthly LAI anomalies below -1 (above 1) stdev
<b>Western-Europe</b>	<b>WEUR</b>	<b>-1</b>	<b>15</b>	<b>48</b>	<b>55</b>	<b>5(1)</b>	<b>5(0)</b>
Western Mediterranean	WMED	-10	15	35	45	0(7)	4(4)
Eastern Europe	EEUR	15	30	45	55	2(1)	0(2)
Balkans	BALK	15	30	40	45	3(3)	1(4)
Western Russia	WRUS	30	60	55	67	0(1)	1(3)
Lower Volga	LVOL	30	60	45	55	2(1)	2(1)
India	INDI	73	85	12	27	3(0)	2(1)
Southwestern China	SWCH	100	110	20	32	0(2)	0(6)
Northern China	NRCH	110	120	30	40	0(3)	0(4)
<b>Murray-Darling</b>	<b>MUDA</b>	<b>140</b>	<b>150</b>	<b>-37</b>	<b>-26</b>	<b>6(0)</b>	<b>7(0)</b>
California	CALF	-125	-115	30	42	2(0)	5(0)
Southern Plains	SPLN	-110	-90	25	37	0(3)	0(4)
Midwest	MIDW	-105	-85	37	50	1(2)	1(3)
Eastern North	ENRT	-85	-70	37	50	0(3)	0(7)
Nordeste	NDST	-44	-36	-20	-2	0(3)	1(2)
Pampas	PAMP	-64	-58	-36	-23	2(2)	2(0)
Sahel	SAHL	-18	25	13	19	2(0)	1(2)
<b>East Africa</b>	<b>EAFR</b>	<b>38</b>	<b>51</b>	<b>-4</b>	<b>12</b>	<b>2(3)</b>	<b>1(7)</b>
Southern Africa	SAFR	14	26	-35	-26	2(0)	2(1)

2605

Table II: Set up of the experiment used in this study. LDAS\_ERA5 and LDAS\_HRES have an analysis (assimilation of surface soil moisture, SSM, and leaf area index, LAI) and a model equivalent (open-loop, no assimilation), LDAS\_fc4 and LDAS\_fc8 are model runs initialized by either LDAS\_HRES open-loop or analysis. N/A stands for not applicable.

Experiments (time period)	Model version	Atmospheric forcing	Domain & spatial resolution	DA method	Assimilated observations	Observations operators Model equivalents	Control variables
LDAS_ERA5 (2010 to 2018)	ISBA Multi-layer soil model CO <sub>2</sub> -responsive version (Interactive vegetation)	ERA5	Global, ~0.25 °x 0.25°	SEKF	SSM (ASCAT)	Second layer of soil (1-4cm)	Layers of soil 2 to 8 (1-100cm)
LDAS_HRES (04/2016 to 12/2018)		IFS-HRES	North Western Europe ( <b>WEUR</b> ) and Murray-Darling River basin ( <b>MUDA</b> ) (see spatial extend in Table I) ~0.10° x 0.10°		LAI (GEOV1)	LAI	LAI
LDAS_fc4 (2017 to 2018)				N/A	N/A	N/A	N/A
LDAS_fc8 (2017 to 2018)		N/A	N/A	N/A	N/A		



2610 Table III: Evaluation datasets and associated metrics used in this study.

<b>Datasets used for the evaluation</b>	<b>Source</b>	<b>Metrics associated</b>
In situ measurements of soil moisture (ISMN Dorigo et al., 2011, 2015)	<a href="https://ismn.geo.tuwien.ac.at/en/">https://ismn.geo.tuwien.ac.at/en/</a>	<b>R for both absolute and anomaly time-series</b> , unbiased RMSD and bias
In situ measurements of river discharge	See Table S1	Nash Efficiency (NSE), Normalized Information Contribution (NIC) based on NSE,
In situ measurements of evapotranspiration (FLUXNET-2015)	<a href="http://fluxnet.fluxdata.org/data/fluxnet2015-dataset/">http://fluxnet.fluxdata.org/data/fluxnet2015-dataset/</a>	R, unbiased RMSD, Bias, NIC on R values
Satellite derived surface soil wetness index (ASCAT, Wagner et al., 1999, Bartalis et al., 2007)	<a href="http://land.copernicus.eu/global/">http://land.copernicus.eu/global/</a>	R and RMSD
Satellite derived Leaf Area Index (GEOV1, Baret et al., 2013)	<a href="http://land.copernicus.eu/global/">http://land.copernicus.eu/global/</a>	R and RMSD
Satellite-driven model estimates of land evapotranspiration (GLEAM, Martens et al., 2017)	<a href="http://www.gleam.eu">http://www.gleam.eu</a>	R and RMSD
Upscaled estimates of Gross Primary Production (GPP, Jung et al., 2017)	<a href="https://www.bgc-jenna.mpg.de/geodb/projects/Home.php">https://www.bgc-jenna.mpg.de/geodb/projects/Home.php</a>	R and RMSD
Solar Induced Fluorescence (SIF) from GOME-2 (Munro et al., 2006, Joiner et al., 2016)	See references	R
Interactive Multi-sensor Snow and Ice Mapping System (or IMS) snow cover	<a href="https://www.natice.noaa.gov/ims/">https://www.natice.noaa.gov/ims/</a>	Differences

## Figures

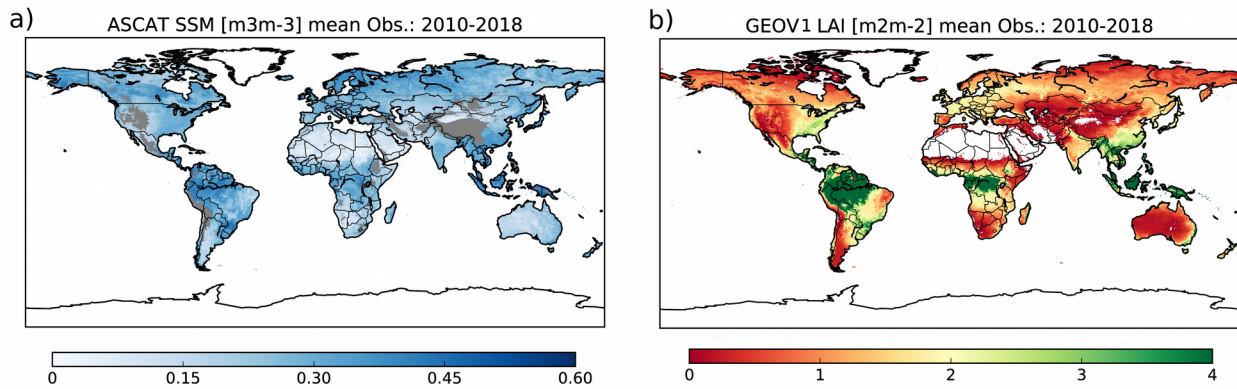


Figure 1: (a) Surface soil moisture (SSM) from the Copernicus Global Land Service (CGLS) for pixels with less than 15% of urban areas and with an elevation of less than 1500 m above sea level, (b) GEOV1 leaf area index (LAI) from CGLS, for pixels covered by more than 90 % of vegetation, averaged over 2010 to 2018. SSM is obtained after rescaling the ASCAT Soil Wetness Index (SWI) to the model climatology, grey areas on (a) represent filtered out data (see Section 2.3).

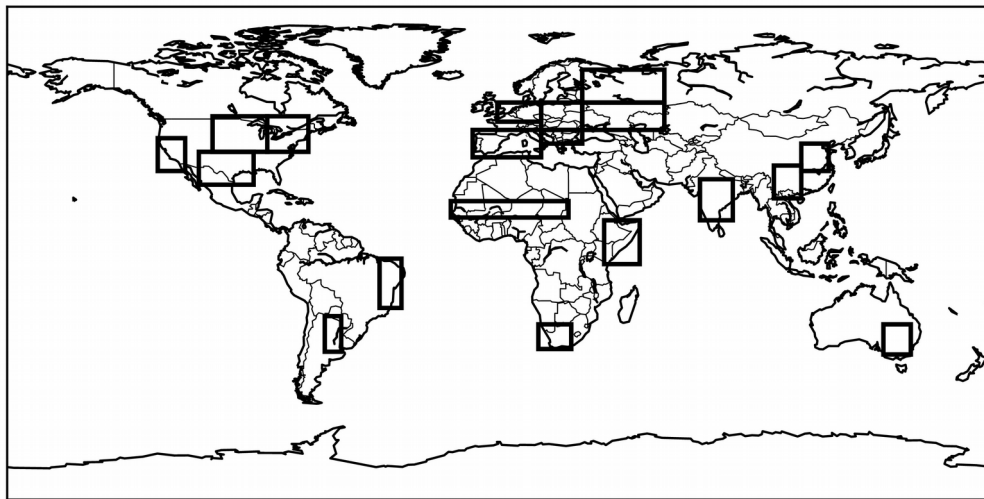


Figure 2: Selection of 19 regions across the globe known for being potential hot spots for droughts and heat waves, see section on experimental setup.

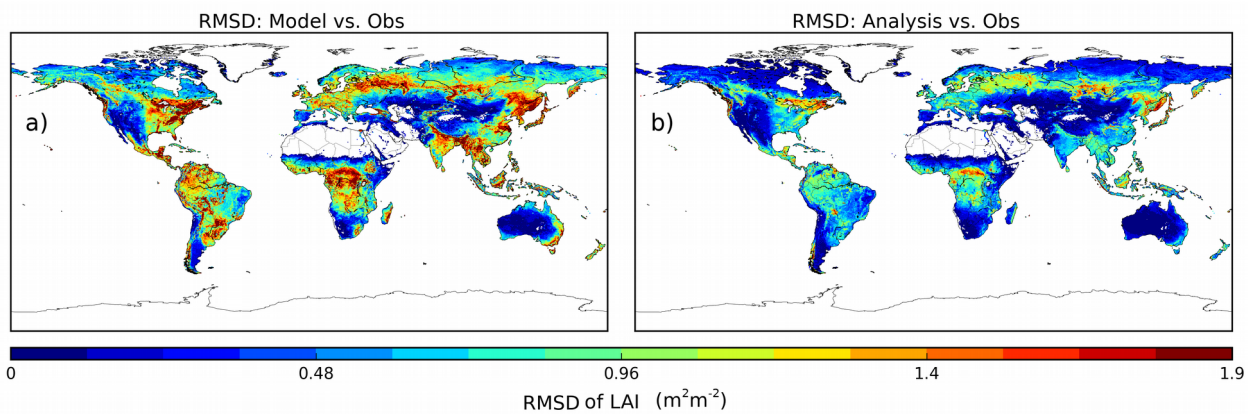


Figure 3: RMSD values between observed Leaf Area Index (LAI) and LDAS\_ERA5 (a) before assimilation and (b) after assimilation of surface soil moisture (SSM) and LAI.

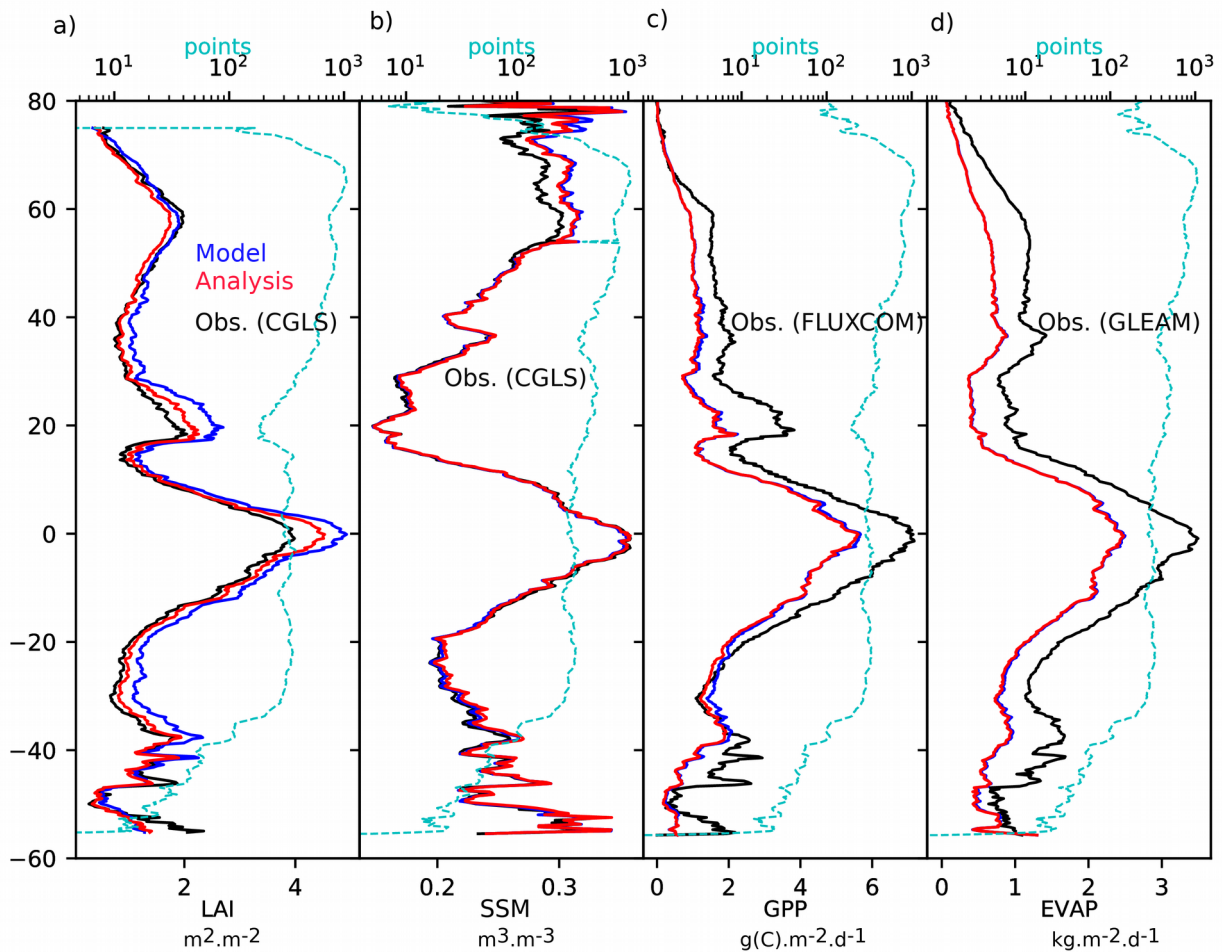


Figure 4: Latitudinal plots of (a) Leaf Area Index (LAI), (b) Surface Soil Moisture (SSM), (c) Gross Primary Production (GPP) and (d) Evapotranspiration for LDAS\_ERA5 before assimilation (Model, blue solid line) and after assimilation (Analysis, red solid line) as well as observations (black solid line). Cyan dashed line represents the number of points considered per latitudinal stripes of  $0.25^\circ$ .

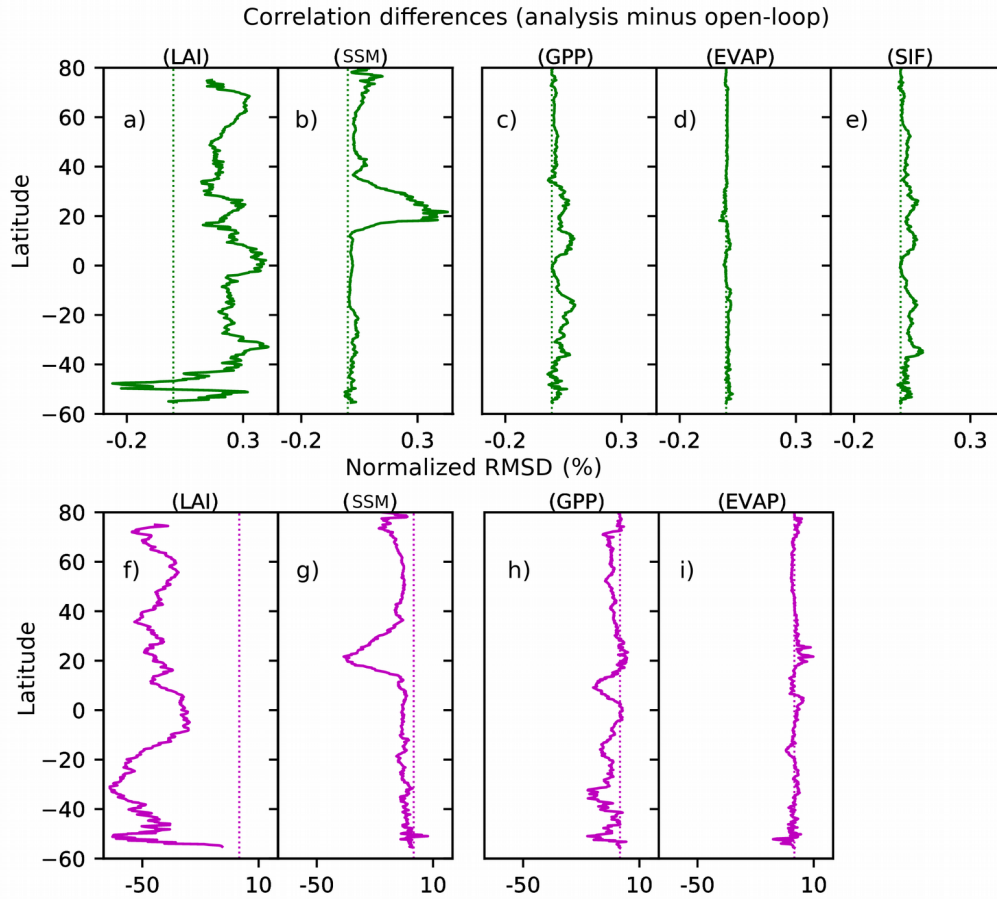


Figure 5: Latitudinal plots of score differences (analysis minus open-loop) for a) correlation, b) RMSD for Leaf Area Index (LAI), c) correlation, d) RMSD for Surface Soil Moisture (SSM 1-4 cm), e) correlation, f) normalized RMSD for Gross Primary Production (GPP), g) correlation, h) RMSD for evapotranspiration (EVAP) and i) correlation for Sun-Induced Fluorescence (SIF). Scores were computed based on monthly average over 2010-2018 for LAI and SSM, 2010-2013 for GPP, 2010-2016 for EVA and 2010-2015 for SIF. For SIF only differences in correlation are represented. Dashed lines represent the zero lines (equal scores for open-loop and analysis).

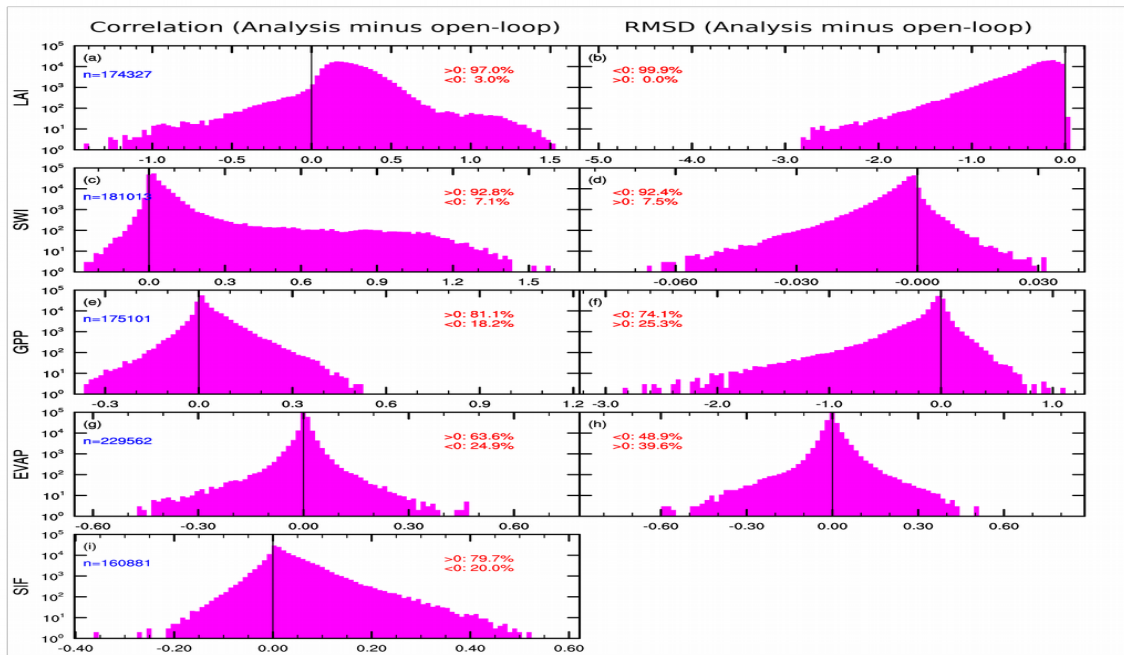
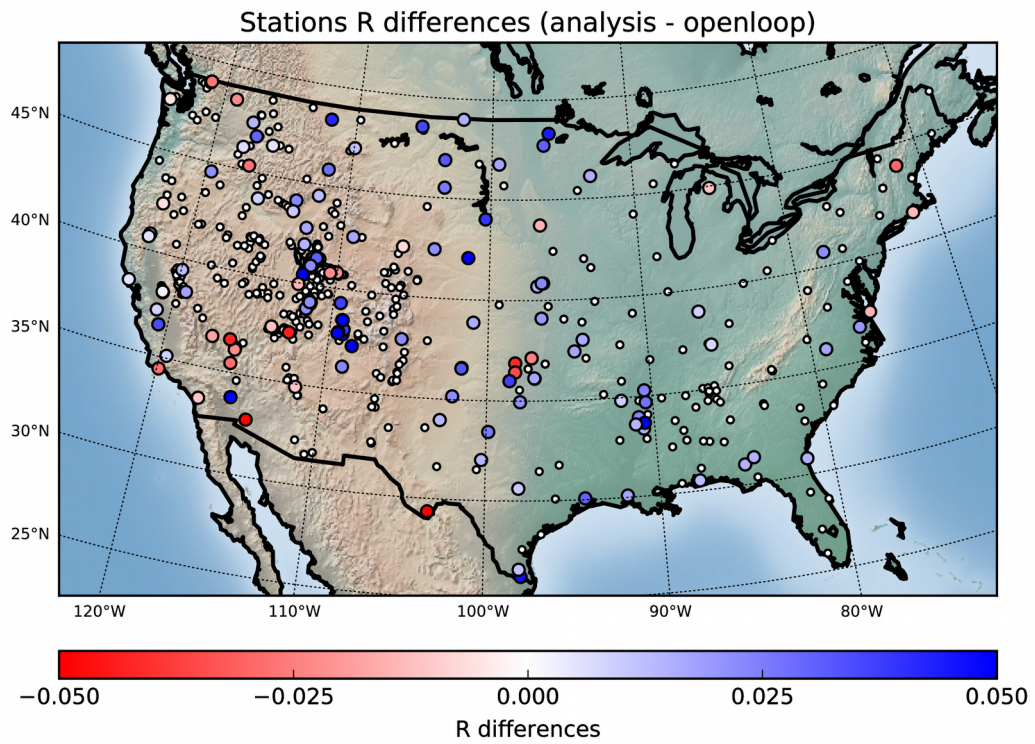


Figure 6: Histograms of score differences (correlation and RMSD, analysis minus open-loop) for a),b) Leaf Area Index (LAI), c),d) Surface Soil Moisture (SSM 1-4 cm), e),f) Gross Primary Production (GPP), g),h) evapotranspiration (EVAP) and i) Sun-Induced Fluorescence (SIF). Scores were computed based on monthly average over 2010-2018 for LAI and SSM, 2010-2013 for GPP, 2010-2016 for EVAP and 2010-2015 for SIF. For SIF only differences in correlation are represented. Number of available data (in blue) as well as the percentage of positive and negative values (in red) are reported. Note that for sake of clarity, the y-axis is logarithmic.

2635

2640



*Figure 7: Map of correlations (R) differences (analysis minus open-loop) for stations available over North America. Small dots represent stations where R differences are not significant (i.e. 95% confidence intervals are overlapping), large circles where differences are significant.*

2645

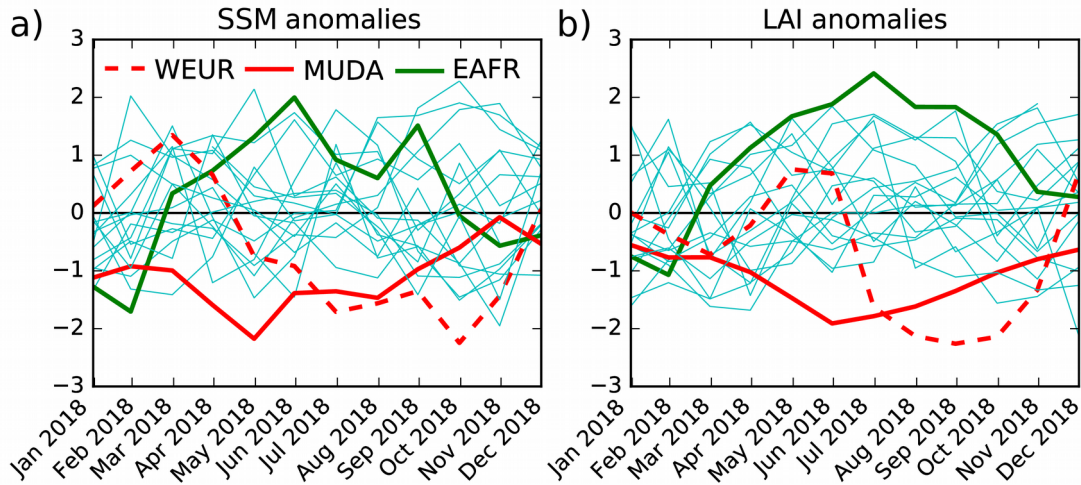


Figure 8: 2018 monthly anomalies scaled by standard deviation of analysed (a) Surface Soil Moisture (SSM, 1-4 cm) and (b) Leaf Area Index (LAI), with respect to 2010-2018, for the 19 regions presented in Table 1 and Figure 2. Solid red line, dashed red line and solid green line represent regions MUDA, WEUR and EAFR. Solid cyan line represent all other boxes (see Table 1 and Figure 2).



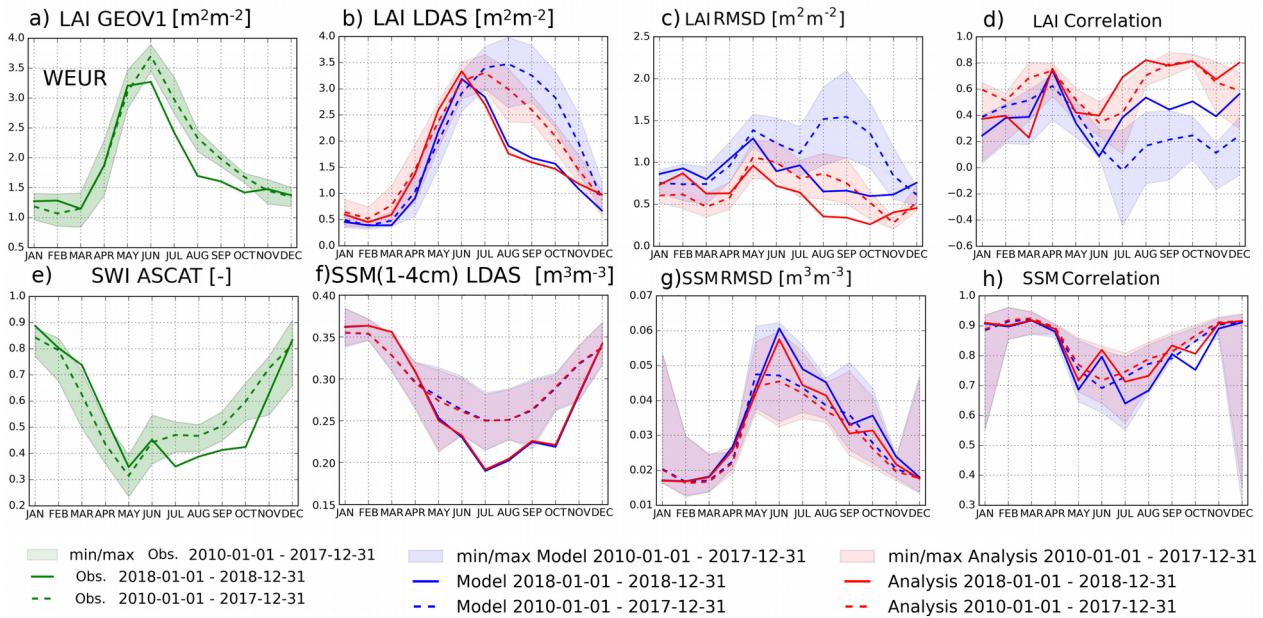


Figure 9: Seasonal cycles of a) observed Leaf Area Index (LAI) from the Copernicus Global Land Service (GEOV1, CGLS), b) LAI from the open-loop (in blue) and the analysis (in red), c) LAI RMSD values between either the open-loop or the analysis and the LAI GEOV1 for the Western Europe (WEUR) area (see Table I for geographical extent). d) same as (c) for correlation values. e), ASCAT Soil Wetness Index (SWI) from CGLS, f, g) and h) same as b), c) and d) for Surface Soil Moisture (SSM). Note that in g) and h) ASCAT SWI has been converted to SSM using the CDF-matching-technique seasonal linear rescaling discussed in section 2.3 on assimilated Earth Observations dataset. For each panels dashed line represents the averaged over 2010-2017 along with the minimum and maximum values, the solid line is for year 2018.

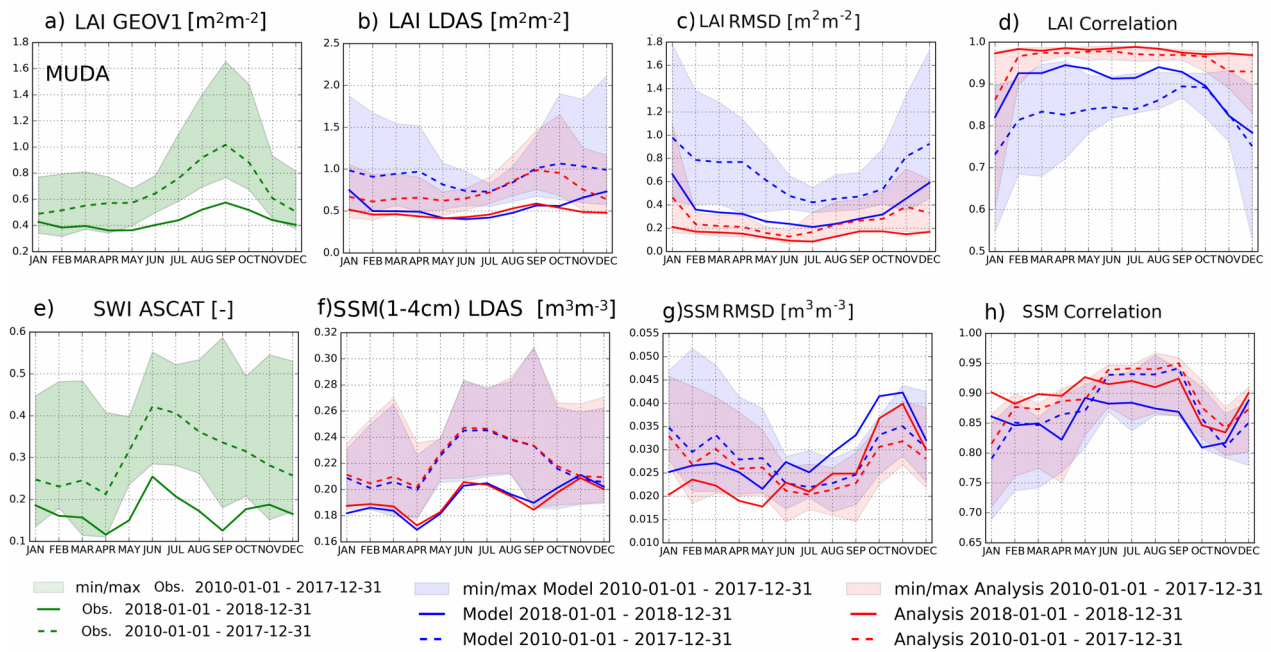


Figure 10: Same as Figure 9 for the Murray-Darling river (MUDA) area in south eastern Australia.

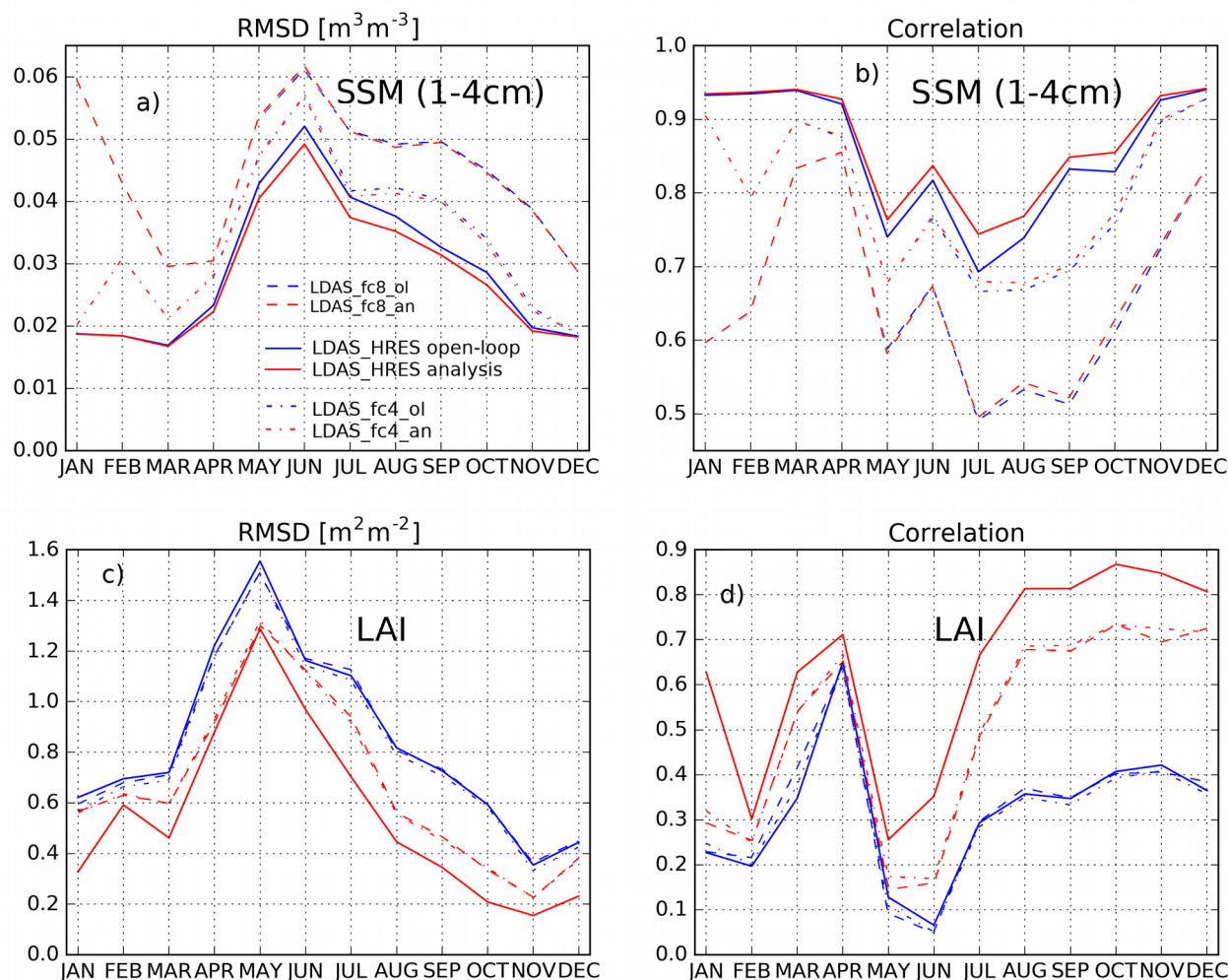


Figure 11: Upper panel, seasonal (a) root mean square differences (RMSD) and (b) correlation values between surface soil moisture (SSM) from the second layer of soil (1–4 cm) from the model forced by HRES (LDAS\_HRES, open-loop in blue solid line, analysis in red solid line) and ASCAT SSM estimates from the Copernicus Global Land Service project over 2017–2018 over the WEUR area. Scores between SSM from the second layer of soil of LDAS\_HRES 4-day (dashed/dotted blue – when initialised by the open-loop- and red – when initialised by the analysis- lines) and 8-day (dashed blue and red lines) forecasts and ASCAT SSM estimates are also reported. Lower panel (c) and (d), same as upper panel between modeled/analyzed Leaf Area index (LAI) and GEOV1 LAI estimates from the Copernicus Global Land Service project.

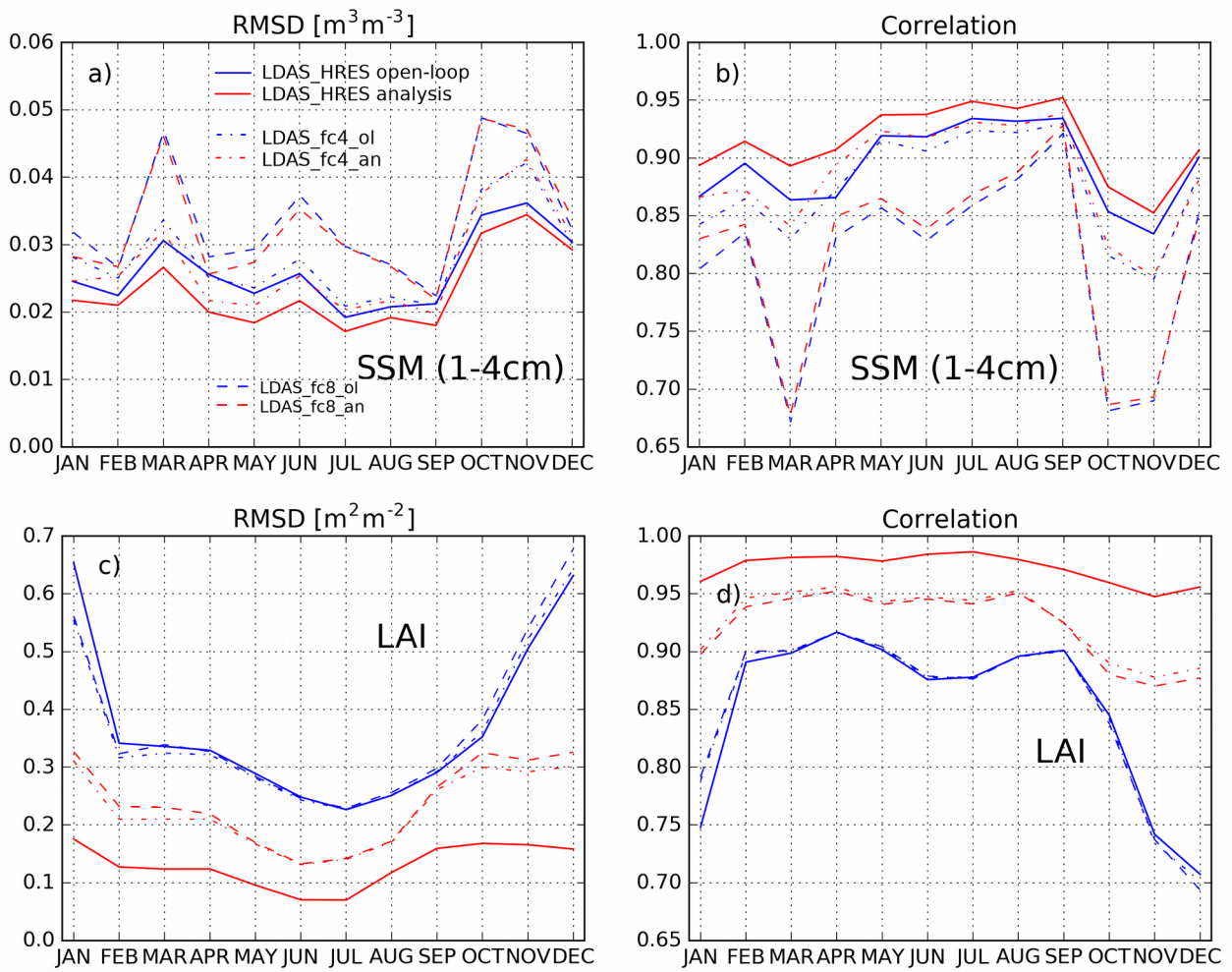


Figure 12: Same as Figure 11 for the Murray-Darling river (MUDA) area in southeastern Australia.

2660

2665

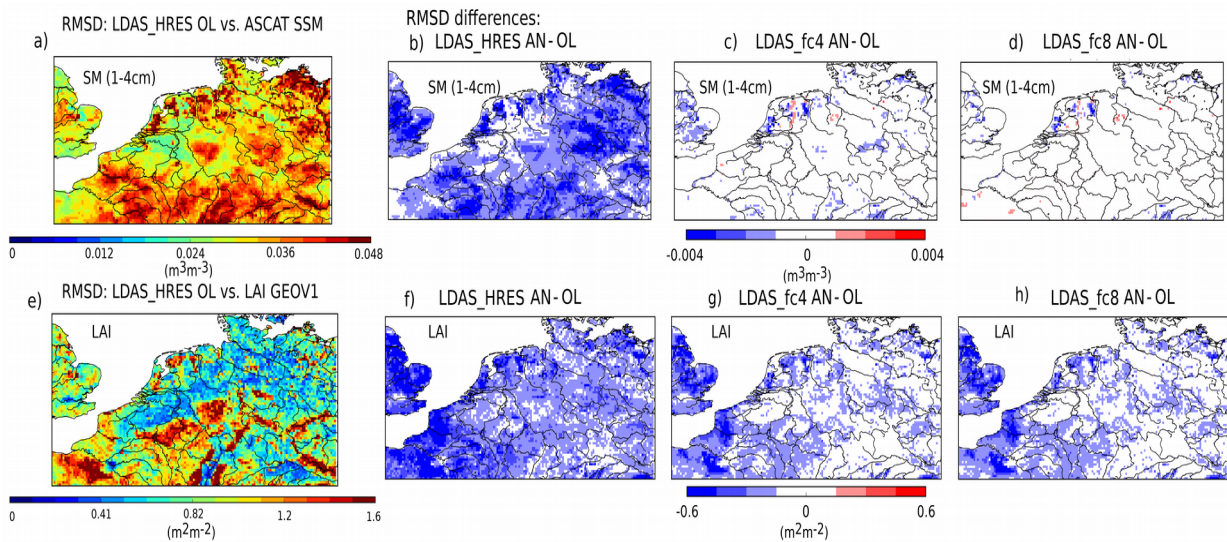


Figure 13: Top row, (a) RMSD values between LDAS\_HRES open-loop and ASCAT SSM estimates from the Copernicus Global Land Service (CGLS) over 2017-2018 for the WEUR domain, (b) RMSD differences between LDAS\_HRES analysis (open-loop) and ASCAT SSM. (c), (d) and (e) Same as (b) between LDAS\_fc4 initialised by the analysis (open-loop) and LDAS\_fc8. Bottom row, same as top row for Leaf Area Index (LAI) from the different experiments and LAI GEOV1.

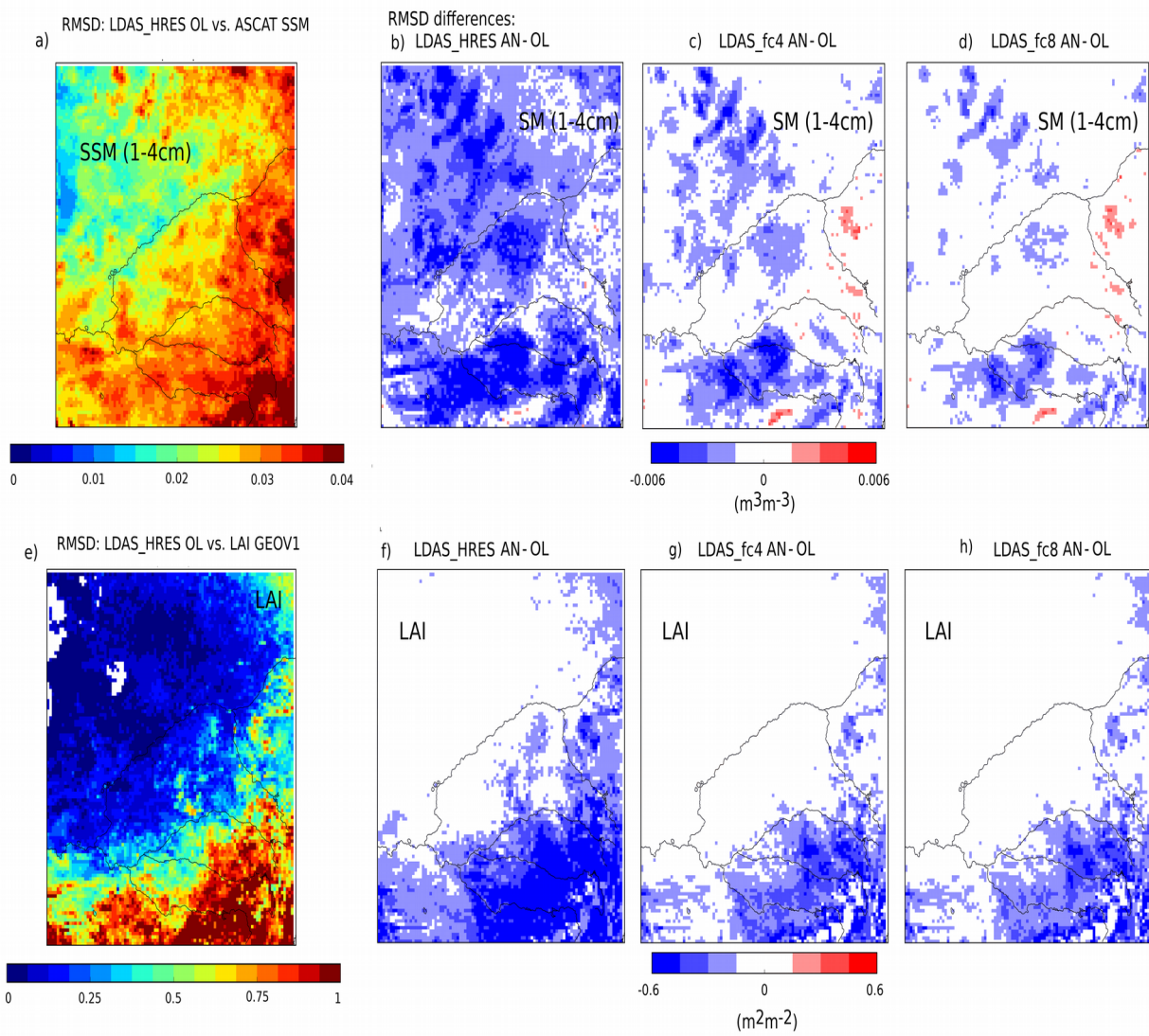
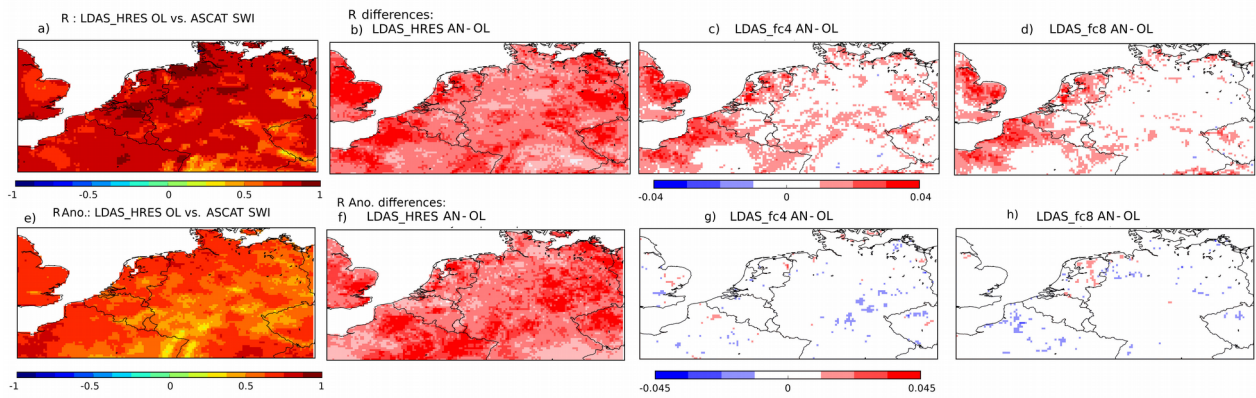
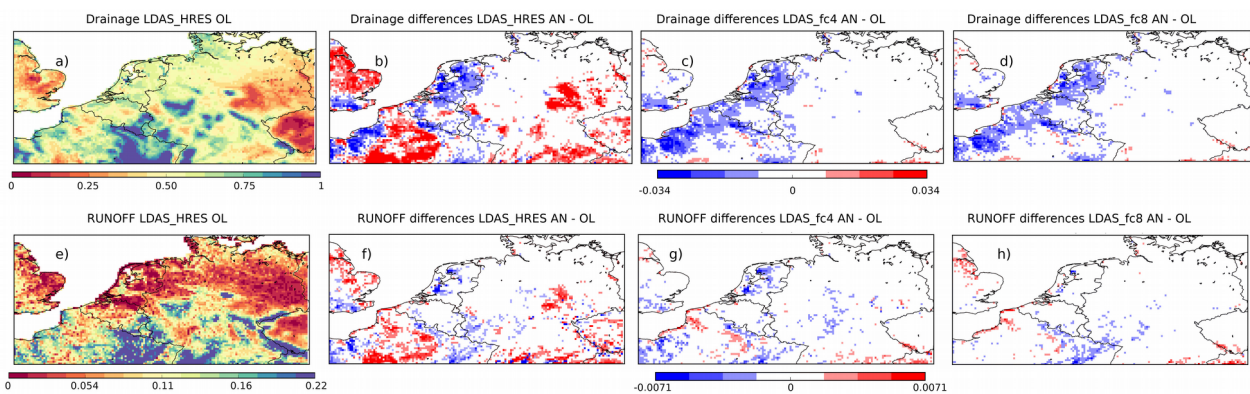


Figure 14: Same as Figure 13 or the Murray-Darling river (MUDA) area in south-eastern Australia.



**Figure 15:** Top row, (a) R values between LDAS HRES open-loop and ASCAT SWI estimates from the Copernicus Global Land Service (CGLS) over 2017-2018 for the WEUR domain, (b) R differences between LDAS HRES analysis (open-loop) and ASCAT SWI. (c) and (d) same as (b) between LDAS\_fc4 initialised by the analysis (open-loop) and LDAS\_fc8. Bottom row, same as top row for R values based on anomaly time-series.



**Figure 16:** Top row, (a) drainage values for LDAS HRES open-loop over 2017-2018 for the WEUR domain, (b) drainage differences between LDAS HRES analysis and open-loop. (c), (d), same as (b) between LDAS\_fc4 initialised by the analysis and LDAS\_fc4 initialised by the open-loop, between LDAS\_fc8 initialised by the analysis and LDAS\_fc8 initialised by the open-loop. Bottom row, same as top row for runoff. Units are  $\text{kg.m}^{-2}.\text{day}^{-1}$